Towards Environmental Resilience in Pulp and Paper Manufacturing: Water Consumption and Carbon Dioxide Emission Reductions

by

Amod Dilip Parkhi

A dissertation submitted to the Graduate Faculty of
Auburn University
in partial fulfillment of the
requirements for the Degree of
Doctor of Philosophy

Auburn, Alabama
August 6, 2022

Keywords: WinGEMS, Water reduction, Scaling, Carbon dioxide capture, Techno-economic analysis, Optimization

Approved by

Zhihua Jiang, Chair, Auburn Pulp and Paper Foundation Assistant Professor of Chemical Engineering, Auburn University
Selen Cremaschi, Co-chair, B. Redd & Susan W. Redd Endowed Eminent Scholar Chair Professor of Chemical Engineering, Auburn University
Mario R. Eden, Joe T. and Billie Carole McMillan Professor of Chemical Engineering, Auburn University
Thomas Elder, Research Scientist, USDA-Forest Service, and Professor Emeritus, School of Forestry, Auburn University
Lauren E. Beckingham, Chair, Assistant Professor of Civil & Environmental Engineering

Abstract

The objective of this research is to reduce freshwater consumption and carbon dioxide emission from the pulp and paper industry. Specifically, we investigated the feasibility of reducing freshwater consumption in the bleach section, one of the largest freshwater consumers in pulp and paper manufacturing by recycling white water from the paper machine. Then, we carried out a techno-economic analysis of solvent-based carbon dioxide capture from limekiln flue gas, the primary source of fossil fuel-based emissions from the pulp and paper industry.

Windows General Energy and Material Balance Systems (WinGEMS) was used to develop a process simulation model of an integrated softwood line of a Kraft pulp mill for the bleaching section and the paper machine section capturing the material, water, energy, and the Non-Process Elements (NPEs). Steady-state equations for the Elemental Chlorine Free (ECF) bleaching sequence $D_0E_{OP}D_1E_PD_2$ are included in the simulation capturing the effects of Brown-stock washers (BSW) and the extraction stage washers on the chemical consumption and the pulp brightness. The simulation model prepared can predict changes in the kappa number, brightness, and the COD values with changes in the operating parameters. Industry and literature data were used to validate the ECF bleaching simulation model, and the difference was in the range of 0.2 to 5.5% for final stage brightness and the post-first extraction pulp kappa number, respectively.

Then we simulated the effect of stepwise replacement of the freshwater used in the bleach washer showers with the white water on scaling tendency in the bleach section. The partition of calcium ions, the primary NPE in white water, between the fiber walls and the surrounding liquor was studied using the Donnan equilibrium model. The dynamic data exchange (DDE) feature in WinGEMS was used to link the Donnan equilibrium model with the bleaching section simulation. After simulating white water addition, the free calcium ions were calculated using the value of the

distribution coefficient 'λ' and taking the inputs of the metal ion concentration from the ECF bleaching section of the WinGEMS model. The free calcium ions predicted by the Donnan equilibrium model were used to calculate the saturation index (SI) in the bleaching section. The maximum amount of white water recycled in the bleaching section without the scale formation is determined by the SI value sensitivity analysis.

Of the three major sources of CO_2 in pulp and paper manufacturing, the Lime Kiln is the only source of fossil fuel-derived CO_2 and has the highest concentration of CO_2. In this work, we, for the first time, performed a techno-economic analysis (TEA) of a monoethanolamine (MEA) solvent-based CO_2 capture from the pulp and paper mill's Lime Kiln section using the CAPCOST modular program.

The flue gas specifications were obtained from published limekiln data of a theoretical pulp and paper mill. The process was simulated in Aspen Plus and linked to CAPCOST using a python script for the cost calculations. The CO_2 capture cost estimates were compared to the only CO_2 capture costs data available in the literature for limekiln flue gas. Comparing the cost breakdown between the published data and this study, the capital cost difference was found to be highest for the stripper and the compression and dehydration sections.

We further examined the TEA and process flowsheet optimization by processing flue-gas using actual mill data from two different mills. A derivative-free optimization (DFO) solver was used to optimize the flowsheet and minimize the CO_2 capture costs. Additionally, we analyzed possible steam integration from within the mills and explore potential in-mill CO_2 applications and their impact on the total CO_2 capture costs. After taking into account the steam savings and CO_2 utilization, the total capture costs were -$2.5 per tonne of CO_2 for Mill A and $2.6 per tonne of CO_2 for Mill B.

Acknowledgments

I would like to acknowledge my advisors Dr. Zhihua Jiang and Dr. Selen Cremaschi for their consistent guidance and encouragement. I appreciate my advisors for giving me the required freedom and opportunity to conduct work on different research topics. This has helped me explore different ideas put forth by various researchers in different fields. I would also express my deepest gratitude to the Auburn University Chemical Engineering department for their support. Special thanks to Dr. Jiang, Dr. Cremaschi, and Dr. Eden's research group members for their help with my doubts. I would also like to thank my committee members Dr. Mario Eden and Dr. Thomas Elder and my university reader Dr. Lauren Bechingham for their input towards my research and my dissertation document.

I would also like to mention the chance that I got to visit various pulp and paper mills during my research. I would like to thank the mills for providing me with the data for my research. Also, I would thank the mill personnel for the field visits which helped me to gain a better understanding of the overall process. I would also thank the pulp and paper industry itself for accommodating me into a vast realm of manufacturing and helping me build up on my previous industry knowledge and further grow as an industry individual.

I would like to extend my gratitude to Dr. Ramsis Farag, and Dr. Burak Aksoy for their support. The amount of experimental work that I was able to accomplish would not have been possible without the help and guidance of Dr. Ramsis Farag and Dr. Burak Aksoy. I would also mention Dr. Illari Filpponen for his input and discussions during the early time of my research work. I am also thankful to the members of the Alabama Center for Paper and Bioresearch Engineering (AC-PABE) for their support. Also thank you to Dr. Tapas Acharjee for providing his valuable time and input during my experimental work.

Words would not serve justice to the moral support provided by many different individuals that I met during my time here and before coming to Auburn. I am not sure about the words that I should use for my Mom, Kalyani Parkhi, my biggest source of inspiration and motivation. Thank you for your moral and ethical teachings that made me what I am today. Thank you to my sister, Amruta Parkhi, and my brother-in-law Amogh Pande for their constant support and guidance throughout. I am thankful to all my friends Vinita Shinde, Rajas Bhalerao, Ritankar Bhattacharya, Ashraf Ali, and Yeseul Choi for their support and help during my stay at Auburn.

Table of Contents

Abstract 2

Acknowledgments 4

Table of Contents 6

List of Tables 10

List of Figures 12

List of Abbreviations 15

Chapter 1. Introduction 17

Chapter 2. Background 22

2.1 Kraft pulping process 22

2.2 Water in the pulp and paper industry 24

2.3 Record for water reduction in the pulp and paper industry 27

2.3.1 Simulation-based techniques 28

2.3.2 Mathematical techniques used for water reduction 33

2.3.3 Sources of carbon dioxide from the pulp and paper industry 46

2.3.3.1 Recovery boiler 46

2.3.3.2 Bark Boiler 47

2.3.3.3 Rotary Lime Kiln 48

2.3.4 Techno-economic analysis of solvent-based CO_2 capture from the pulp and paper mills 49

Chapter 3. WinGEMS simulation of a 5-stage elemental chlorine-free bleaching of softwood .. 58

3.1 Introduction 58

3.2 Methodology 59

3.2.1 WinGEMS simulation 60
3.2.1.1 5-stage ECF bleach section process simulation 61
3.2.1.2 WinGEMS simulation of a bleaching stage 62
3.2.2 Industrial data collection 69
3.3 Results and discussions 70
3.3.1 Mill A data validation 70
3.3.2 Mill B data validation 71
3.4 Conclusions and prospects 72
Chapter 4. White-water recycling in ECF bleaching: prediction of scale buildup 74
4.1 Introduction 74
4.2 Methodology 75
4.2.1 WinGEMS simulation and the Donnan equilibrium model linking 76
4.2.2 Donnan equilibrium model 77
4.2.3 Scale formation 78
4.2.3.1 Calcium oxalate 78
4.2.3.2 Calcium carbonate 79
4.2.3.3 Saturation index 79
4.3 Results and discussion 80
4.3.1 Sensitivity analysis 80
4.3.1.1 Calcium oxalate scaling 81
4.3.1.2 Calcium carbonate scaling 84
4.3.1.3 Effect of pH on the SI value 85
4.3.1.4 D_2 and D_1 chlorine dioxide stage 86

4.3.1.5 Effect of temperature on the SI values of D_0 stage 88
4.4 Conclusions 89
Chapter 5. Techno-Economic Analysis of CO_2 Capture from Pulp and Paper Mill Lime Kiln ... 91
5.1 Introduction 91
5.2 Process simulation and economic analysis 94
5.2.1 Kraft pulp and paper mill 94
5.2.2 Aspen Plus simulation of the MEA-based absorption process for CO_2 capture from Lime Kiln 95
5.2.3 Economic analysis of the MEA-based absorption process 99
5.3 Overview of the reference study economic analysis 100
5.3.1 CO_2 capture setup of the reference study 100
5.3.2 Economic analysis of the reference study 100
5.4 Results and discussions 101
5.4.1 CO_2 capture costs evaluation and comparison with the reference study 101
5.4.2 Sensitivity of the capture cost for the base case of this study 109
5.5 Conclusions and future directions 112
Chapter 6. Carbon dioxide capture from the Kraft mill Lime Kiln: process and techno-economic analysis 114
6.1 Introduction 114
6.2 Process simulation and optimization framework 115
6.2.1 Kraft pulp and paper mill 115
6.2.2 ASPEN Plus process simulation 115
6.2.3 Optimization environment 117

6.2.4 Economic analysis 119
6.3 Results and discussions 121
6.3.1 Derivative-Free Optimization (DFO) parametric study 121
6.3.1.1 Effect of absorber stages 125
6.3.1.2 Effect of stripper stages 126
6.3.1.3 Effect of stripper inlet temperature 127
6.3.1.4 Effect of the solvent lean loading 127
6.3.1.5 Effect of Monoethanolamine weight percentage 128
6.3.1.6 Effect of the amount of CO_2 capture 130
6.3.1.7 Effect of DCC stages on capture costs 130
6.3.1.8 Effect of flue-gas temperature on capture costs 131
6.3.2 Integration of the CO_2 capture system within a pulp and paper mill 132
6.3.2.1 Economic impact of the steam integration on the CO_2 capture costs 132
6.3.2.2 In-mill CO_2 utilization 135
6.3.3 Sensitivity analysis 137
6.4 Conclusion and prospects 140
6.5. Acknowledgment 141
Chapter 7. Conclusions and future work 142
References 147

List of Tables

Table 2.1 Process water usage in the pulp and paper industry 25

Table 2.2 Various software used for water reduction from the pulp and paper industry 29

Table 2.3 Various techniques for water reduction from the PPI..... 34

Table 2.4 Carbon dioxide capture system..... 50

Table 2.5 Post-combustion carbon dioxide capture from the pulp and paper industry 52

Table 2.6 CO_2 capture rates required for studied CO_2 utilization processes 57

Table 3.1 ECF beaching steady-state equations 68

Table 3.2 5-stage ECF bleaching section WinGEMS simulation model validation..... 71

Table 5.1 Economic analysis assumptions, utility costs, and raw material prices..... 95

Table 5.2 Lime Kiln flue gas data..... 97

Table 5.3 Property package and the equipment model used..... 98

Table 5.4 Summary of CO_2 capture costs for the base case 101

Table 5.5 Equipment-wise breakdown of the capital costs..... 102

Table 5.6 Operating cost details ($ million/y) 105

Table 5.7 Energy consumption of the main equipment 106

Table 5.8 Stripper section costing: CAPCOST..... 107

Table 5.9 Specification for main equipment in this study 108

Table 5.10 CO_2 capture process section-wise cost breakdown..... 109

Table 6.1 Lime Kiln fluegas data..... 116

Table 6.2 Optimal process configuration for the MEA-based CO_2 capture system 122

Table 6.3 Optimized flowsheet equipment costs and specification..... 123

Table 6.4 CO_2 capture costs..... 124

Table 6.5 Impact of CO_2 capture on the steam and electricity balances..... 134

List of Figures

Figure 1.1 The sources of carbon dioxide from a Kraft pulp and paper mill 19

Figure 2. 1 Overview of an integrated Kraft pulp and paper mill and a linerboard mill with CO_2 sources..... 24

Figure 2.2 Fresh and wastewater flows in an integrated bleached Kraft mill..... 26

Figure 2.3 Freshwater consumption in each section of a pulp and paper mill..... 27

Figure 2.4 Concepts used for freshwater minimization 29

Figure 2.5 Simulation steps in the study..... 31

Figure 2.6 Stepwise process to find an effluent management solution for a mill using computer simulation..... 33

Figure 2.7 General water pinch analysis project structure..... 38

Figure 2.8 Three-step study used for water reduction 39

Figure 2.9 Energy reduction in a kraft mill..... 40

Figure 2.10 Methodology overview to study the water and energy interactions in Kraft pulping process..... 41

Figure 2.11 Strategies for water closure 42

Figure 2.12 Water superstructure for water recycling and reuse 43

Figure 2.13 Process integration and process simulation coordination..... 44

Figure 2.14 Typical Kraft Recovery Boiler 47

Figure 2.15 Babcock and Wilcox Bark Boiler..... 48

Figure 2.16 Lime Kiln in calcium loop..... 49

Figure 2.17 Post-combustion carbon capture system applicability for the pulp and paper industry 51

Figure 2.18 Quantifying CO_2 emissions from each site 55

Figure 3.1 Unit operations in Pulp Bleaching..... 61

Figure 3.2 WinGEMS simulation of a bleaching stage 62

Figure 3.3 D_0 stage tower compound block..... 63

Figure 3.4 D_0 stage washer compound block..... 64

Figure 3. 5 E_{OP} stage tower compound block 65

Figure 3.6 E_{OP} stage washer compound block 66

Figure 3.7 5-stage ECF bleaching sequence 67

Figure 4.1 Proposed freshwater replacement by white water 76

Figure 4.2 D_2 stage SI sensitivity analysis..... 82

Figure 4.3 D_1 stage SI sensitivity analysis..... 83

Figure 4.4 D_0 stage SI sensitivity analysis..... 84

Figure 4.5 Ep and Eop stage SI sensitivity analysis 85

Figure 4.6 Effect of pH on the SI values for the D_0 stage 86

Figure 4.7 Effect of pH on the SI value for D_2 stage and Effect of pH on the SI value for D_1 stage 87

Figure 4.8 Temperature effect on the SI values..... 89

Figure 5.1 Overview of a Kraft pulp and paper mill..... 94

Figure 5.2 Aspen Plus model of CO_2 capture 97

Figure 5.3 CO_2 compression train..... 98

Figure 5.4 Factors considered in CAPCOST for estimating equipment costs..... 103

Figure 5.5 CAPEX and OPEX comparison 106

Figure 5.6 Capture cost sensitivity with the flue gas CO_2 mol% and steam costs 110

Figure 5.7 Capture costs sensitivity with the MEA and electricity costs 111

Figure 6.1 ASPEN Plus flowsheet of CO_2 capture 117

Figure 6.2 The derivative-free optimization framework 119

Figure 6. 3 Impact of absorber stages on capture costs 126

Figure 6.4 Impact of stripper stages on capture costs 126

Figure 6.5 Impact of stripper inlet temperature on capture costs 127

Figure 6.6 Impact of solvent lean loading on capture costs 128

Figure 6.7 Impact of solvent concentration (wt. %) on capture costs 129

Figure 6.8 Impact of the amount of CO_2 capture (%) on capture costs 130

Figure 6.9 Impact of the DCC stages on capture costs 131

Figure 6.10 Impact of flue-gas temperature on capture costs 131

Figure 6.11 Steam extraction point for the capture process 133

Figure 6.12 Capture costs as a function of flue gas flowrate and flue gas CO_2 concentrations . 138

Figure 6.13 Capture costs as a function of MEA costs 139

Figure 6.14 Capture costs as a function of electricity costs 139

List of Abbreviations

Ø	Diameter
λ	Distribution coefficient
$f_{Ca^{2+}}$	Activity coefficient for calcium ions
$f_{C_2O_4^{-2}}$	Activity coefficient for oxalate ions
K_{sp}	Solubility product
$[M^{2+}]_s$	Metal ion concentration in the solution
ADt	Air-dried tonne
AF	Annualization factor
BSW	Brown stock washing
C	Chlorine bleaching stage
C_i	Carboxylic acid concentration in mmol per O.D. kg pulp
CAPEX	Capital investments
COD	Chemical oxygen demand
CEPCI	Chemical engineering plant cost index value
D	Chlorine dioxide
D_0	First chlorine dioxide stage
D_1	Second chlorine dioxide stage
D_2	Third chlorine dioxide stage
DCC	Direct contact cooler
DCF	Discounted cash flow
DDE	Dynamic data exchange
DFO	Derivative free optimization

E	Extraction
Ep	Extraction stage reinforced with peroxide
E_{OP}	Extraction stage reinforced with oxygen and peroxide
ECF	Elemental chlorine-free
GHG	Greenhouse gases
i	Interest rate
K_i	Carboxylic acid dissociation constant
m	Plant operating years
MEA	Monoethanolamine
MWh	Mega-watt hour
NPEs	Non-process elements
OPEX	Operating costs
PCC	Precipitated calcium carbonate
PPI	Pulp and paper industry
SI	Saturation index
TAC	Total annulized cost
TCR	Total capital requirement
TEA	Techno-economic analysis
t/h	Tonnes per hour
WinGEMS	Windows general energy and material balance system
WW	White water

Chapter 1. Introduction

Industrial activities are a significant source of air, water, and land pollution, making it a leading cause of pollution worldwide [1]. Among the Industrial activities, the pulp and paper industry (PPI) is one of the largest manufacturing industries converting lignocellulosic materials into pulp, paper, board, and other cellulose-based products. The PPI environmental impact account for the release of wastewater, solid waste like sludge, and air emissions [2]. The PPI generates the sixth-largest amount of industrial air, water, and land emissions in the U.S., accounting for 4% of the total industrial releases in 2019 [3].

Of the total 322,000 million gallons per day of water usage in the U.S., the industrial water withdrawal is around 5%. In the industrial water withdrawal, the PPI stands at third rank in demand for water [4,5]. Starting from raw material preparation to pulp washing and paper machines, water is an integral part of the process and is used for several purposes in pulp and paper manufacturing [6]. Although the PPI is a large water user, the industry consumes only a tiny amount of freshwater. Consequently, almost the same amount of wastewater is generated for every cubic meter of freshwater used [6,7]. As a result, the freshwater reduction would reduce nearly the same amount of wastewater discharge from the PPI. Considering the amount of water used in the PPI, several measures are developed to reduce fresh water consumption. These measures include an extensive study of water networks for individual mill sections, novel water recycling and reuse, and water and energy use strategies vis both the intra and intersectional mill scale integration [8–16].

On account of the increasing water stewardship, in U.S. pulp and paper manufacturing, there was a reduction of 6.9%, from 11,281 gallons of water per ton of product to 10,503 gallons of water per ton of product from the 2005 baseline to that in 2018 . Further water reduction within the industry is becoming more challenging due to technical and economic factors [17]. One of the

critical limiting factors for process integration and water recycling is the buildup of Non-Process Elements (NPEs). The NPEs accumulate at various locations in the mill as the level of closure increases causing severe problems like corrosion, plugging, scaling, and deposition [15], [17] imposing a limit on the amount of water reuse and recycling in the mills.

Because water consumption in the bleaching section and the paper machine section account around 75% of the total mill freshwater consumption, this research is focused on water reduction in the Elemental chlorine-free (ECF) bleaching section and predicting the scaling tendency due to white water recycling from the paper machine section to the bleaching section. A 5-stage ECF bleaching sequence was simulated in WinGEMS for the first time. The ECF bleaching WinGEMS simulation enables an analysis of important pulp properties like the kappa number and pulp brightness along with the effluent quality in terms of chemical oxygen demand (COD). Extending the applicability of the simulation, we simulated the effect of stepwise replacement of the freshwater used in the bleach washer showers with the white water in the paper machine section. The changes in the calcium ions in the bleach section effluent were recorded and scaling tendency was predicted in the bleaching section.

Along with high freshwater utilization, the Department of Energy (DOE) has categorized paper manufacturing (NAICS 332) as an energy-intensive sector [18]. In 2019, the industrial sector accounted for 32% of the total U.S. energy consumption, of which 6% was consumed by the PPI [19]. Much on-site energy is generated by burning waste wood, bark (i.e., hog fuel), and spent cooking chemicals (i.e., black liquor) [20], leading to carbon dioxide (CO_2) emission. A modern pulp and paper mill emits 1-3 tons of CO_2 per air-dried ton of pulp produced [21]. In 2020, the PPI in the U.S. released 1.32% CO_2 emissions of the total industrial releases [22].

Regarding the CO_2 emissions, the primary sources of CO_2 from a Kraft mill are the recovery boiler, the biomass boiler, and the Lime Kiln (Figure 1.1) [23]. Over 80% of the CO_2 emissions from the PPI are from the burning of residual biomass, making the PPI very attractive in biomass-based CO_2 capture and industrial CO_2 capture [24-25].

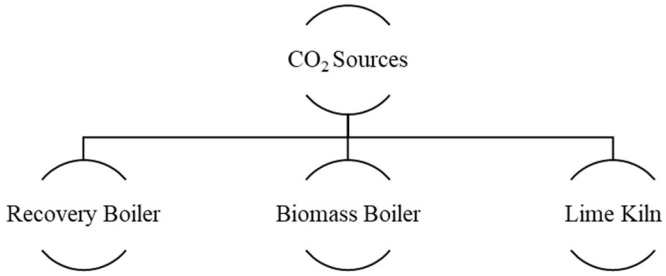

Figure 1.1 The sources of carbon dioxide from a Kraft pulp and paper mill

The Lime Kiln section is the only major CO_2 source in the pulp and paper with fossil fuel-based emissions with the highest concentration of CO_2 in the flue gas.

Control of greenhouse gases using the option of carbon dioxide capture and storage is attractive as it allows the continued use of fossil fuels without contributing significantly to greenhouse gas emissions [24]. There are three main capture systems associated with different combustion processes [25–29]: 1) Post-combustion, 2) Pre combustion, and 3) Oxy-fuel process. Capturing CO_2 from the flue gas mixture produced by burning fossil fuels and biomass in the air is termed post-combustion capture The carbon dioxide in the flue gases from PPI falls in the post-combustion capture module due to gas pressure and CO_2 concentration conditions [30,31].

Solvent-based technologies for CO_2 capture have been studied extensively for oil & gas, iron & steel, cement, and chemical productions [32]. However, limited research on solvent-based CO_2 capture in the literature has been done for the cause of CO_2 capture from the PPI [21],[33–35]. Some research has also been carried out on calcium looping (CaL) and the black liquor

gasification combined cycle (BLGCC) technology for decarbonization [36,37]. As per the Environmental Protection Agency's policy [38], CO_2 emissions from biomass combustion for energy production are treated as carbon neutral. This very reason for treating the biobased CO_2 as carbon neutral limits the economic incentives for investments in capturing biogenic CO_2 [39], posing a challenge in selecting technology to capture CO_2 from the PPI. Owing to the scarcity of costing data, Leeson et al. [32], in their techno-economic analysis and systematic review of carbon capture and storage from various industries, do not include the PPI. The report has given the costing data from only two literature data points for CO_2 capture from the PPI.

With the high concentration of Lime Kiln flue gas CO_2, and the limited economic data availability of CO_2 capture from the pulp and paper industry, this research worked on the CO_2 capture from the Lime Kiln section flue gas and studied the techno-economic analysis and process and flowsheet optimization of MEA-based CO_2 capture.

The dissertation is organized as follows. Chapter 2 provides a review of background information relevant to this research. Chapter 3 describes the build-up of WinGEMS simulation of the bleaching sequence providing details on the different blocks used in the simulation preparation and validation. Chapter 4 provides details about the scaling tendency in the bleaching section due to the replacement of the bleach shower's freshwater with paper machine section white water. The 5-stage ECF bleaching section simulation was used to study the scaling tendency. This chapter also elaborates on the integration of the Donnan equilibrium model with the WinGEMS model using the dynamic data exchange (DDE) feature in WinGEMS. The sensitivity analysis provides the maximum freshwater that can be replaced in the bleaching section. Chapter 5 focuses on the CO_2 capture from published limekiln data of a theoretical pulp and paper mill. Aspen plus flowsheet was prepared to simulate the monoethanolamine (MEA) based CO_2 capture and the

CAPCOST modular program was linked to the flowsheet using a python script. This chapter provides the cost breakdown and the economic analysis methodology comparison with published literature data on Lime Kiln CO_2 capture. Chapter 6 extends the approach used in Chapter 5 to examine the flue gas from two actual mills and performs a techno-economic analysis. Further, Chapter 6 provides details on the process and flowsheet optimization. To reduce the capture costs, steam integration and in-mill CO_2 application were studied taking into account the Section 45Q – Internal revenue code. Chapter 7 summarizes the conclusions and future work of this research.

Chapter 2. Background

2.1 Kraft pulping process

The process by which the fibrous raw material is reduced to a fibrous mass is referred to as pulping. As shown in Figure 2.1, wood logs are debarked and converted to chips in the mill's wood preparation section. Along with chip fines, the wood bark is burned in the bark boiler for steam generation, in which CO_2 is formed. The chips are then fed to the digester for cooking. The cook is maintained at maximum temperature, usually about 170°C, for up to 2 hours to complete reactions. The cooking chemicals are sodium hydroxide (NaOH) and sodium sulfide (Na_2S) in a water solution, which is called white liquor. Residual liquor and the cooked pulp are then separated by brown stock washing, typically using a multi-stage counter-current washing sequence. Weak black liquor leaving the brown stock washers, with a solids content between 13 and 17%, is concentrated in a multi-effect evaporator. The concentrated black liquor, with solid content between 60 and 80% solids, is burned in a recovery boiler for chemical and energy recovery - this burning of concentrated black liquor results in CO_2 emissions from boiler flue gases. The reboiler smelt is dissolved in water to form green liquor and causticized with the reburned Lime (CaO) to form white liquor to be used in the cooking process, completing the cycle [40].

In an integrated pulp and paper mill, the pulp is processed into the stock used for papermaking, either directly or after a bleaching process, with different chemicals under different conditions to take the pulp to the desired level of brightness. The papermaking process includes pulp blending specific to the desired paper product, dispersion in water, beating and refining, and any necessary wet additives. The pulp then goes to the headbox. The pulp goes to the paper machine from the headbox, and then after a series of drying operations, the pulp is formed into paper [41].

For a linerboard mill, the pulp, after cooking, is refined and washed. In some cases, fibers recovered from previous corrugated boxes get added to the washed pulp's mixer. The brown-colored pulp is then formed into a sheet by the paper machine [42,43].

CO_2 emissions from the bark boiler and recovery boiler fall under biogenic CO_2 as the CO_2 is released due to burning wood-derived fuels. The wood bark is burned in the bark boiler, and strong black liquor from the multiple effect evaporators is burned in the recovery boiler, respectively. In the Lime Kiln, CO_2 is released in the calcium carbonate decomposition process, involving fossil fuel burning [21]. Figure 2.1 also gives the location of primary CO_2 sources from the pulp and paper industry.

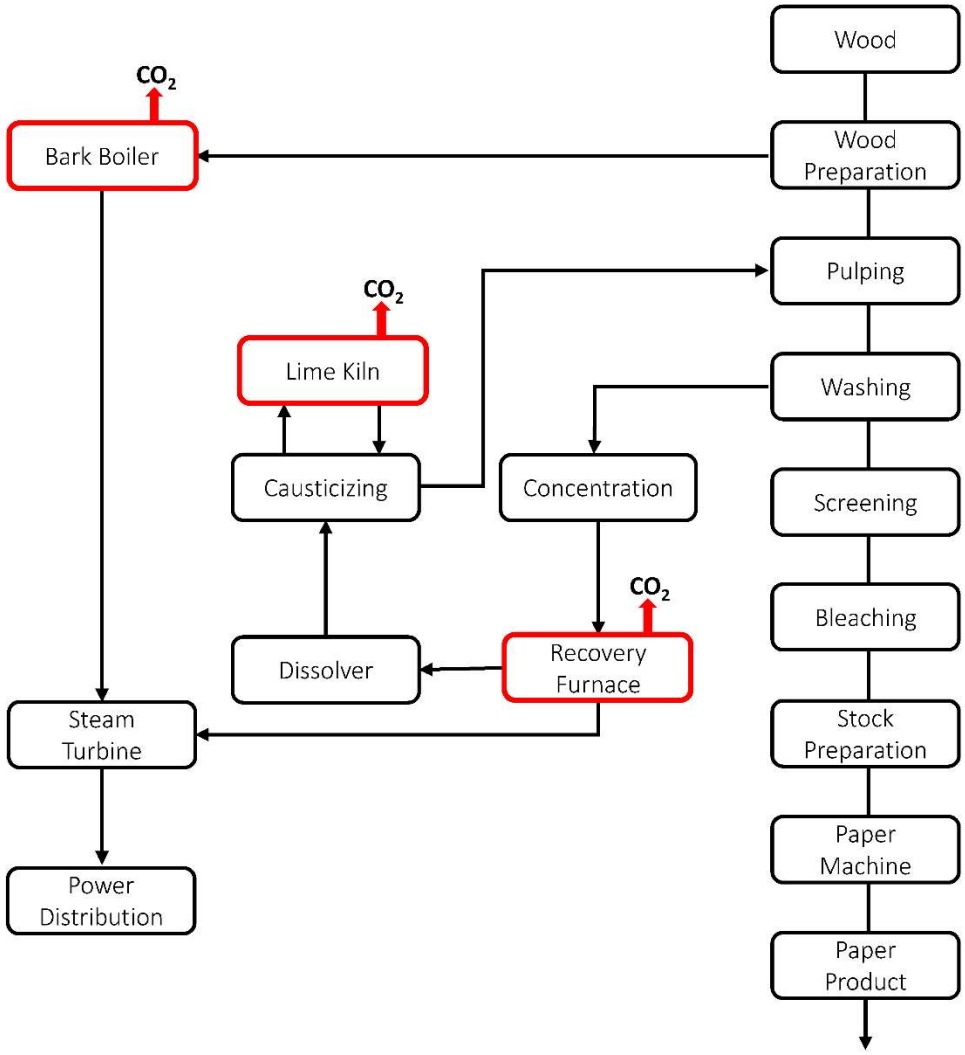

Figure 2.1 Overview of an integrated bleached Kraft pulp and paper mill and a bleached linerboard mill with CO_2 sources

2.2 Water in the pulp and paper industry

Water is an integral part of paper manufacture, required from wood preparation to fiber conditioning and classification. The application of water in PPI ranges from pulping, bleaching, etc., as a solvent (e.g., chemical recovery, additive preparation, etc.) to its physical application as a conveyor of the final product or intermediary material [5] (Table 2.1).

Table 2.1 Process water usage in the pulp and paper industry

Mill section	Usage of process water	Reference
Wood handling/preparation	Cleaning and de-icing the logs. In defibrator to separate heavy materials from the chips.	[40], [44]
Pulping	Used as steam and process water in digesters for chip cooking, chemical preparation, used as a solvent in pulp washing, and recovery of chemicals employed in lignin removal from the wood. As a lubricant in mechanical pulping.	[5], [40], [45,46]
Bleaching	To convey heat/cool pulp stock, medium in which delignification or bleaching reaction occurs, separation of bleached pulp and reactants from the pulp, dissolve organic and inorganic materials.	[47]
Recovery	Solvent in the recovery section	[5]
Papermaking	For dilution of the stock, production processing, fiber conditioning, and classification.	[5]

Also, the water requirements in a mill are a strong function of product type, process type, and general mill practice. In addition, the industry's quality requirements and manufacturing process specifications contribute to a large amount of high-quality water consumed [48]. Large non-integrated paper and board mills, using purchased pulp for their paper production [49], had the lowest median water use. In contrast, the dissolving pulp mills had the greatest median water use of around 11 times the previous one [50]. The water consumption can further be broken down

into different process areas within the pulp and paper mill. Figure 2.2 depicts freshwater and wastewater flows in the paper and pulp manufacturing process [51].

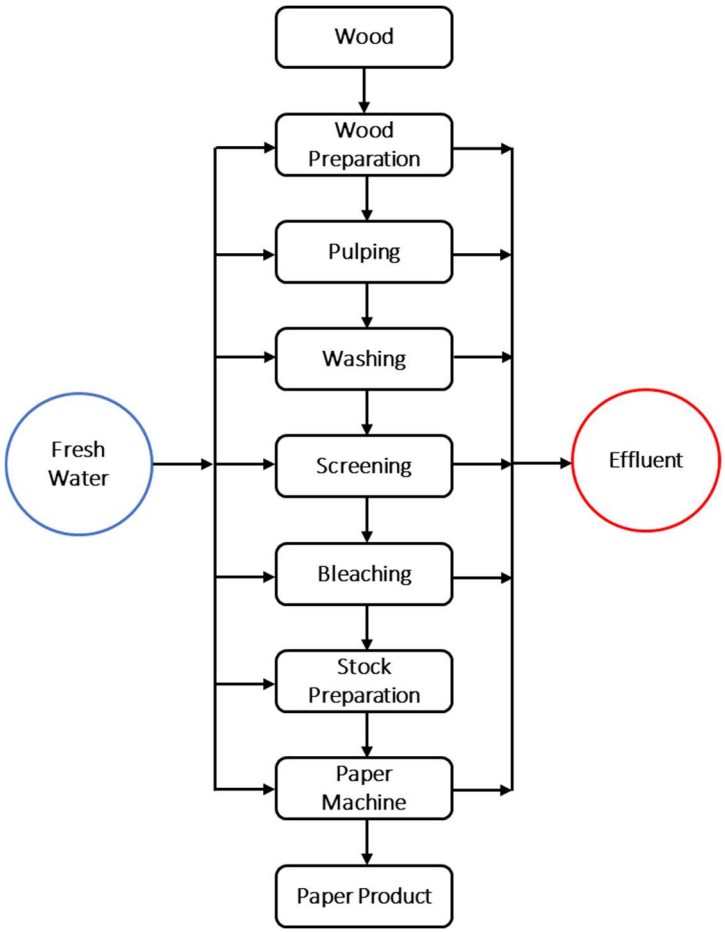

Figure 2.2 Fresh and wastewater flows in an integrated bleached Kraft mill

Of the various process areas in a typical integrated bleached Kraft mill, the paper machine and pulp production process areas account for around 75.0% of the total mill freshwater consumption, with pulp production alone contributing to 40.0% of the freshwater consumption [48]. Figure 2.3 represents the section-wise freshwater consumption in a pulp and paper mill.

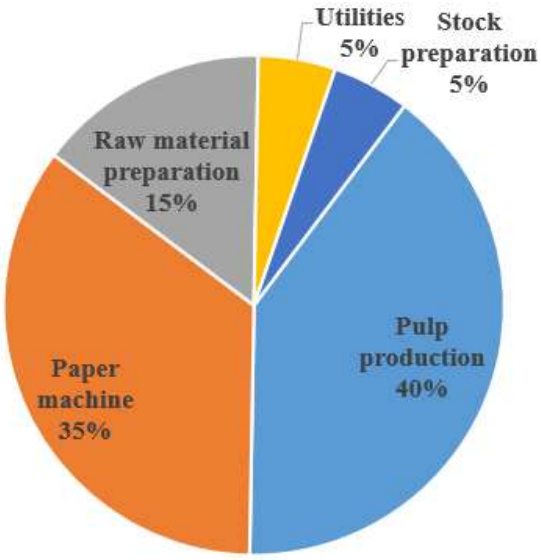

Figure 2.3 Freshwater consumption in each section of a pulp and paper mill

The large quantity of water required in pulp and paper manufacturing and its distribution over the mill's different process areas has led to several innovative and thought-provoking water reduction steps. Pulp production and the paper machine section are typically the largest freshwater consumers; the most significant potential for freshwater reduction exists in these two areas [48],[50].

2.3 Record for water reduction in the pulp and paper industry

Efforts are continuously directed for water reduction, reuse, and recycling from the PPI. The amount of water recycled can depend on product type, supply availability, effluent disposal, equipment availability, and economics [5],[50]. However, advanced technology and innovation have increased water reuse throughout the industry. The mathematical methods used for water reduction involve studying the process and process parameters using process simulations as the initial step. Additionally, exploring the impact of process modifications on water utilization has

also been studied using process simulations. The following section talks about simulation-based techniques followed by the mathematical techniques for water reduction.

2.3.1 Simulation-based techniques

Computer simulation and modeling represent a convenient tool for assessing process modification, raw material, and end product changes [46]. Simulation and modeling in the PPI can provide an overall image of the mill operations and assist in better operation ability to decrease the effluent discharge and analyze the environmental impact. Computer simulation serves as a cost-effective measure of many tools to find the most appropriate operating conditions for a paper mill. The process changes are simulated and represent a valuable tool for evaluating process changes [52].

Process modeling has been used chiefly to design or improve the existing plants and explain how an optimal solution should look. On the other hand, computer simulations and modeling have proved to be useful not only in pinpointing novel pathways for maximizing the water recovery but also providing ideas of potential problems, bottlenecks control strategy, etc. through a rigorous global analysis for freshwater and wastewater discharge in paper and pulp mill [53], [15]. With the tools of process modeling and simulations at disposal, there is an abundant opportunity to understand further and strengthen the know-how of various industrial process components. Process modeling has also been used to simulate different mill sections and investigate options for water reduction. Table 2.2 provides the simulation software used, the area of application, and the study's scope (water, energy, or NPEs).

Table 2.2 Various software used for water reduction from the pulp and paper industry

Area of application	Simulation software	Scope			References
		Water	Energy	NPEs	
Bleaching	WinGEMS	•		•	[54]
Bleaching	WinGEMS/CADSIM	•		•	[15]
Paper machine	WinGEMS	•			[46]
Effluent treatment/Water recycling	WinGEMS	•			[55]

Targeting water reduction in the bleaching section, Jour P et al. [54] studied the Elemental Chlorine Free (ECF) bleach section to identify options for significantly reducing freshwater usage and the effluent discharge in the bleach section of a softwood kraft market pulp mill. Three concepts were studied using WinGEMS simulation to minimize the use of freshwater (Figure 2.4).

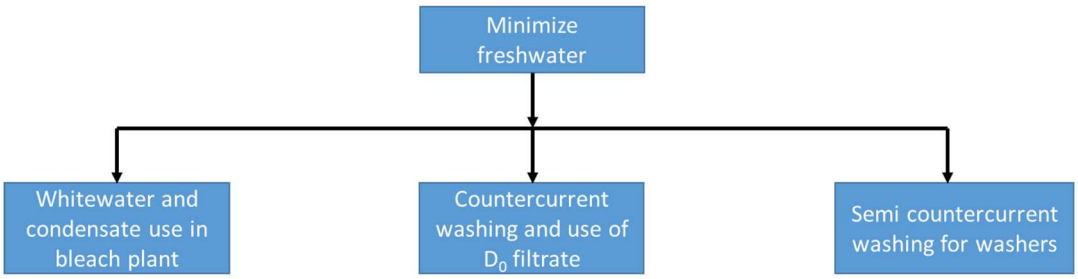

Figure 2.4 Concepts used for freshwater minimization

The first concept was to use white water and condensate in the bleach section. The first concept led to a decrease in freshwater consumption by 2.7 ton/air dried ton and a reduction in the effluent by the same amount. The second concept was introducing countercurrent washing and increasing the internal use of D_0 filtrate. 97.0% reduction in freshwater usage was achieved by

maximizing both D_0 and E_{OP} filtrates in the bleach section. However, the increased use of both D_0 and E_{OP} filtrates was found to increase the COD carryover to the pulp machine. The third concept was using a semi-countercurrent washing strategy for bleach section washers. The effluent from the D_2 and the EP stage was divided and used equally in the preceding washers. Using the semi-countercurrent method resulted in a freshwater saving of 86.0% across the bleaching section. Considering the impact of NPEs while increasing the use of white water and countercurrent washing, the study highlighted that the highest risk of calcium oxalate precipitation was around the D_0 stage and can be reduced by decreasing the pH and/or increasing the D_0 stage temperature.

De Oliveria et al. [15] used WinGEMS and CADSIM simulators to build a flowsheet for a five-stage bleach section OD(E_{OP})DP oxygen delignification (O); chlorine dioxide (D); peroxide and extraction (E_{OP}); chlorine dioxide (D); hydrogen peroxide (P). The researchers linked the CADSIM simulator to Visual MINTEQ (NICA-Donnan Model) to describe specific and non-specific binding between a metal with various functional groups on the lignin-fiber structure. Methodology and the simulation used in the study were divided into several steps (Figure 2.5).

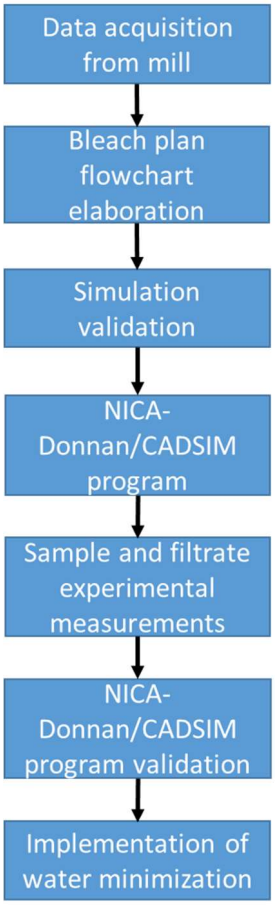

Figure 2.5 Simulation steps in the study

The freshwater savings of 74.0% were achieved using alkaline filtrate (E_{OP}) in the P washer to substitute the freshwater. The study showed a significant change in the E_{OP} and the 2nd D stage metal ion concentrations. The NPEs distribution study over the bleaching sequence showed some interesting results. The simulation results showed that the E_{OP} and the 2nd D stage significantly changed with increased calcium, manganese, and magnesium concentrations in the E_{OP} filtrate. However, the study reported decreased ferric concentrations in E_{OP} stage filtrate. The study states that special attention needs to be given to the increase in the manganese in the E_{OP} stage and calcium in the D_1 stage because of the operational problems.

To increase the water loop closure of the stock preparation and the paper machine wet end, D. Ravnjak et al. [46] studied the possibility of a process equipment change, substituting the existing internal floatation water system with a poly-disk filter for water reuse on the wet end of a paper machine of a paper mill. WinGEMS was used to create a model of the wet end of the papermaking process. The model preparation was based on the input streams and the process quantities measurements. The prepared model was validated by comparing the measured values to the calculated output values. The possibility of broke reuse and a process equipment change was studied employing the model. As per the model, the freshwater use can be reduced to almost half and the wastewater generation by approx. 20.0% at an unchanged production rate. Based on the COD increase due to water recycling, the study concluded that closing the water loop without additional water treatment would not bear any desired results.

Mansfield M et al. [55] used a WinGEMS model of a paper mill producing specialty fine paper to build a baseline model to simulate various effluent treatment and recycling options. The steps involved in using a computer simulation to achieve a zero effluent solution for a mill are shown in Figure 2.6. The researchers tested several biological treatment systems and found that treated sewage water could be eliminated using a biological kidney.

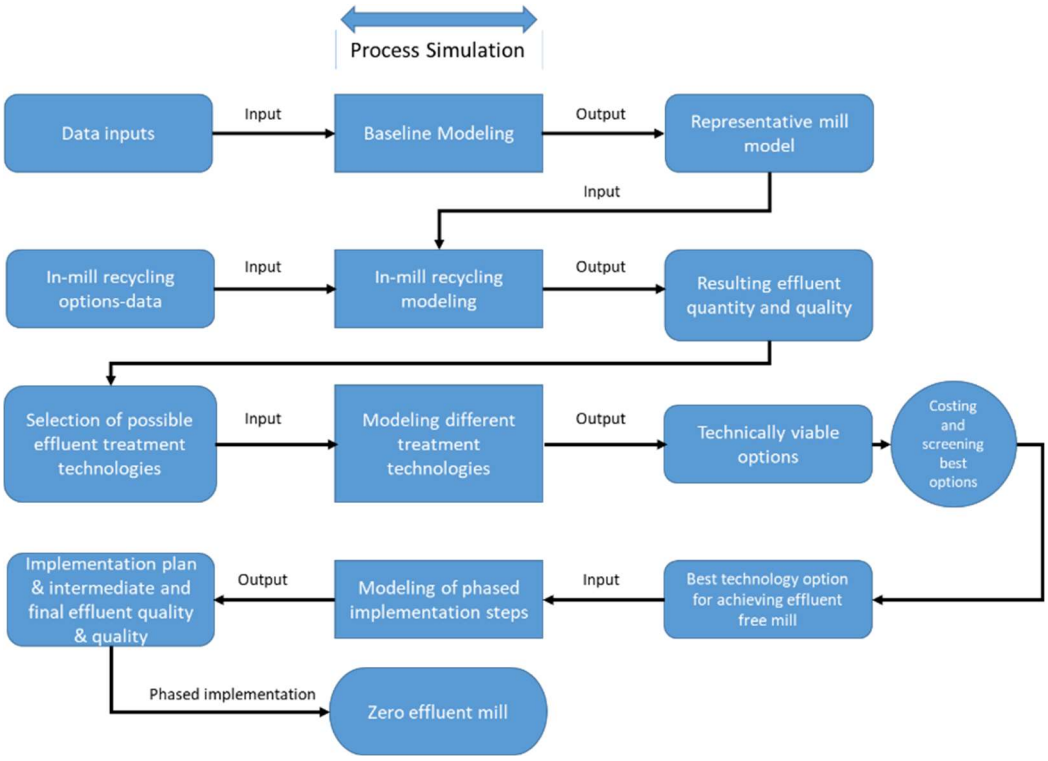

Figure 2.6 Stepwise process to find an effluent management solution for a mill using computer simulation

The water COD levels were dropped as the biological kidney removed COD.

2.3.2 Mathematical techniques used for water reduction

The earlier studies on water conservation mainly included practices resulting from a cohesive knowledge of the overall pulp and paper mill operations [5]. Initial efforts were placed on designing the water networks by working on the source and sink concept. Inter and Intra mill recycling concepts included water use within a particular section or from one network to another. Some specific approaches have been used to design water networks. While most work on water synthesis has been focused on a single water network, some research has also been focused on interplant water integration [9]. Table 2.3 gives the various mathematical techniques used for water reduction from the PPI, the mill sections where these methods are studied, and the scope (water, energy, or NPEs).

Table 2.3 Various techniques for water reduction from the PPI

Technique	Mill section(s)	Scope			References
		Water	Energy	NPEs	
Water Pinch Analysis (WPA)	Pulping, bleaching, and paper machine section.	•		•	[14]
	Kraft paper board mill	•	•		[56]
	Papermill	•			[57]
	Kraft mill	•		•	[9]
	Bleaching section and cooling tower	•	•		[58]
	Kraft mill	•	•		[59,60]
Multi-Period problem	Stock preparation, washing, bleaching, pulp machine, and re-causticizing	•	•		[61]
Mathematical modeling	Bleaching section.	•			[62,63]
Nonlinear programming optimization (NLP)	Kraft mill	•		•	[7]
	Brown stock washing	•	•		[64]
Target study	White water network and the alkaline loop of a de-inking process.	•			[8]
Mixed Integer Non-Linear Programming (MINLP)	Kraft mill	•	•		[65]

The bleach section is one of the largest freshwater consumers in a Kraft pulp mill, in some cases accounting for almost half of the total water consumption in a Kraft mill [66]. The large amount of water consumed in the bleaching section provides an opportunity to reduce freshwater. With efforts diverted towards reducing fresh water and limiting the effluent releases to the water treatment plants, there has been a reduction of freshwater consumption by almost 50.0% from the inial value of 50.0m^3 per ADt in the early 1980s to 25.0m^3 per ADt in recent years. However, freshwater reduction in the bleaching section of a paper and pulp mill could increase the concentrations of impurities. These impurities interfere with the regular operation of the bleaching section and affect routine plant operations. A thorough analysis of the bleaching section would help to analyze the optimum values of process conditions and parameters which would help to reduce the amount of freshwater consumed without causing any undesired conditions.

Taking account of it, Dogan and A. Guniz [62] developed a steady-state model for six-stage chlorination–extraction–hypochlorination–chlorine dioxide–extraction–chlorine dioxide (CEHDED) bleaching system. They optimized various bleach towers and the washer process variables. The study simulated the whole bleach section using a FORTRAN source code. The lowest value of the process parameters was selected for wash water optimization. Also, the impact of this reduced wash water flow value was studied on the total dissolved solids. The optimization for the entire bleach section leads to a decrease in 28.0% of the wash water used and a corresponding decrease of 2.9% of total dissolved solids. The study further concluded that the extraction and hypochlorination stages most effectively lowered the dissolved solid's discharge.
Further, working on minimizing freshwater consumption and reducing effluent generation, S. Shukla et al. applied a process integration approach to the bleaching section of an integrated mill [67]. The mill selected in this study uses a conventional Chlorination-Extraction-Hypochlorination

(CEH) bleaching sequence. In addition, the study did a water targeting study, taking COD as the target impurity, and reported a freshwater reduction of 20.8% in the bleaching section. The main focus of this study was the reduction in bleach tower washer wash water.

In a chlorine-based bleaching section to reduce the COD discharge, wastewater minimization of a four-stage CEHH (Chlorination–Extraction–Hypo chlorination 1–Hypo chlorination 2) bleach section was investigated using a steady-state mathematical model by V.P.Singh et al. [63]. To formulate the unit operation models, the authors used mass balances on liquor, fibers, kappa number, chemicals, and COD. Process variable optimization was performed for each bleaching tower's temperature, concentration, residence time, and pulp consistency. For the parameters considered, a maximum reduction of 1.5% was reported in the COD from the chlorination stage while using the lowest allowable values of all the optimization parameters.

Pinch technology has been used extensively in the refining and petrochemical industries to reduce energy usage. However, while applying the pinch analysis to the PPI, complex interactions exist between water and energy. These complex interactions have led to methodologies that combine heat and water integrations [68]. Application of material pinch analysis in the regions where the miscible phase networks encountered in the PPI poses a problem. Working on these interactions, Jacob J. et al. did a targeted study determining the maximum targets for reducing freshwater usage and wastewater discharge [8]. Based on this targeted study, the authors presented two network optimization methods to establish a white water configuration to minimize fresh water requirements and wastewater rejects for an integrated thermomechanical pulp (TMP) and newsprint mill. As per the presented water optimization methods, the water network rearrangement could eliminate the need for a filtration step of a de-inking plant's alkaline zone and with a possible two-thirds reduction in freshwater consumption in the white water network of an integrated

newsprint mill. However, the method's applicability needs to be investigated for other pulp and paper processes.

The research work of Shukla et al. [14] applied the WPA technique to an integrated paper mill using a Kraft pulping process, through water cascade analysis to process the pulping, bleaching, and paper machine sections. The study states that the critical limiting constraint depends on the process and the integration streams. Considering different recycling streams in the bleaching section, the study emphasized that the adsorbable organic halogens (AOX) were the critical limiting constraint while recycling the bleaching effluents in a bleaching plant. In contrast, the COD is a vital limiting constraint if the pulp mill and the paper machine effluents are recycled in the bleaching section. After process integration from the mill's identified sections, the freshwater demand and the wastewater generation were reduced by 28.9% and 30.2%, respectively.

Further, applying the pinch analysis for combined energy and water analysis, Savulescu et al., in their study [56], did a combined water and energy analysis at a kraft paperboard mill. The pinch analysis general project structure consisted of several steps (Figure 2.7).

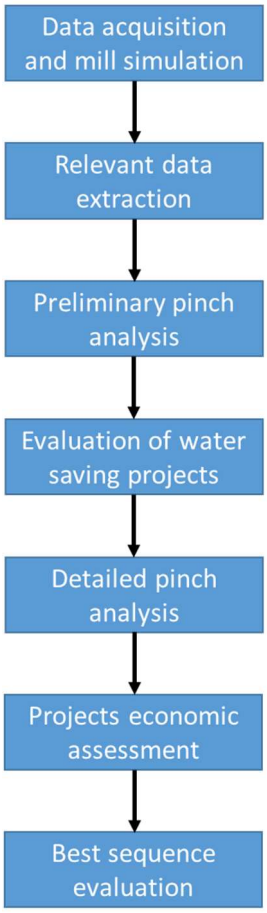

Figure 2.7 General water pinch analysis project structure

Four projects based on the investigation related to the effluent reductions were selected for implementation in the mill: 1) Two projects covering the white water treatment and reuse at paper machine showers, 2) White water reuse at the broke thickener, and 3) Segrigating non-contaminated water from white water. The authors projected water savings would reduce 6,000 m^3/d in freshwater consumption and effluent generation. In addition, implementing the combined heat recovery and water reuse projects was found to reduce the effluent temperatures by 3.0°C, reducing the load on cooling towers.

Also, applying water pinch analysis to a paper mill regenerating paperboard, Liang et al. [57] did a three-step study to reduce the overall water consumption (Figure 2.8). The first was to

determine the contaminant. The colloidal substrate was considered a harmful contaminant for the paper mill. The second was the determination of the water sources and water sinks. In addition to fresh water, some water-consuming processes could be potential sources for other water-consuming processes depending on the inlet contaminant concentration requirements. The third was the determination of limiting concentrations of the contaminant.

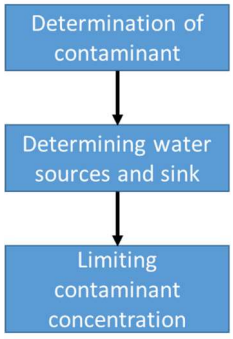

Figure 2.8 Three-step study used for water reduction

The research uses a graphical procedure to draw a graph with purity as its vertical axis and water flow rate as its horizontal axis. The results from the pinch analysis showed that the mill was able to achieve a zero effluent discharge. The pinch analysis application to the mill led to a no wastewater discharge, and the treated water was reused without harmful effects on the production and paperboard quality. Based on the data from the pinch analysis, the water consumption rate was reduced from 90.0-110.0m^3 to 1.6m^3 per ton of paper production.

Towers M. [58] identified opportunities for reducing energy costs related to water usage in a Canadian Kraft mill in two phases. Phase one included steam reduction through pinch analysis and benchmarking, and in phase two, water reduction was explored as a means of energy reduction. Two primary sources of clean water usage were highlighted, 1) the open washing stage before the bleach section and 2) the bleach section itself (Figure 2.9). The kraft mill this study worked on

switched from a six-stage to five-stage bleaching process; as a result, the open washer was an extra bleach section washer. This washer's removal saved approximately 7600.0 l/min of fresh warm water. Further, a filter management strategy based on the principle of a split, jump-stage, counter-current recycling was devised to reduce the fresh water in the bleach section. Implementing this strategy, the blech plant effluent was decreased by more than 20.0 m^3.

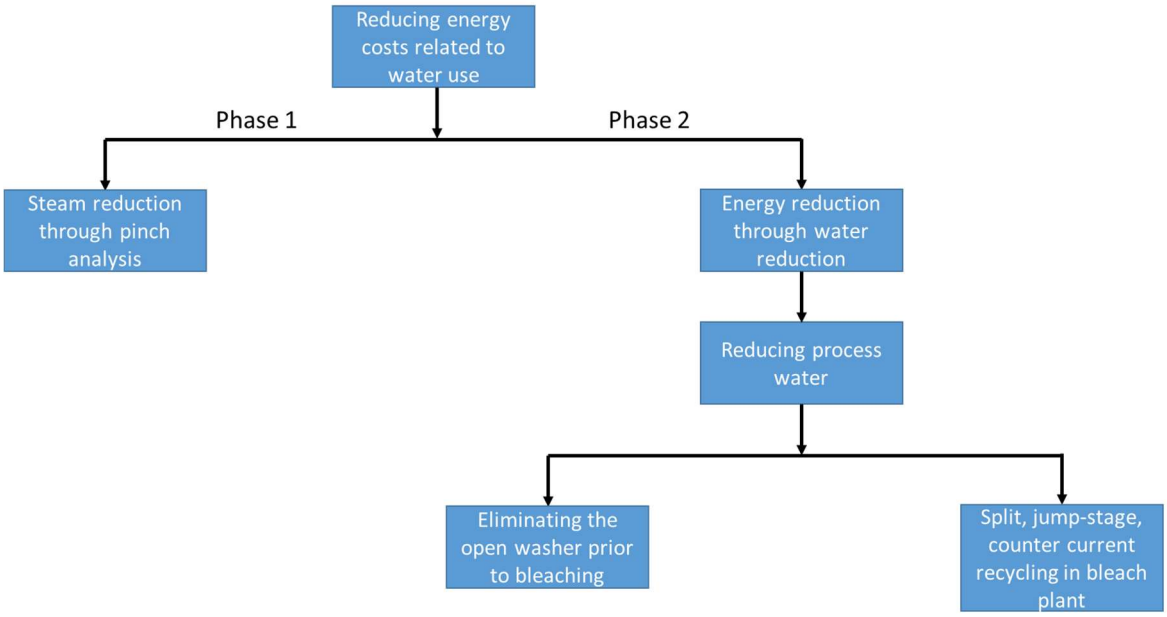

Figure 2.9 Energy reduction in a kraft mill

Significant steam saving was realized by reducing the water usage in the mill. Water reduction alone saved 49.0% more steam in winter than in summer. The study also pointed out that water reduction should be considered with process integration techniques. To achieve significant water reduction, a mill must simultaneously reduce the water needs of both the heat recovery and the process areas.

Mateos-Espejel E et al. [60] developed a systematic methodology to study interactions between energy and water in the kraft pulping process and applied it to an operating mill. The methodology consisted of 5 parts [69] (Figure 2.10).

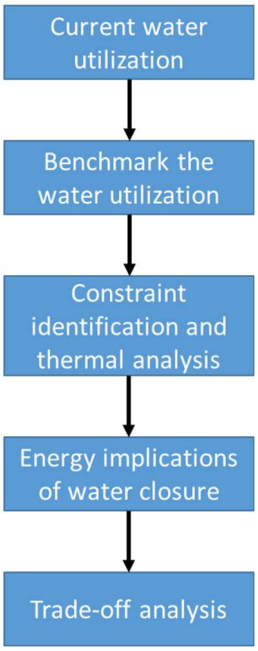

Figure 2.10 Methodology overview to study the water and energy interactions in Kraft pulping process

Four strategies were identified to reduce water, steam, and cooling requirements, and their energy implications were studied (Figure 2.11).

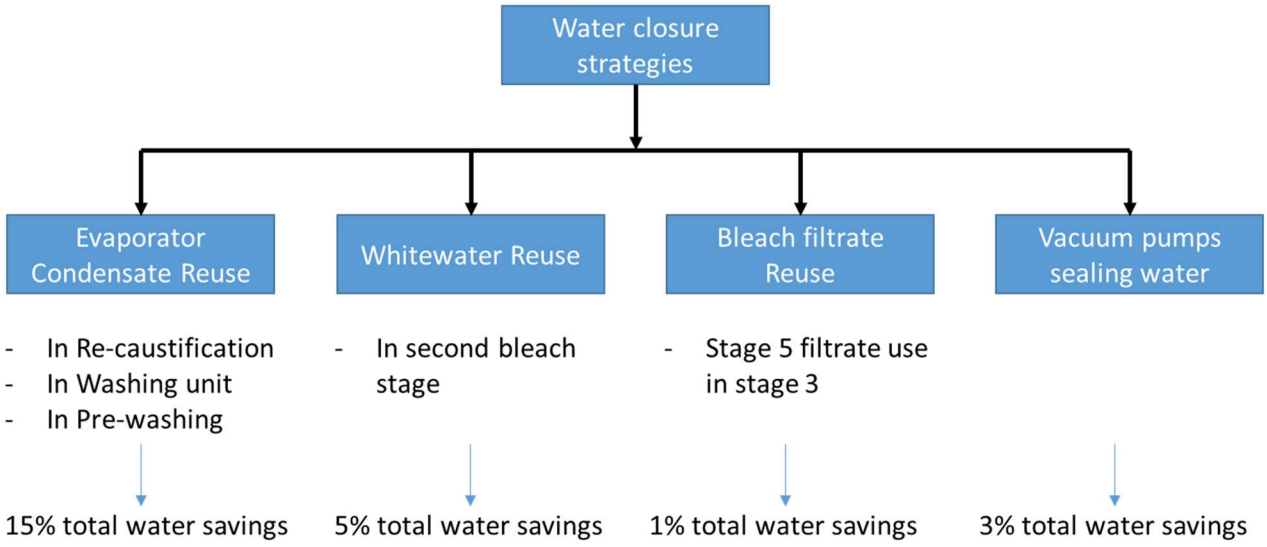

Figure 2.11 Strategies for water closure

As a result, a total savings of 24.0% of total water was realized in addition to a savings of 14.0 MW of steam and 13.1 MW cooling demand. The report mentions the energy implications of the water closure strategies, leaving behind the quality of the effluent and the applicability of various techniques concerning the accumulation of impurities due to reduction in freshwater utilization in the mill.

Kermani et al. [61] developed an optimization methodology based on Mixed Integer Linear Programming (MILP) for simultaneous optimization of water and energy (SOWE). They applied the optimization methodology to a Canadian softwood Kraft pulping mill. The researchers proposed a water superstructure for recycling and reuse (Figure 2.12).

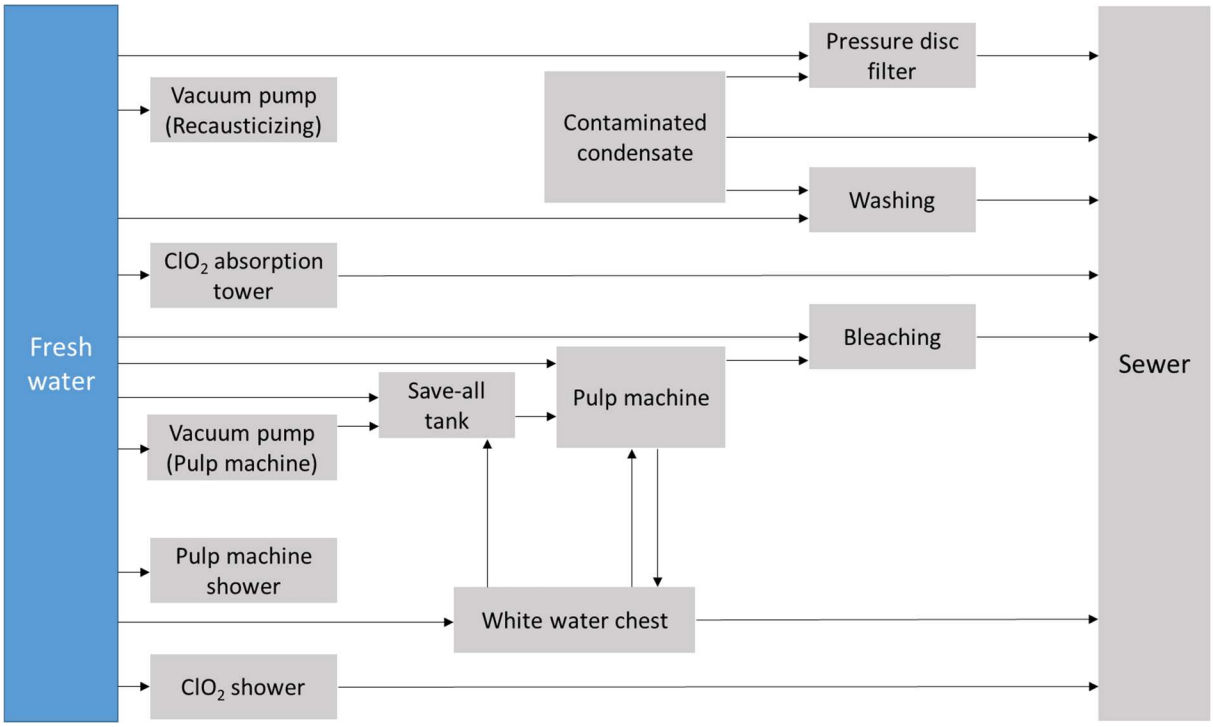

Figure 2.12 Water superstructure for water recycling and reuse

As a result, a total water reduction of 17.0% was reported without any hot utility. In addition, a decrease of 34.0% in the total cost was also achieved due to the reduced operating costs resulting from reducing total water consumption.

One of the critical parameters limiting water recycling and freshwater utilization is the NPEs, which accumulate in the system. Lovelady EM. in the study [7] used mass integration to optimize water networks in the Kraft process and developed a mathematical model to track water and primary NPEs throughout the pulping process. The overall approach applied was to coordinate two crucial activities of process integration and process simulation (Figure 2.13). Mass integration techniques were the primary focus of the process integration tools for water and NPEs.

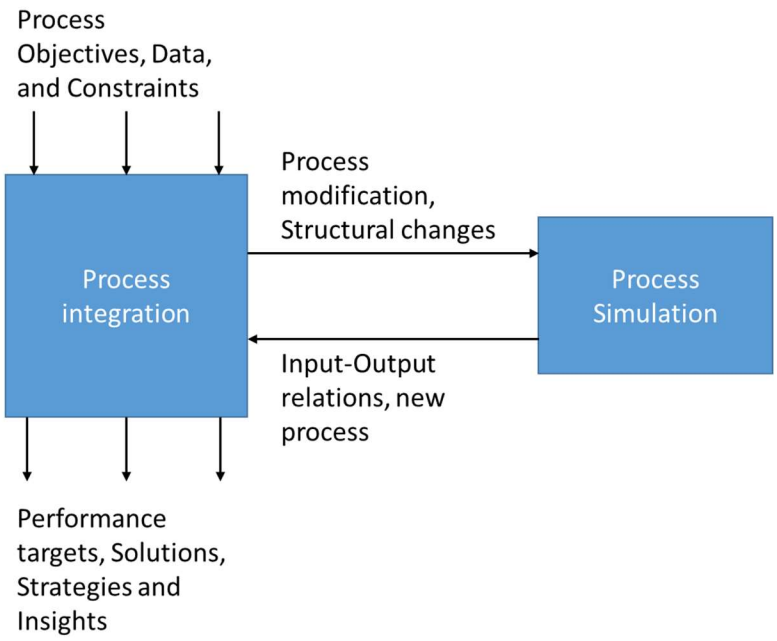

Figure 2.13 Process integration and process simulation coordination

The mass integration objective was to maximize water utilization and satisfy all the process requirements and constraints. The water reduction in the mill was achieved in three systematic ways 1) Direct recycling, 2) Single interception, and 3) New technology enabling self-recycling. Their results demonstrated a significant decrease in water usage. For their case study, a 23.0% decrease in the freshwater was achieved by simple recycling, reusing of wastewater, interception technologies gave a further increase of 62.0% reduction in the water usage, and the highest, 81.0% reduction in water usage, was observed when the NPEs removal technologies allowing self recycling were developed and used.

Chew et al. [64] proposed an NLP optimization problem to minimize water and energy consumption in a pulp and paper mill's brown stock washing system (BSWS) through wash water reuse/recycling. The NLP model is solved using LINGO optimization software. BSWS mass and energy balance were simulated with CADSIM and adopted as the base case for the study. The

objective function minimizes the total cost, including fresh water and energy costs. The objective function is solved subject to the constraints on the washer mass balance, twin roll press mass balance, heat balances, and the constraints on the dissolved solids and the displacement ratio. The NLP optimization results show a possible 23.0% and 17.0% reduction in water and energy. Ibrić et al. [65] applied simultaneous synthesis of non-isothermal water networks to a Kraft pulping mill for water, energy, and the total annualized cost (TAC) reduction. The freshwater consumption was reduced by approx. 34.0% compared to the reference case using water from the pulp machine into the washing section and reusing stock preparation water to the bleaching section. The hot utility consumption dropped to zero with a slight increase in the cold utility consumption. The decrease in water and energy consumption leads to a reduction of approx. 50.0% in the operating and approx. 28.0% in the total annualized costs.

The benefits of applying mathematical modeling tools and simulation techniques have not been fully realized due to the complex dynamics of the papermaking process and rigid operational practices. The reasons for not realizing the full potential of modeling and simulations can be attributed primarily to 1) Complicated nature of the process in terms of raw material characterization, wood chips from different kinds of trees may contain other elements, reaction kinetics that is fundamental for the simulation intending to detect, control and analyze are challenging to figure out. 2) NPEs like transition metals Manganese, Iron, Magnesium, Calcium enter the process mainly from the wood chips released in the process of delignification, part of it coming from impure chemicals, like makeup NaOH, makeup Lime, mill water, and chemical reagents, or from pipes and equipment [70]. In the case of an open mill, the NPEs are purged naturally from the system in the product; however, for closing a mill, these elements tend to build up, resulting in increased equipment corrosion, detrimental plugging, problematic scaling, and

deposit formation, and can adversely affect the papermaking process. 3) The final quality of the paper depends on many process elements, in a complex and nonlinear way, the control actions being usually based on the skill and difficult to quantify. The wet dynamics are convoluted and not fully understood [70]. The points mentioned above make it difficult to model and simulate the whole process, i.e., simulating and optimizing wood chips to paper.

2.3.3 Sources of carbon dioxide from the pulp and paper industry

There are three major sources of CO_2 emissions from the pulp and paper industry. The recovery boiler, the bark boiler, and the Lime Kiln.

2.3.3.1 Recovery boiler

In a Kraft mill recovery boiler, concentrated black liquor is burned in the furnace, and the reduced inorganic chemicals come out from the bottom of the furnace (Figure 2.14). In a Kraft pulp mill, the recovery boiler serves three main functions 1) burn the organic material in the black liquor to generate high-pressure steam, 2) recycle and regenerate spent chemicals in black liquor, 3) minimize the discharge of several waste streams in an environmentally friendly way. The exhaust gases containing CO_2 are generated during black liquor combustion [71].

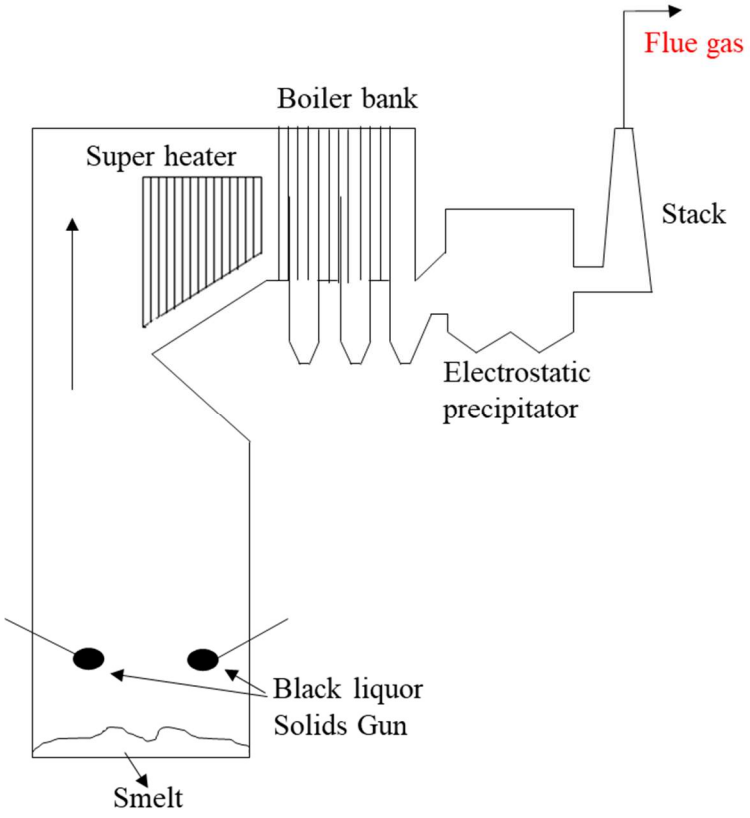

Figure 2.14 Typical Kraft Recovery Boiler

2.3.3.2 Bark Boiler

Wood and bark residues from the raw material preparation are burned in the bark boilers (Figure 2.15). The exhaust gases containing CO_2 are generated due to the wood bark and residue combustion.

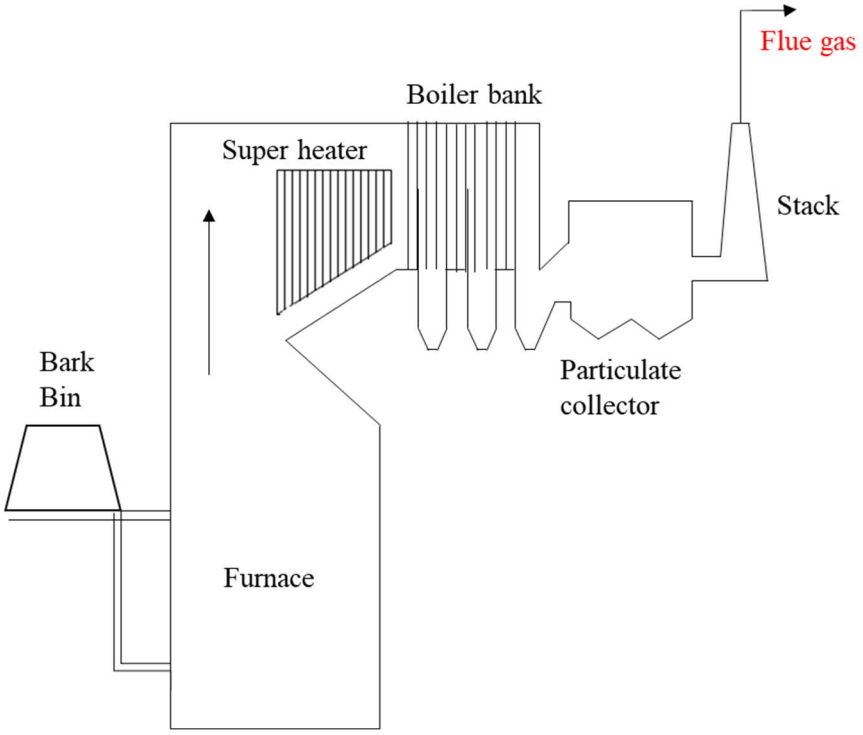

Figure 2.15 Babcock and Wilcox Bark Boiler

2.3.3.3 Rotary Lime Kiln

Rotary Lime Kilns are refractory lined large steel tubes. They are slightly inclined at an angle of 3.0-4.0 degrees to the horizontal and are slowly rotated. A burner, fired with either natural gas or oil, is installed on the fuel's downhill sideburns [72,73] (Figure 2.16). The reaction product from the causticizers, calcium carbonate ($CaCO_3$), is regenerated to CaO in the Lime Kiln with heat from burning fossil fuel typically according to the reduction reaction [74]:

$CaCO_3 \rightarrow CaO + CO_2 \uparrow$…….. (1)

Fossil fuel combustion provides the necessary temperature for the reduction reaction and in-process releases the CO_2 [75].

$Fossil\ Fuels + O_2 \rightarrow CO_2 \uparrow$……(2)

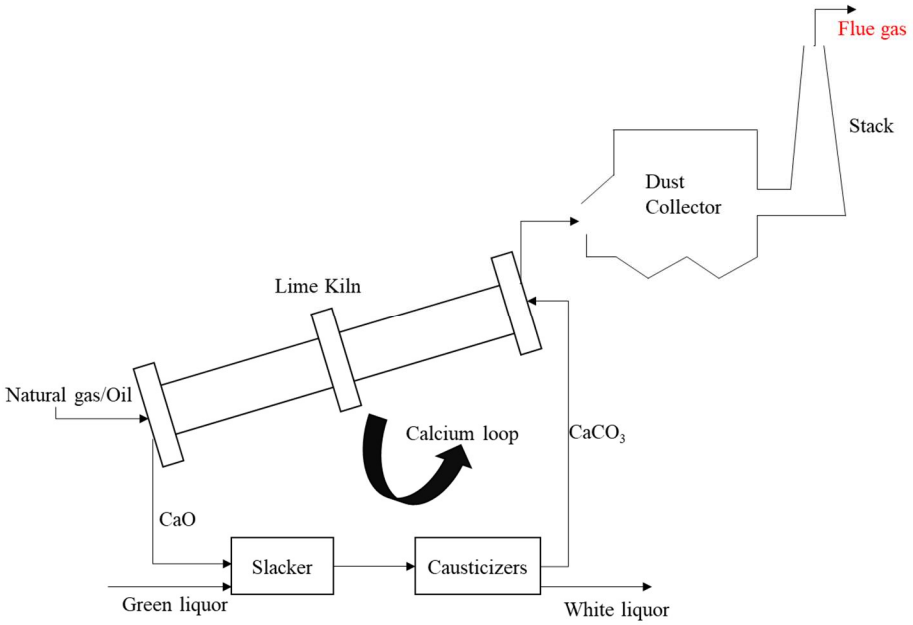

Figure 2.16 Lime Kiln in calcium loop

2.3.4 Techno-economic analysis of solvent-based CO_2 capture from the pulp and paper mills

Control of greenhouse gases using the option of carbon capture utilization and storage is attractive as it allows the continued use of fossil fuels without contributing significantly to greenhouse gas emissions [24]. There are three main capture systems associated with different combustion processes [25–29].

Table 2.4 Carbon dioxide capture system

Capture System	Description	Application	References
Post-combustion	CO_2 capture from flue gas.	low pressure (1 bar) and low CO_2 content (3.0-20.0%)	
Pre-combustion	CO_2 capture from a gas mixture with predominantly H_2 gas.	Elevated pressures (15-40 bar) and medium (15.0-40.0%) CO_2 content	[25],[76]
Oxy-fuel processes	Oxygen instead of air is used for the combustion process.	Power plants using solid fuels	

Carbon dioxide can be separated from the recovery boiler, bark/hog boiler, and Lime Kiln, treating each as individual point sources or combining these sources [31], [77]. Figure 2.17 gives a possible approach for carbon dioxide capture using post-combustion carbon capture from the pulp and paper mill.

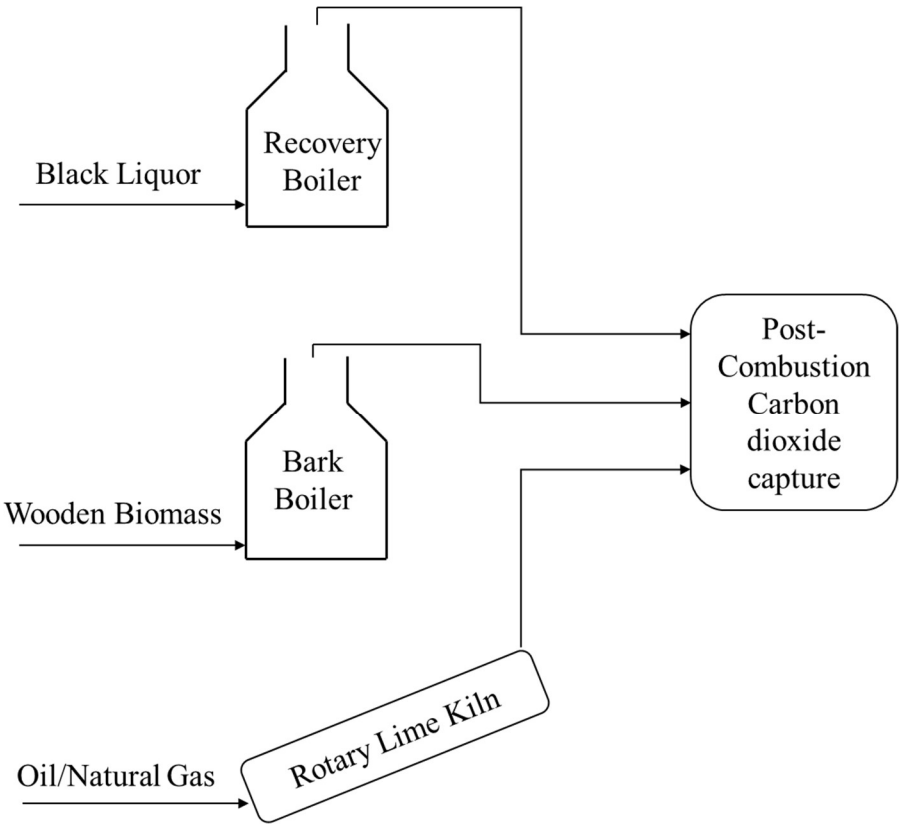

Figure 2.17 Post-combustion carbon capture system applicability for the pulp and paper industry

For CO_2 capture, amine scrubbing is a promising technology. The research in this field is dedicated mainly to process design and optimization to reduce the total energy requirements and thus reduce the CO_2 capture costs [78]. Research is done to capture CO_2 from PPI using post-combustion CO_2 capture technology from the three sources of CO_2 (Table 2.5). The studies so far for the solvent-based CO_2 capture from the PPI have considered a heuristic approach for simulation that leads to a wide range of CO_2 capture costing data.

Table 2.5 Post-combustion carbon dioxide capture from the pulp and paper industry

Technology	Flue-gas source for CO_2 capture			References
	Recovery boiler	Multi-fuel/Bark boiler	Lime Kiln	
Solvent-based CO_2 capture	•	•		[79]
	•			[80]
	•	•		[81]
	•	•		[33]
	•	•	•	[21], [77]
	•			[35]
	•			[82]
	•			[83]
	•	•	•	[84]
	•	•	•	[75]

Considering the chemical absorption with Monoethanolamine (MEA), a benchmarked solvent for CO_2 capture [85,86], K Möllersten et al. [87] suggested that CO_2 capture from the coal industry is the technology suitable for CO_2 capture from the PPI. Considering 90.0% of CO_2 capture from black liquor boiler flue gases and chemical absorption, the preliminary cost of CO_2 capture was $ 34.0 per tonne of CO_2. With black liquor integrated gasification combined cycle and physical absorption, the capture cost was $ 23.0 per tonne of CO_2. The capital costs and the lost electricity production were included in calculating the cost of CO_2 capture.

Hektor and Berntsson [81] considered two alternatives for thermal process integration for reducing the CO_2 capture cost from a fictitious market kraft mill. Alternative one captured CO_2 from the recovery boiler using MEA as absorbent, applying low-pressure steam for solvent

regeneration. Alternative two used a fictive solvent and medium pressure steam for solvent regeneration. At 90.0 % CO_2 recovery, depending on the energy market parameters, for alternative one, the CO_2 capture cost varied between € 25.4 and € 30.7 per tonne of CO_2 whereas, for alternative two, the capture cost changed between € 22.5 and € 27.2 per tonne of CO_2.

Onarheim et al. [21] evaluated two hypothetical reference mills 1) Market pulp mill and 2) Integrated pulp and board mill for different configurations of capturing CO_2 from the flue gases of the recovery boiler, the multi-fuel boiler, and the Lime Kiln. Their results show that it is technically feasible to retrofit amine-based post-combustion CO_2 capture to an existing pulp mill or pulp and board mill. The economic feasibility report [77] evaluated the cost of CO_2 avoided varying the CO_2 tax, incentives for renewable electricity production, exempting CO_2 emissions from tax or not, and rewarded captured and permanently stored CO_2 with negative emissions credit. The cost of CO_2 avoided accounted for € 52.0-66.0 per tonne of CO_2 for a kraft mill and € 71.0-89.0 per tonne of CO_2 for integrated pulp and board mill cases where the CO_2 emissions capture is at 60.0-90.0% of the total site emissions. The study applied the CO_2 capture process to hypothetical mills and did not consider process optimization for the absorption process.

Providing the data for CO_2 capture from the pulp and paper, Stefanía Ósk Garðarsdóttir et al. [35] applied a standard MEA-based CO_2 absorption process to several industries like pulp and paper, oil and gas, steel, cement, and chemical production, with cost estimations to estimate the capital cost for CO_2 capture. The study limited itself to the facilities emitting > 500.0 kt-CO_2/y, as they accounted for more than 50.0% of the industrial fossil-related CO_2 emissions. The study reported a total capture cost of 90.0% CO_2 capture from the recovery boiler at € 61.8 per tonne of CO_2 captured of the various flue gas points discussed. The study concludes that CO_2 capture costs are highly dependent on market conditions. The study considered absorber intercooling an option

for flue gas with CO_2 concentrations higher than 20.0% to improve the process performance. More recently, Chikezie Nwaoha and Paitoon Tontiwachwuthikul[82] investigated two advanced configurations, advanced rich amine four split (ARA4S) and advanced rich amine three split with desorber inter-heating (ARA3S-DI). The study compared the performance of these two techniques with the conventional MEA system and the AMP-MEA blend. The study integrated CO_2 capture into a flue gas exiting from the power boiler of a pulp mill with an annual production capacity of 365,000.0 air dry tonne (ADt) of northern bleached softwood kraft (NBSK) pulp in British Columbia, Canada. To capture all the CO2e emissions attributed to fossil fuel, the study sent flue gas split steam (ca. 55%) from the power boiler to the CO_2 capture plant. At 90.0% of CO_2 capture, the carbon capture process techno-economic assessment revealed that capture costs for the MEA system were lowest at $ 137.6 per tonne of CO_2 or $ 55.5 per ADt Pulp for conventional process configuration. For the AMP-MEA blend, the costs were lowest at $ 125.6 per tonne of CO_2 or $ 50.7 per tonne of ADt for ARA3S-DI.

Prospects for bioenergy with carbon capture and storage (BECCS) in the U.S. PPI was studied by W.J. Sagues et al. [84] at 205 mills. A detailed study assessing the CO_2 emissions from each mill and quantifying the CO_2 emitted from various sources and operations was considered (Figure 2.18).

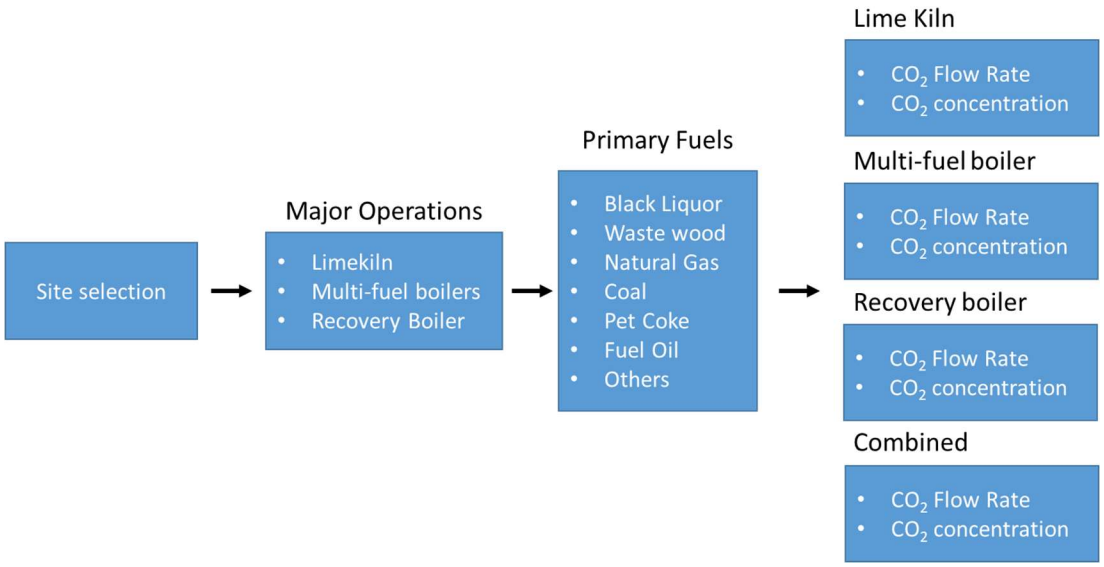

Figure 2.18 Quantifying CO_2 emissions from each site

The study did a top-down, i.e., industry-wide screening, and a bottom-up, chemical modeling technique. One of the crucial conclusions made in the study was regarding the cost comparisons of CO_2 capture amongst the fuels with high and low hydrogen to carbon ratios. The top-down industry-wide analysis concluded that CO_2 capture from coal and biomass combustion is generally less expensive than capturing CO_2 from natural gas combustion. Also, the top-down economic analysis revealed that CO_2 capture from Lime Kiln and recovery boiler is less costly than the multi-fuel boiler. The cost estimates of CO_2 capture from the industry-wide top-down analysis ranged from -$0.6 to $12.7 per tonne of CO_2. Also, the capture cost for CO_2 capture from the Lime Kiln and recovery boiler was less costly than the multi-fuel boiler.

Further, four mills were selected based on the top-down industry-wide screening. The Levelized capital and operating expenses for CO_2 capture were estimated using chemical process models and were assessed using AspenTech process simulation software. The bottom-up analysis estimated CO_2 capture costs for the four mills in the range from -$19.0 to $23.0 per tonne CO_2 considering a $50.0 per tonne CO_2 tax credit (Section 45Q utilization tax credit). The report also highlighted

that process intensification and innovations like the partial oxy-fuel combustion combined with post-combustion CO_2 capture and calcium looping CO_2 capture would help to reduce the CO_2 capture costs. Taking leverage of the Section 45Q utilization tax credit, the report emphasizes pathways for CO_2 utilization such as lignin precipitation and calcium carbonate filling would be potential cash flow opportunities.

More recently, Parkhi et al. [88] did a techno-economic analysis of a conventional MEA solvent-based CO_2 absorption process for pulp and paper mill Lime Kiln presenting a comparative study with a previously published research [21]. The study evaluated CO_2 capture cost by linking the CAPCOST modular program to Aspen plus using a python script. Lime Kiln flue gas from the literature [21] was processed and the capture cost arrived at $ 76.0 per metric ton of CO_2. The study did a detailed analysis of the capital and the utility cost citing the difference in the approaches used for capture cost calculation with the literature work.

Also, Kuparinen et al. [75] studied the potential CO_2 capture within two kraft mill operations from the PPI using MEA based post-combustion process. The report also mentions the utilization of CO_2 for different applications in the PPI. For on-site CO_2 utilization, tall oil manufacturing, lignin extraction, and precipitated calcium carbonate (PCC) production were studied. The amount required to meet the CO_2 for a specific application depends on the sources of CO_2 capture and the mill type (Table 2.6).

Table 2.6 CO_2 capture rates required for studied CO_2 utilization processes

	CO_2 capture rate		
	Recovery boiler (%)	Bark boiler (%)	Lime Kiln (%)
Mill A (softwood kraft mill)			
Tall oil production	0.2-0.3	0.5-0.8	1.4-2.1
PCC production	0.9	2.6	7.1
Lignin separation	1.6	4.5	12.4
Tall oil+PCC+Lignin	2.7	7.9	21.6
Mill B (Eucalyptus kraft mill)			
Lignin separation	1.1-1.8	-	7.0-11.7

The research provides a global scenario for biobased CO_2 capture and concludes that the technical potential for CO_2 in pulp mills is notable and accounts for almost 3% of the global CO_2 capture.

Chapter 3. WinGEMS simulation of a 5-stage elemental chlorine-free bleaching of softwood

3.1 Introduction

Simulation modeling and analysis help to gain insight into a complex system and achieve the development and testing of new operating or resource policies and new concepts or systems without disturbing the actual system [89]. In particular, process simulation modeling favors a better understanding of the mechanisms of processes for the pulp and paper industry [70]. Also, process simulation modeling helps to evaluate any modifications or changes in a section of the pulp and paper manufacturing process . The commercial software available for the pulp and paper industry comprises various modular units representative of various operations, an executive program that is responsible for the administration of modular units, and databases of physiochemical and thermodynamic properties of all components in the process [15].

WinGEMS is widely used in the pulp and paper industry to model various sections of the pulp and paper mill [52,53,90,91]. However, few studies have given attention to understanding the bleaching section of a pulp and paper mill using the simulation approach. De Oliveira et al., [15] carried out a global analysis of a bleach mill plant in Brazil, using WinGEMS and CADSIM simulators, and the NICA- Donnan Model to predict Non-process elements (NPEs) distribution. The prepared model made a good NPE behavior assisting the pulp mill with the buildup of those elements. C. Litvay et al., [92] modeled the NPEs in the hardwood bleach plant by linking an excel spreadsheet to solve the ion-exchange equilibrium using the dynamic data exchange to WinGEMS software. The WinGEMS model vastly improved the ability of this mass and energy balance program to model and predict the distribution of non-process elements in the bleach plant. Recently, Jour P et al., [54] studied an Elemental Chlorine Free (ECF) bleach plant of a softwood

kraft market pulp mill.to identify options for significantly reducing freshwater usage and the effluent discharge in the bleach plantThe ECF model was also used to predict the impact of white-water recycling in the bleach plant. The study highlighted that the highest risk of calcium oxalate precipitation was around the D_0 stage and can be reduced by decreasing the pH and/or increasing the D_0 stage temperature. These studies focused on the application of the bleach plant WinGEMS simulation without providing details on the simulation build-up. Further, the impact of various process parameters and the bleach plant conditions on the important pulp properties were not studied.

The present study, for the first time, models an entire ($D_0E_{OP}D_1E_PD_2$) 5-stage ECF bleaching sequence using the steady-state delignification and brightening ECF equations in WinGEMS simulation software . Our approach makes use of different WinGEMS blocks and a combination of various blocks to simulate different bleaching stages in the bleaching sequence. Initial inputs to the bleaching sequence model were taken from published bleaching data of softwood. Further, validation of the bleaching section was done using data from two softwood mils. The prepared 5-stage ECF bleaching model was then used to predict the important properties such as the pulp kappa number, pulp brightness, and the effluent COD.

3.2 Methodology

In this work, we used WinGEMS software to develop a steady-state process. The simulation model for the 5-stage ECF bleaching section captures the material, water, energy, andNPEs. Three levels of research work wereconsidered for simulation 1) Unit operation, 2) Combination of unit operations, and 3) Combination of various processes. The combination of steady-state kinetics equations for delignification and brightening stages were taken from the literature to model the chemical consumption, pulp brightness, and effluent COD. Simulation was built up using blocks,

representing a particular unit operation, and streams, representing the transfer of material from one bleach tower to another. Input data for the simulation build-up was taken from an integrated softwood mill operating with a typical $D_0E_{OP}D_1E_PD_2$ 5-stage ECF bleaching sequence. The operational data including the temperature, consistency, the wash water flowrates, and various chemical charges necessary for the bleach section model are taken from the softwood mill. Further, the prepared simulation is validated with another integrated softwood mill data.

3.2.1 WinGEMS simulation

GEMS (General Energy and Material balance System) is a modular program designed to perform mass and energy calculations. In this software, the calculations are grouped in different modules called blocks. GEMS is extensively used for material and energy balances in pulp and paper mills [93–95]. WinGEMS makes use of a modular approach, dividing the system into smaller parts called modules. This makes it possible to simulate many different processes using a finite number of calculation blocks. A simulation project is created by diagramming a process using GEM blocks and streams. WinGEMS consists of two integrated parts:

- Windows interface allows the building of a project, controls the interactive execution, and presents the results.
- Process subroutines and process modules that are arranged to model a given process.

WinGEMS has a library of over 75 pre-built process blocks those help in the development of a simulation which is built up using blocks, representing a particular unit operation, and streams, representing the transfer of material from one bleach tower to another. Compound blocks are used when a large simulation of the tower and washers is made. The shortcoming of this program is that it does not contain any chemistry. The simulation uses only mass balance calculations [96]. As

bleaching is a process with chemical reactions, the kinetics equations for delignification and brightening are need to be taken from the previous research data.

3.2.1.1 5-stage ECF bleach section process simulation

The simulation model is prepared for the 5-stage ECF bleaching $D_0E_{OP}D_1E_PD_2$. As shown in Figure 3.1 [47], all bleaching treatments have certain unit operations and processes in common. The mixture of chemicals and pulp passes into a reactor that provides sufficient residence time for the bleaching reaction to occur, after the reaction the material is then transferred to the washer to remove reacted lignin and dissolved material and wash the pulp, although the chemical addition is different for different stages and applications

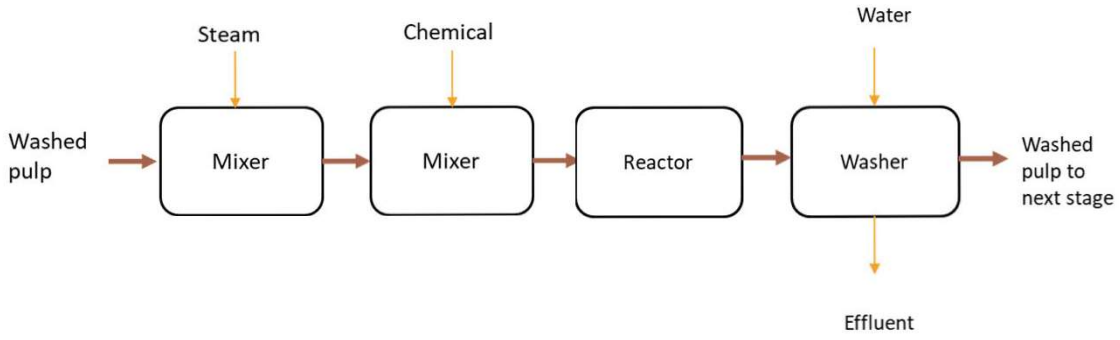

Figure 3.1 Unit operations in Pulp Bleaching

3.2.1.2 WinGEMS simulation of a bleaching stage

Figure 3.2 shows the WinGEMS simulation of a typical bleaching stage. For each bleaching stage, two compound blocks are prepared, one compound block for the bleach tower and another compound block for the bleach tower washer.

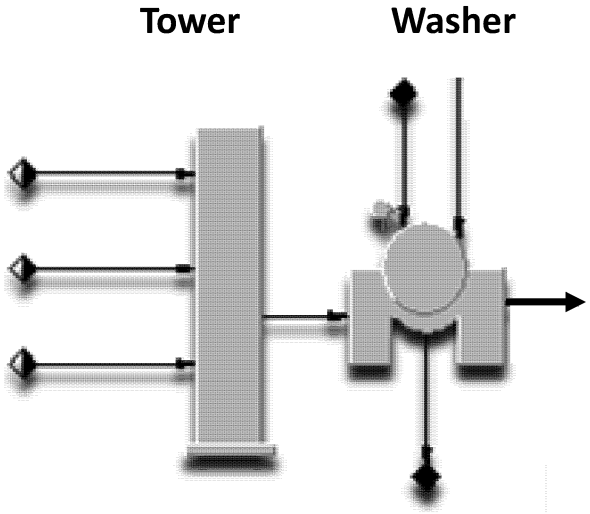

Figure 3.2 WinGEMS simulation of a bleaching stage

In the chlorine dioxide stages, D_0, D_1, and D_2, the compound block for the bleaching tower consists of a CHARGE block to simulate chlorine dioxide addition, another CHARGE block to simulate acid addition, and a REACTION block to simulate the delignification reaction. The acid addition is dependent on the system pH requirement, and the chlorine dioxide addition is on the entering pulp's kappa number. For the alkaline extraction stages, E_{OP} and E_P, the CHARGE blocks are used to simulate the addition of sodium hydroxide, oxygen, and hydrogen peroxide as a percentage on pulp. After the chemical addition, the pulp enters the bleaching tower. The reaction takes place in the reaction tower and the reacted pulp is then washed in the washer.

The incoming pulp properties of kappa number and brightness are stored in the STORE block within the compound block. Also, the steady-state delignification and brightness equations are stored in the STORE blocks. The equations are referred to while calculating the pulp properties, delignification, and pulp brightness in a particular stage. The washer compound block consists of WASH and DILUTE blocks. The washer operates with a defined dilution factor. The effluent quantity and the quality depend on the washer-defined outlet consistency and the shower water quality. The COD is calculated based on the delignification in the first two stages and the pulp yield loss.

Chlorine dioxide stage compound block

Figure 3.3 shows the WinGEMS internal layout of the D_0 stage bleaching tower compound block and Figure 3.4 shows the D_0 stage washer compound block.

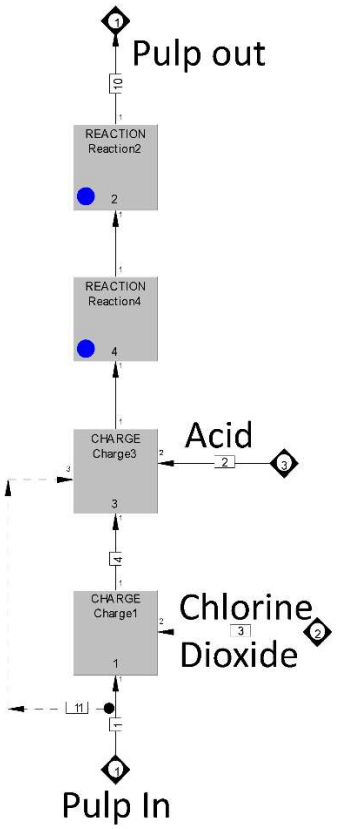

Figure 3.3 D_0 stage tower compound block

CHARGE, REACTION, and the STORE blocks constitute the main blocks for the D_0 stage bleach tower while DILUTE, WASH, and MIX blocks are used in the washer compound block. Chlorine dioxide and acid are charged using CHARGE block. The blue dots in the reaction blocks represents the use of pulp properties of kappa number, the temperature, and the chemical charges required in the steady-state equations of the delignification in the D_0 stage and pulp brightness calculation in the D_1 and the D_2 stages.

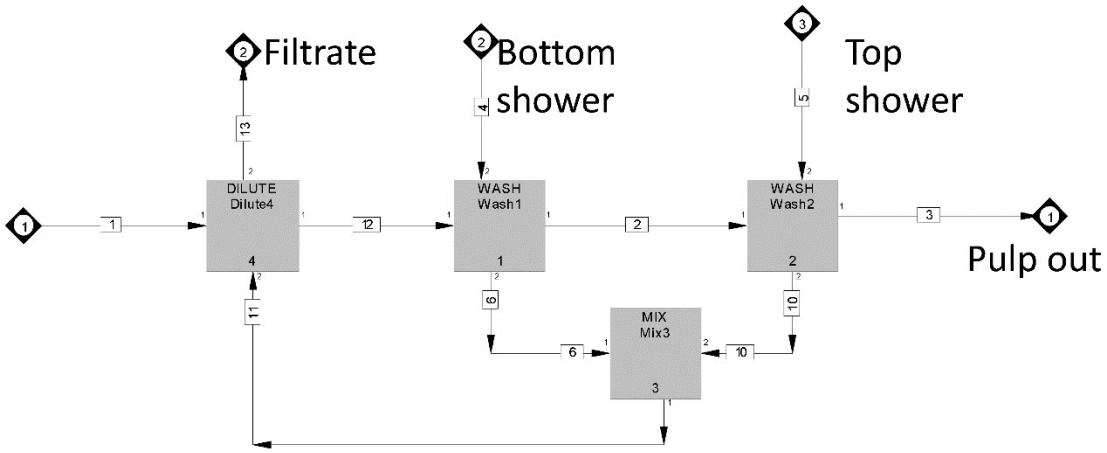

Figure 3.4 D_0 stage washer compound block

The reacted pulp then flows into the washer for washing. The pulp leaving the tower is diluted to the required vat consistency and then washed. For the D_0 stage, fresh water is used in the bottom and E_{OP} stage effluent in the top shower for pulp washing and adjusting the pulp pH, the excess water leaves the system as effluent for processing. In the WASH block, the outlet consistency of the pulp, washer efficiency factor, and dilution factors are defined. The pulp after washing in the washers goes to the next stage.

The D_1 and D_2 stages are simulated similarly to account for the chlorine dioxide addition on pulp and with a similar compound block layout for the washers. In the D_1 stage washer

compound block, the freshwater is used in the bottom shower, and the E_P stage effluent is used in the top shower for pulp washing and pH adjustment as per the pH conditions in the E_P stage. Further, fresh water is used in both, the bottom and the top showers in the D_2 stage washer.

Extraction stage compound block

Figure 3.5 shows the WinGEMS internal layout of the E_{OP} stage bleaching tower compound block and Figure 3.6 shows the E_{OP} stage washer compound block.

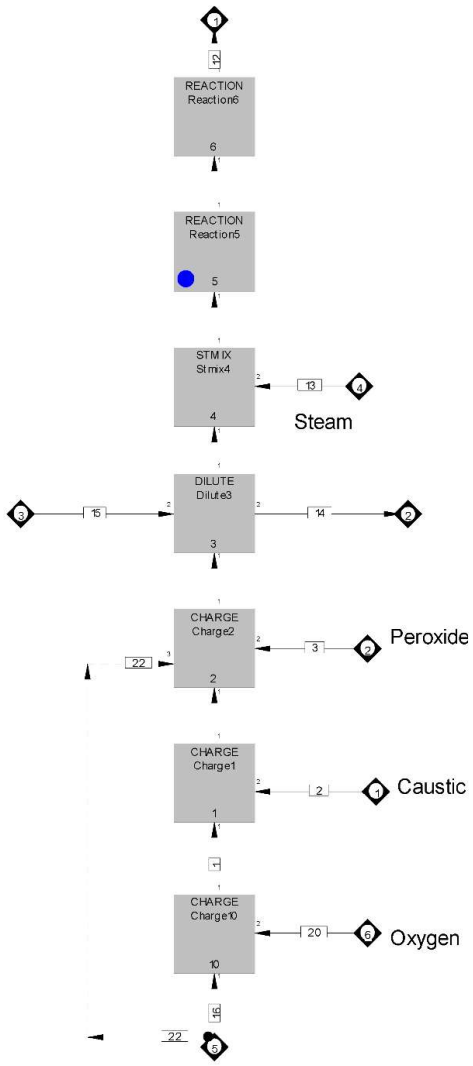

Figure 3.5 E_{OP} stage tower compound block

CHARGE, REACTION, DILUTE, STMIX, and the STORE blocks are the main blocks for the extraction stage, while DILUTE, WASH, and MIX blocks are used in the washer compound block. The pulp from the D_0 stage washer enters the E_{OP} stage. Three CHARGE blocks charge oxygen, sodium hydroxide, and peroxide on pulp. DILUTE block dilutes the pulp to the desired E_{OP} stage consistency. The temperature in the EOP stage is controlled by steam addition to the pulp. The STMIX block simulates the steam addition to the desired temperature. The steam required to reach the desired temperature is back-calculated in the STMIX block. The STORE block stores the steady-state equations, the parameters necessary to solve the steady-state equations, and the brightness equations. The COD calculations are based on the simulated yield losses in the bleach tower.

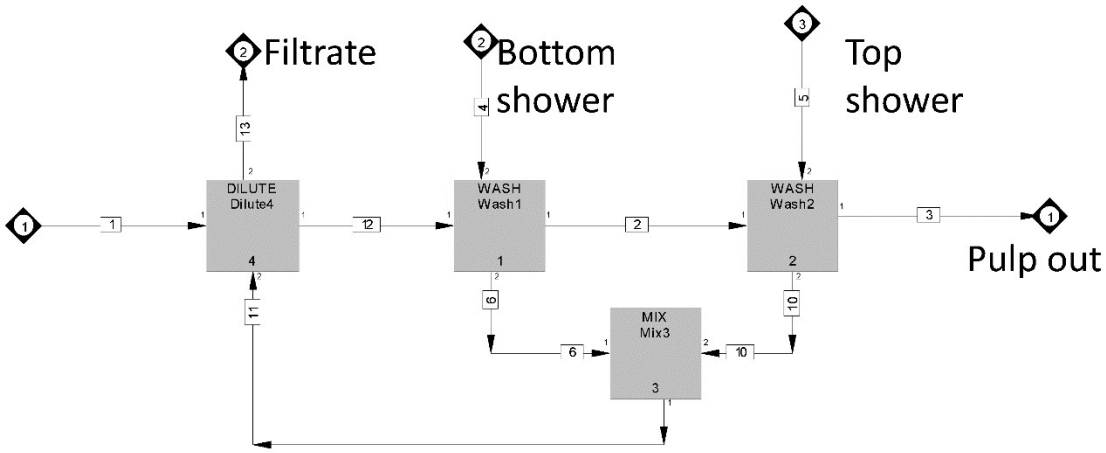

Figure 3.6 E_{OP} stage washer compound block

The reacted pulp from the extraction stage goes into the washer compound block for washing. The pulp leaving the tower is diluted to the required vat consistency. For the E_{OP} stage, the pulp is washed using fresh water in the bottom and the D_1 stage effluent in the top shower. For the E_P stage, the pulp is washed in the pulp washers using the D_2 stage effluent in the bottom

shower and fresh water in the top shower. The excess water leaves the system as effluent for processing. In the WASH block, the outlet consistency of the pulp, washer efficiency factor, and dilution factors are defined. The pulp after the washer goes to the next stage. The compound block of the E_P stage is simulated similarly to account for the sodium hydroxide and peroxide addition on pulp with a similar compound block layout for the tower washers.

Figure 3.7 gives the WinGEMS simulation for the entire $D_0E_{OP}D_1E_PD_2$ 5-stage ECF bleaching sequence. The pulp from the brown-stock washer enters the ECF bleaching sequence and is delignified in the D_0E_{OP} stage and brightened to the required brightness in the $D_1E_PD_2$ stage.

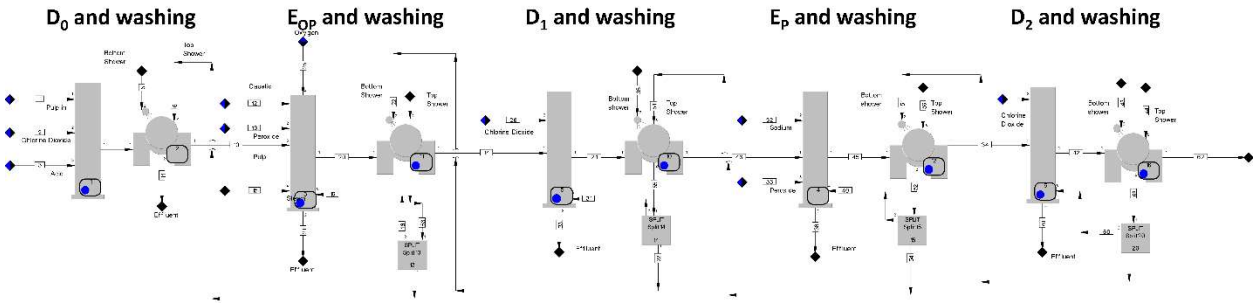

Figure 3.7 5-stage ECF bleaching sequence

Steady-state equations

Table 3.1 gives the steady-state equations used in the 5-stage ECF bleaching sequence. The first two stages (D_0E_{OP}) form the delignification stages of the bleaching sequence and contain the delignification equations and the pulp brightness equations, and the $D_1E_PD_2$ stages represent the pulp brightening stages of the bleaching sequence and contain the pulp brightness equations. The equations of individual stages are stored in the STORE blocks in the compound blocks of each bleach tower and the tower washers.

Table 3.1 ECF beaching steady-state equations

Stage	Steady-state Equations	Reference
D_0E_{OP}	$[Kappa^*] = \frac{[Kappa]}{[Kappa_0]}$ $[Kappa^*] = \frac{1}{\left(\frac{[ClO_2] - \gamma.[C.O]}{2A'} + 1\right)^2}$ $\frac{k}{s} = a_1 * K^2 + a_2 * K + a_3$ $\frac{B}{100} = 1 + \frac{k}{s} - \sqrt{2 * \frac{k}{s} + \left(\frac{k}{s}\right)^2}$	[97–99]
D_1	$D_{1\ Brightness} = c_{01} - \frac{\beta_{11}}{x_1 + \frac{\beta_{11}}{c_{01} - B_E}}$ $\beta_{11} = 4.535 * Kappa_E + 0.44 * C.O._{TDS} - 7.434$	[100]
E_P	$E_{P\ Brightness} = 0.765 * D_{1\ Brightness} + 21.8$	[101]
D_2	$D_{2\ Brightness} = 92 - \frac{\beta_2}{x_2 + \frac{\beta_2}{92 - B_{EP}}}$ $\beta_2 = 0.25 * B_{EP} + 23.0$	[101]

D_0E_{OP}

Improved modified generalized steady-state equations for the D_0E_{OP} delignification stages were used to predict the kappa number for an amount of bleach (chlorine dioxide) consumed. Normalized kappa number ($Kappa^*$) was calculated from the values of D_0 stage chlorine dioxide charge and the value of A'. A' is the stoichiometric parameter that accounts for the extraction stage temperature (°C) and the percentage of peroxide used in the E_{OP} sage. The factor '$\gamma.[C.O]$' in the equation of $[Kappa^*]$ represents the chlorine dioxide consumption by the brown stock washer carry-over. The value of chloride consumption was considered 10% of the total chlorine dioxide

charge. The brightness of the pulp after the D_0E_{OP} stage was calculated using the Kubelka-Munk equation. The factor '$\frac{k}{s}$' required in the Kubelka-Munk equation was calculated using the extraction stage pulp kappa number and the values of a_1, a_2, and a_3. The values of coefficient a_1, a_2, and a_3 for softwood pulp were taken from [97].

D_1 stage

To calculate the D_1 stage pulp brightness, the asymptotic D_1 brightness limit, chlorine dioxide charge, post-extraction brightness, and washer carryover values were considered. The equation parameter 'β_{11}' is a function of extracted kappa number '$Kappa_E$' and the total dissolved solids carryover per ton of pulp from the extraction stage '$C.O._{TDS}$'.

E_P stage

The E_P stage pulp brightness was calculated using the D_1 stage pulp brightness.

D_2 stage

The equation used to calculate the D_2 stage brightness was similar to the equation used to calculate the D_1 stage brightness. However, the E_P extraction stage washer carryovers were not considered in the brightness equation of the D_2 stage.

3.2.2 Industrial data collection

First, to simulate a 5-stage blech section, the layout for the bleach section was taken from a softwood mill in the southern U.S (Mill A). The mill was operating with a typical Elemental Chlorine Free (ECF) bleaching sequence of five bleaching stages. The incoming kappa number for softwood pulp into the bleaching sequence was 30.0. The bleach plant's operational data including the temperature, consistency, the wash water flowrates, and various chemical charges were taken from the mill. The data for the simulation built up was a 3-month average data. The simulation model was validated with the data from Mill A and from another softwood mill in the southern

U.S (Mill B), The value of COD was taken from literature data. Both mills were operating with a 5-stage $D_0E_{OP}D_1E_PD_2$ ECF bleaching sequence.

3.3 Results and discussions

Simulated values of the important pulp properties are shown in Table 3.2 The major pulp properties considered were the E_{OP} stage pulp kappa number, E_{OP} stage pulp brightness, the E_{OP} stage COD, and the D_2 stage brightness.

3.3.1 Mill A data validation

For Mill A, the inlet kappa number was 30.0. The kappa number for the E_{OP} stage was 5.1 and the corresponding brightness was at 50.0% ISO. The E_{OP} stage kappa number calculated using simulation is 6.1. The difference between the calculated and the industry value of the E_{OP} stage kappa number was 5.5%. The brightness calculated for the E_{OP} stage is 49.5 % ISO as against the industry value of 50.0% ISO. The final brightness of the Mill A pulp after the bleaching section was 88.0% ISO and the value calculated using the simulation model is 89.6% ISO. The percentage difference between the important pulp properties of the pulp kappa number and the pulp brightness for Mill A was in the range of 1.0 % to 5.5%.

3.3.2 Mill B data validation

The entering pulp kappa number for Mill B was 25.0. The E_{OP} stage pulp kappa number was 4.9 and the calculated kappa number was 4.7. The corresponding calculated brightness for the E_{OP} was 52.7% ISO. The final pulp brightness was calculated at 89.6 % ISO and the industry value was 89.8% ISO. The difference in the pulp properties for the Mill B data was in the range of 0.2 to 4.0%.

Table 3.2 5-stage ECF bleaching section WinGEMS simulation model validation

Variable	Mill A Data*	Simulation Data	Difference (%)	Mill B Data**	Simulation Data	Difference (%)
Pulp inlet Kappa number (SW)	30.0	30.0		25.0	25.0	
E_{OP} Extraction Stage						
Kappa number	5.1	5.4	5.5	4.9	4.7	4.0
Brightness (%ISO)	50.0	49.5	1.0	-	52.7	-
COD (Kg/t)	53.0[#]	54.1	2.0	-	-	-
D_2 stage final Brightness (%ISO)	88.0	89.6	1.8	89.8	89.6	0.2

* Mill A (3-month average)
** Mill B (9-month average)
# Literature value

The Mill A and B were operating with different values of incoming kappa numbers. The chemical charge of chlorine dioxide in the D_0, D_1, and D_2 stages and the temperature, oxygen, peroxide, and sodium hydroxide charge in the extraction stages for both mills were also different. The simulation model prepared for the bleaching section is capable of predicting the pulp properties for different conditions of the incoming pulp and the process conditions in the bleaching section.

3.4 Conclusions and prospects

In this work, a generic WinGEMS simulation of a 5-stage ECF bleaching of softwood was prepared to predict the changes in kappa number, brightness, and the COD values with changes in the operating conditions and parametersIn this simultaion, steady-state delignification models were used in combination with pulp brightening models to predict the important pulp properties for a particular level of chemical charge and process conditions in the bleaching section.

The brown stock washed pulp kappa number, chemical charges, bleach tower washer water consumption, and other process conditions were inputs to the model. The outputs of the model are the pulp brightness, the kappa number of the E_{OP} stage, COD of the bleach section, and the final pulp brightness. These outputs were validated with the data from two different softwood mills. The difference between the industry data and the simulation results in terms of major pulp properties of the kappa number and the brightness were in the range of 0.2 to 5.5%. The industry data validation showed that the prepared bleach section model can be used on different softwood mills with different operating conditions and process parameters. Future work will focus on the experimental validation of the 5-stage bleaching model.

The steady-steady delignification and the brightening models were used in this study. Steady-state models help to simplify and understand the process and reduce the process complexities. However, the processes in the pulp and paper industry seldom reach a steady-state condition. Time-based changes in the reaction of pulp with chemicals need to be considered while modeling the bleaching section. Further, a high degree of interaction exists in various processes in the pulp and paper industry and these interactions need to be considered while working on the bleach section models.

The next chapter applies the prepared 5-stage bleach section WinGEMS simulation model and studies the reduction of freshwater in the bleaching section. We linked the Donnan equilibrium model with the prepared bleaching simulation using the dynamic data exchange feature in WinGEMS. We study the partition of calcium ions between the fiber walls and the surrounding liquor using the Donnan equilibrium model. Then, we evaluate the changes in the bleaching section concerning scaling as a result of paper machine white water recycling into the bleaching section.

Chapter 4. White-water recycling in ECF bleaching: prediction of scale buildup

4.1 Introduction

The pulp and paper industry (PPI), with water withdrawal of around 5% of the total, is one of the major consumers of water in the US manufacturing sector [4,5]. Considering the amount of water used in the PPI, several measures have been undertaken to reduce fresh water consumption. Further water reduction within the industry is becoming more challenging due to technical and economic factors. One of the limiting factors for process integration and water recycling is the buildup of Non-Process Elements (NPEs). The NPEs accumulate at various locations in the mill as the level of closure increases causing severe problems like corrosion, plugging, scaling, and deposition causing a problem in the mill operations [15,17]. This imposes a limit on the amount of water reused and recycled in the pulp and paper mills. Specifically for the bleaching section, the issue of scaling is encountered as many dissolved species and NPEs accumulate in the process loops [66].

Case studies, fundamental chemistry, and a detailed equilibrium analysis on calcium oxalate scaling have been discussed earlier for the digester and the bleach section [102–104]. Also, NPEs were modeled for a hardwood bleach section of MeadWestvaco Evadale mill with an ion-exchange equilibrium [92]. To model the NPEs, the study developed an ion-exchange equilibrium in an excel spreadsheet and linked the spreadsheet by dynamic data exchange to WinGEMS. The model developed was used to calculate the bound and free concentrations for H^+, Na^+, Mg^{2+}, Ca^{2+}, Mn^{2+}, and Ba^{2+} for the bleach section to evaluate the replacement of existing D_0 and Eop stage diffusion washers with presses. The model prepared predicts the calcium ions concentrations throughout the bleach section, however, the scaling tendency of the calcium was not studied. Recently, Jour et al., [54] studied elemental chlorine free (ECF) bleaching plant aiming to reduce the freshwater usage in the bleach section and reduce the effluent volume. A base case WinGEMS

simulation model was prepared and used to evaluate increased closure for a softwood kraft market pulp bleaching section. The research further studies the risk of calcium oxalate scaling in the D_0 stage. The paper concludes that the risk of scale deposition in the D_0 stage can be reduced by decreasing the pH and/or increasing the D_0 stage temperature. However, a complete bleaching section analysis concerning scaling was not conducted in the study.

In the present work, we aim at reducing the freshwater consumption in the shower water of a 5-stage elemental chlorine free (ECF) bleaching section. Firstly, we linked WinGEMS and Donnan equilibrium theory using the dynamic data exchange feature (DDE) in WinGEMS. We automated the macro-enabled excel file to calculate the Ca^{2+} ions distribution and the scaling parameter using visual basics coding. Secondly, after using the WinGEMS bleach section model earlier prepared, we analyze the Ca^{2+} ion distribution as a result of replacing the bleach shower freshwater with the paper machine white water. Then, we estimate the distribution of Ca^{2+} in the bleaching section using the Donnan equilibrium theory and predict the calcium oxalate and calcium carbonate scaling using the saturation index calculations. A sensitivity analysis of the saturation index (SI) by replacing the shower freshwater with white water was carried out. The sensitivity analysis also studies the changes in the value of SI with changing process parameters like the system pH, the temperature, the pulp consistency, and the calcium ion concentration in white water.

4.2 Methodology

A base case bleaching model for a 5-stage ECF bleaching ($D_0E_{OP}D_1EpD_2$) capturing the material, water, and NPEs was linked with the Donnan equilibrium model using the dynamic data exchange (DDE) feature. Data for the analytical measurements for the ions and the process conditions of the temperature, pH, and the fiber charge along the fiber line in the bleach section are taken from P.

Huber et al., [105]. Also, the values of metal ions entering the bleaching section through the brown stock-washed pulp are taken from the study. Stepwise replacement of the bleaching section freshwater was simulated and the partition of calcium ions was studied between the fiber walls and the surrounding liquor using the Donnan equilibrium model. The concentration of free Ca^{2+} ion in the surrounding liquor along with the concentrations of the oxalate ion and the carbonate ions are used to predict the calcium oxalate and the calcium carbonate scaling in the acidic and the extraction stages respectively.

4.2.1 WinGEMS simulation and the Donnan equilibrium model linking

This study was carried out using Valmet WinGEMS version 5.4. The 5-stage ECF bleaching section simulation earlier prepared was used to simulate the freshwater replacement by white water (WW) Figure 4.1. Figure 4.1 also shows the points of freshwater addition in the bleaching section to be replaced by the white water.

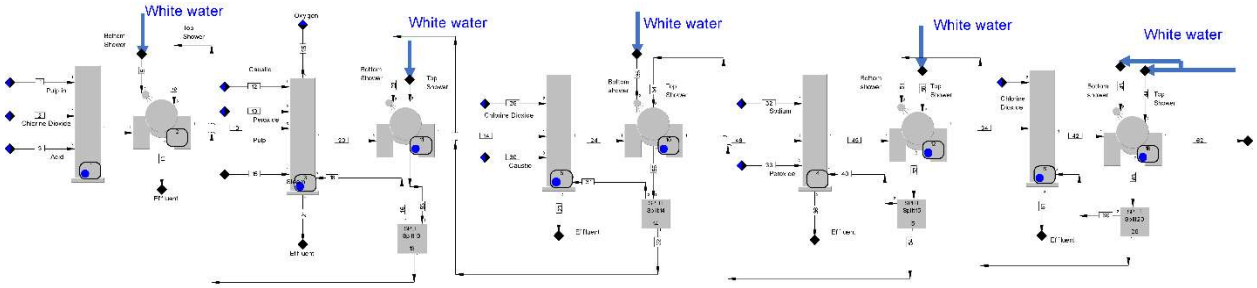

Figure 4.1 Proposed freshwater replacement by white water

DDE feature in WinGEMS which allows to import and export of data to an excel spreadsheet [106] is used to simulate the white-water addition in the bleaching stage of shower water. The freshwater in the bleach tower washers was replaced in steps from 0.0 to 100% and the changes in the concentrations of the Ca^{2+} ions in the effluents were ported via DDE to the excel file after each iteration. After simulating white water addition, the changes in the effluent, and the

pulp quality concerning the Ca^{2+} ions serve as an input to the Donna Equilibrium in the excel file. For every iteration, the free Ca^{2+} ions are calculated using the value of the distribution coefficient 'λ' and taking the inputs of the other metal ion concentration from the ECF bleaching section of the WinGEMS model. After calculating the free Ca^{2+} ions, the solubility product and the saturation index values in macro-enabled excel predict the calcium oxalate and calcium carbonate scaling in the bleaching section.

4.2.2 Donnan equilibrium model

The Donnan equilibrium model in Eq. 3 is used to calculate the value of the distribution coefficient [107].

$$\frac{2\,[M^{2+}](\lambda^3-1)}{V+F(\lambda^2-1)} + (\boldsymbol{\lambda}^2-1)[H^+]_S - \boldsymbol{\lambda}\frac{K_i\times\frac{C_i}{F}}{K_i+\boldsymbol{\lambda}\times[H^+]_S} = 0 \qquad (3)$$

where $\boldsymbol{\lambda}$ represents the distribution coefficient for different ion species, M^{2+} denotes the total divalent metal ion in mol per O.D. kg pulp, V is the total liquid volume in l per kg O.D. pulp and is the pulp consistency parameter, F is the water content in the fiber wall and the value is 1.4 l per kg O.D. pulp, C_i and K_i are the concentration in mmol per O.D. kg pulp and the dissociation constant for the carboxylic acid and $[H^+]_S$ is the solution pH. WinGEMS does not perform predictive pH calculations and to reach a particular pH value, the OH^- ion concentrations need to be manipulated. The manipulation needs to be done using a REACT or CHARGE block in WinGEMS. Instead of using these blocks for pH modulation, the value of pH was entered in the excel file manually.

After the calculation of the distribution coefficient, the free ion concentration for the Ca^{2+} ion is calculated using Eq. 4 [107].

$$[M^{2+}]_s = \frac{1}{V+F(\lambda^2-1)} \times M^{2+} \quad (4)$$

Where s is the solution phase and $[M^{2+}]_s$ is the concentration of the metal ion in the solution phase.

4.2.3 Scale formation

Scale formation is a localized chemical precipitation process described using the solubility product convention [104]. After calculating the value of free Ca^{2+} ions, the calcium oxalate and the calcium carbonate scale formation are studied. Salts, where both the anion and cation are divalent, are typically sparingly soluble or insoluble and cause scale to form. Typically, calcium oxalate scaling forms in the chlorine dioxide (acidic) stages, and the calcium carbonate scaling forms in the extraction (alkaline) stages [108].

4.2.3.1 Calcium oxalate

The free calcium ion $[Ca^{2+}]$ concentration calculated from Eq. 4 along with the oxalate ion concentration is used to calculate the solubility product for the calcium oxalate scaling. In previous studies the value of the solubility product is taken constant, however, the solubility product varies as the temperature changes. The effect of temperature on the oxalate ion dissociation and the solubility product is considered as per the study [109]. The solubility product (K_{sp}) value for calcium oxalate is calculated as per Eq. 5.

$$[Ca^{2+}]f_{Ca^{2+}} \times [C_2O_4^{-2}]f_{C_2O_4^{-2}} = K_{sp} \quad (5)$$

Where $f_{Ca^{2+}}$ is the value of the activity coefficient for calcium ions and $f_{C_2O_4^{-2}}$ is the activity coefficient for oxalate ions. The value of the activity coefficient is calculated using Eq. 6.

$$ln[f] = \frac{Az^2\sqrt{I}}{1+ba\sqrt{I}} \quad (6)$$

In Eq. 6, A and b are temperature-dependent constants, a is the hydrated size of the ion and is 6.0 for the Ca^{2+} ion and I is the ionic strength. The value of ionic strength is calculated as the average of the summation of the cation multiplied by the square of its charge and anion multiplied by the square of its charge.

Further, the formation of $C_2O_4^{-2}$ from the oxalate ion is governed by chemical reactions Eqs. 7 and 8, with temperature-based reaction rate constants pK_1 and pK_2 respectively [109]. The value of the oxalate ion concentration is taken from [105].

$$\frac{[HC_2O^-{}_4][H^+]}{[H_2C_2O_4]} = K_{a1} \tag{7}$$

$$\frac{[C_2O^-{}_4][H^+]}{[HC_2O_4-]} = K_{a2} \tag{8}$$

4.2.3.2 Calcium carbonate

The solubility product (K_{sp}) value for calcium carbonate is calculated as per Eq. 9 [110].

$$[Ca^{2+}][CO_3^{-2}] \times f^2_{(CaCO_3)} = K_{sp} \tag{9}$$

$f_{(CaCO_3)}$ is the mean activity coefficient to the solubility product. The value of the activity coefficient is calculated using Eq. 6. The CO_2 dissolution and ionization to CO_3^{-2} is modeled using the equations and the values of the reaction rate constant given in [111].

4.2.3.3 Saturation index

The saturation ratio of the ionic activity product to the actual solubility product at a particular temperature is calculated. To predict the scaling tendency, a base-ten logarithm of saturation level is taken and the obtained values of the saturation index (SI) help to predict the likelihood of scaling. If the system is supersaturated i.e SI value is greater than 1 then there is a tendency of scale to precipitate in the system. At equilibrium, when the value of SI is 0.0, the scale neither forms nor dissolves and the system is undersaturated at a SI value less than 0.0 [109].

4.3 Results and discussion

The WinGEMS and Donnan equilibrium model was used to predict the calcium oxalate scaling in the acidic stages i.e D_2, D_1, and D_0 stages, and calcium carbonate scaling in the extraction stages i.e Ep and E_{OP} as a result of paper machine white water recycling in the bleaching section.

Firstly, stepwise replacement of the D_2 stage bleach tower washer freshwater was simulated. Both the bottom and top shower in the D_2 stage washer use freshwater for pulp washing (Figure 4.1). Initially, the last bleaching stage was selected to replace the freshwater as it is expected to cause a minimum impact on the pulp properties like the kappa number and the pulp brightness. As the white water addition increases, the amount of Ca^{2+} ions in the effluent and the pulp increases. This increase in the Ca^{2+} ions is captured from WinGEMS and calcium carbonate scaling is calculated for the D_2 stage. To further reduce the freshwater consumption, freshwater from each bleaching stage washer was replaced step by step with white water. The changes in calcium ions for all the bleach stages were recorded and the corresponding saturation index was calculated.

4.3.1 Sensitivity analysis

After simulating the freshwater replacement by white water, a SI value sensitivity analysis was performed to predict the value of freshwater replaced without causing a scaling problem. The sensitivity of SI value with changes in the pulp consistency, the solution pH, and the system temperature is studied. The pulp consistency is varied from 1.0 to 15.0% as this range is the typical operating range of consistency for the washer vat to the exit of the washer drum. For different bleaching towers, the freshwater addition on the washer drum is at different locations (Figure 4.1). The consistency of the pulp is different for the water addition at the bottom and the top showers. The values of pH are varied as per the bleach stage pH conditions. The values of SI are evaluated by increasing the amount of freshwater replacement in the blech plant shower water from 0.0 to

100%. To account for the SI sensitivity to the paper machine section white water, the Ca^{2+} ions concentration in the white water is given a swing from 50.0 to 200.0 ppm. The value of 50.0-200.0 ppm is selected based on the white water quality of the paper machine section in the pulp and paper mills.

4.3.1.1 Calcium oxalate scaling

The D_2 stage calcium oxalate SI sensitivity analysis is shown in Figure 4.2. The X-axis shows the amount of freshwater replaced with white water, and the Y-axis represents the SI value. For each pulp consistency, four different trends are plotted to represent the different values of Ca^{2+} ions from 50.0 to 200.0 ppm. As the amount of freshwater replacement by the white water increases, the value of SI increases. This increase is seen across all the consistencies of pulp. For the pulp consistencies of 1.0% and 5.0%, the value of SI for 0.0% freshwater replacement is less than zero. However, for the pulp consistencies of 10.0% and above, the SI value at 0% freshwater replacement is more than 0 indicating the tendency to form scale.

As the value of pulp consistency increases, a decrease in the value of the distribution coefficient 'λ' is observed. As a result as the pulp consistency increases, the values of SI increase. All the SI values for 1.0% consistency are lower than zero indicating the 100.0% replacement of all bleach washer freshwater by white water is possible without the problem of scaling. However, the first instance of scaling is encountered for 5% pulp consistency at 200 ppm white water Ca^{2+} concentration at around 60% freshwater replacement in the D_2 stage washer. For 10.0% and 15.0% pulp consistency the values of SI are zero and above indicating scaling at all the values of white water recycled in all the washers of the bleaching section.

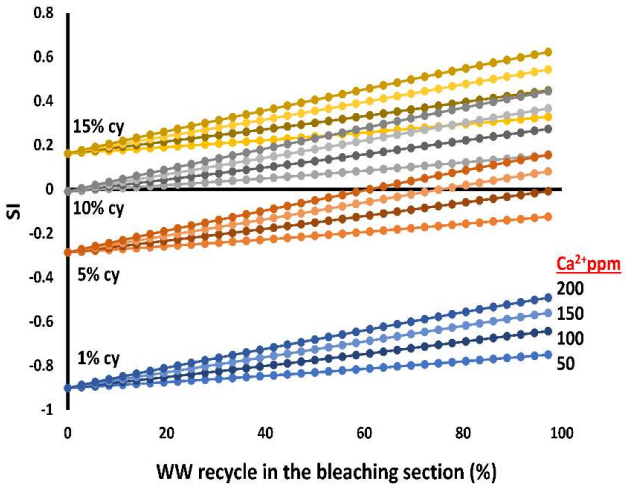

Figure 4.2 D_2 stage SI sensitivity analysis

Figure 4.3 shows the SI value sensitivity for the D_1 stage. For the D_1 stage also, the SI value is less than zero for 1.0% pulp consistency at all the values of freshwater replacement in the bleach section. However, for the 5.0% pulp consistency, the scaling occurs at around 25.0% of white water recycle for the white water Ca^{2+} ion concentration at 200 ppm. At 50 ppm Ca^{2+} ions the freshwater can be completely replaced with white water at 5.0% pulp consistency. For 10.0% and higher pulp consistencies, the values of SI are more than zero for all the amount of freshwater replacement in the bleaching section. The values of SI for the 10.0% and 15.0% pulp consistencies indicate that the freshwater should not be replaced in the washers at the points of medium consistencies.

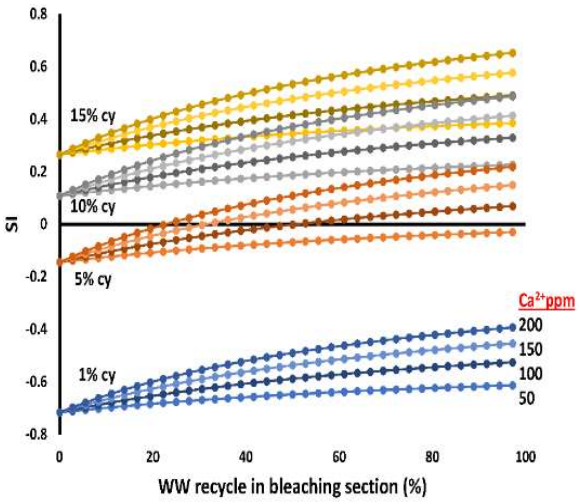

Figure 4.3 D_1 stage SI sensitivity analysis

The SI value sensitivity for the D_0 stage is evaluated (Figure 4.4). For the D_0 stage, the value of SI is less than zero for all the pulp consistencies, all the Ca^{2+} ion concentrations, and all the values of freshwater replacement in the bleach section. The pH value for the D_0 stage is 2.4. At this pH, the divalent oxalate ($C_2O_4^{-2}$) ion is minimal in the system [108]. Although the Ca^{2+} ions are present, the trace amount of $C_2O_4^{-2}$ ions inhibit the calcium oxalate scale formation. As a result

of this, even for 100.0% replacement of freshwater in the bleaching section, the scale formation is not encountered in the D_0 bleaching stage.

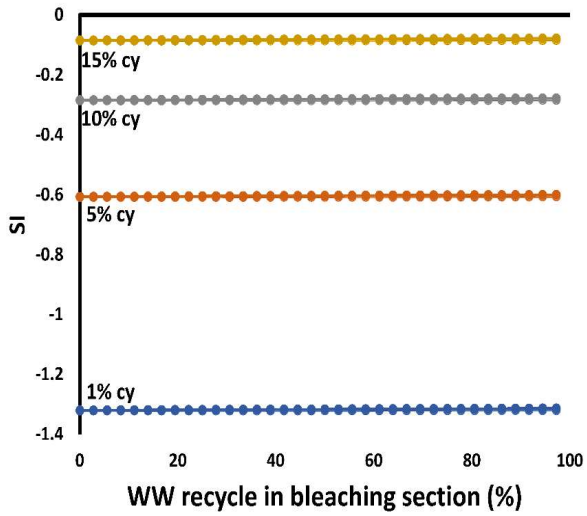

Figure 4.4 D_0 stage SI sensitivity analysis

4.3.1.2 Calcium carbonate scaling

The Ep and E_{OP} stage calcium carbonate SI sensitivity analysis is evaluated in Figures 4.5 respectively. The increase in SI value is across all the pulp consistencies and all the Ca^{2+} ion concentrations in the white water. The values of SI for the Ep and the E_{OP} stages are evaluated at a pH value of 9.0. In the case of alkaline pH, the amount of free Ca^{2+} available is significantly reduced due to the formation of several soluble complexes [66], and the majority of calcite formed in the alkaline stages is carried over by the fibers, and only a small fraction of the calcite is deposited on the equipment [112].

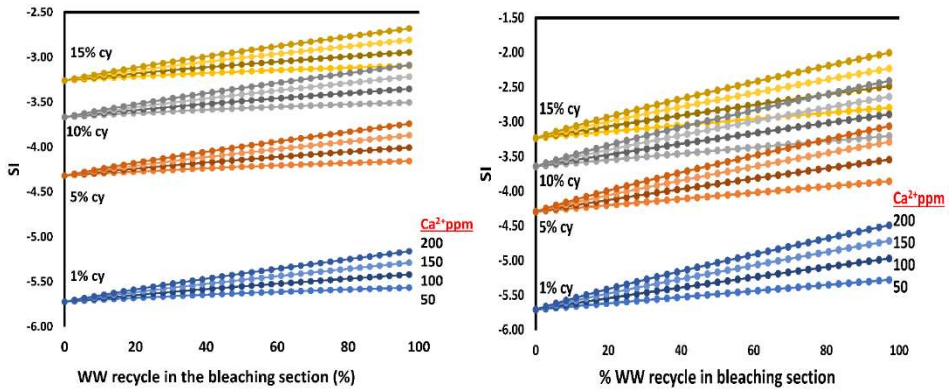

Figure 4.5 Ep and E_{OP} stage SI sensitivity analysis

4.3.1.3 Effect of pH on the SI value

A sudden increase in pH value would occur at the point of addition of alkaline white water to the bleach tower washer drum. To evaluate the sensitivity of SI with pH for the D_0 stage, the pH value was given a swing from 2.5 to 6.0. As seen in Figure 4.6, the value of SI is highly sensitive to a change in system pH and transitions from negative to positive value as the pH increases from 2.5 to 3.0 and reaches a peak value at a pH of around 4.5. This is also following the fact that the critical pH between the hydrogen oxalate ($HC_2O^-{}_4$) and oxalate ($C_2O^{2-}{}_4$) is around 4.0 [112]. After that, the SI value drops and transitions from a positive to a negative value as the pH increases from 4.5 to 6.0. The distribution of SI value is because of the transition in the concentrations of free Ca^{2+} and the oxalate ions. At the pH value of around 4.0, the second proton from the monovalent anion ($HC_2O^-{}_4$) dissociats to form divalent anion ($C_2O^{2-}{}_4$). The formation of divalent oxalate ion and corresponding free Ca^{2+} ion leads to a peak in the value of SI. As the pH goes above 4.5, the free available Ca^{2+} ions decrease, leading to a reduction in the value of SI. Figure 4.6 also provides the value of pH which the system can be operated to reduce the scaling tendency. pH value of 2.5 to reduce or eliminate the calcium oxalate scaling in the first chlorine dioxide stage was also proposed earlier [104].

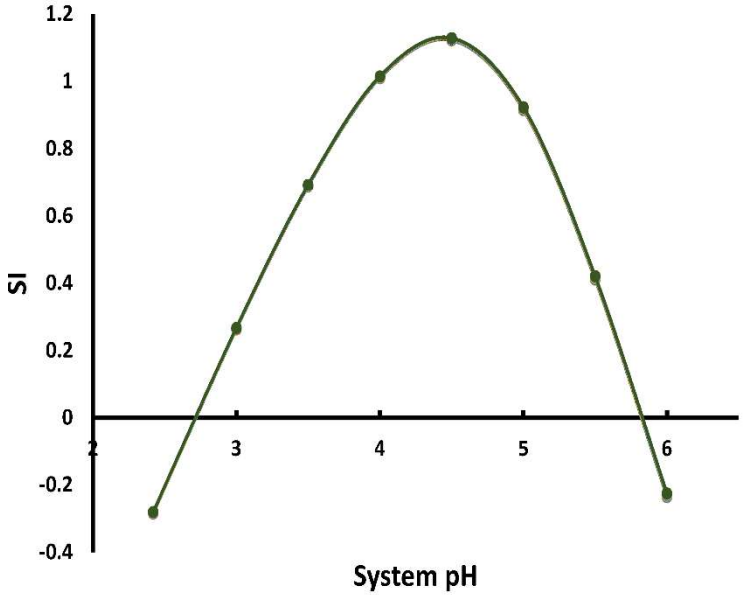

Figure 4.6 Effect of pH on the SI values for the D_0 stage

4.3.1.4 D_2 and D_1 chlorine dioxide stage

To evaluate the sensitivity of SI with pH for the D_2 and D_1 stages, the pH value was changed from 4.2 to 6.0 for the D_2 stage and 4.5 to 6.0 for the D_1 stage (Figure 4.7). The range of pH is selected as the addition of alkaline white water is supposed to increase the system pH. As a result, lower values of pH are not considered. As seen in Figure 4.7, the value of SI reduces as the value of pH increases from 4.2 to 6.0 for the D_2 and the D_1 stages respectively.

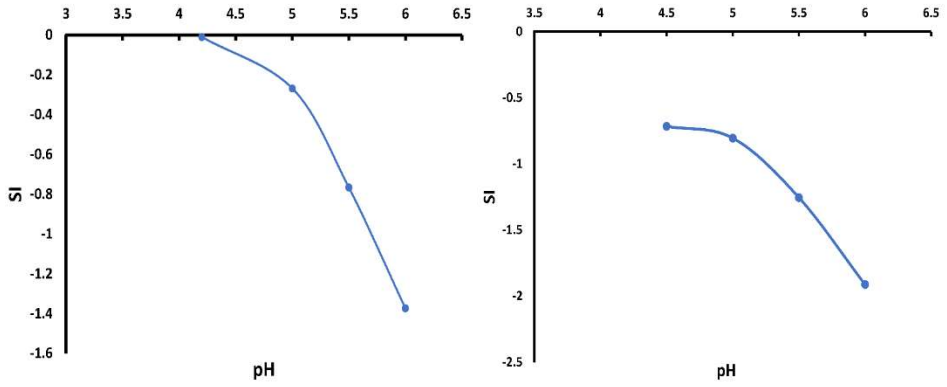

Figure 4.7 Effect of pH on the SI value for D_2 stage and Effect of pH on the SI value for D_1 stage

As the solution pH increases, the amount of Ca^{2+} ions on the fiber surface increases and peaks out. Correspondingly, the free Ca^{2+} ions in the solution decrease. The decreased Ca^{2+} ions with an increase in the pH lead to a reduction in the solubility product and the corresponding saturation index. At lower pH values, the Donnan Equilibrium condition does not exist as the acid groups on the fiber surface are not dissociated. With increasing pH, there is disproportionation in the mobile ions between the fiber wall and the surrounding solution due to the increased concentration of dissociated acid groups within the fiber wall. The value of dissociation constant peaks out at around neutral pH where the acid roups are fully dissociated [107]. For the very same reason of free Ca^{2+} ions reaching the minimal value at neutral pH, the pH sensitivity of the Ep and E_{OP} extraction stages is not considered due to the higher operating system pH. Also, oxalate with a pKa value near 4.0 is a much stronger acid than carbonate, and the solubility of carbonate increases when there is a sudden change in the process condition of pH in the acidic stages of ECF bleaching. At pH less than 3.0, anionic groups on the fiber surface are protonated, and for pH greater than 5.0 most of the dissociated groups are anionic. As a result, the fibers only absorb Ca^{2+} ions at mildly acidic to alkaline pH and are washed away and are present in the system as free Ca^{2+}

ions at acidic pH. Most of the Ca^{2+} ions are carried by the fibers themselves and are released under acidic conditions [66].

4.3.1.5 Effect of temperature on the SI values of D_0 stage

The value of SI is also sensitive to the changes in the system temperatures. At the point of addition of the white water to the washer, there would also be a change in the system temperature. As the D_0 stage operates at the lower values of pH, to evaluate the sensitivity of SI values to temperature, we performed a temperature sensitivity analysis of the SI values (Figure 4.8). The value of temperature varied from 40.0°C to 80.0°C so that the temperature in the study is at around the midpoint value. The system pH vas also varied from 2.0 to 6.0 and the changes in the values of D_0 stage SI was recorded. The values of SI follow the same trend for different temperatures. The SI value transitions from negative to positive, peaks, and then transitions from positive to negative value as seen in Figure 4.8. As the temperature increases, the SI profile shifts to the right. At 40.0°C, the value of SI is zero for a pH value of around 2.3 and at 80°C, the SI value has a zero value at around 3.0 pH. The temperature primarily affects the dissociation of the oxalate ion. The dissociation of oxalate ion is temperature driven and the amount of divalent oxalate ion dissociation also shifts toward the right with increasing temperature [109]. Also, the value of peak SI reduces as the temperature increases, and the peaks are observed at higher pH values for higher temperatures.

At higher pH values, the free Ca^{2+} ions reach a minimum value, and the effect of temperature is not predominant.

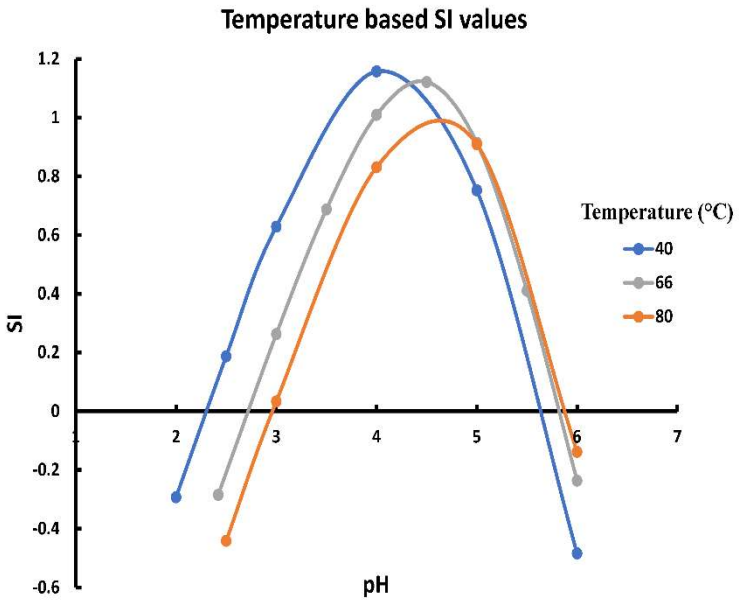

Figure 4.8 Temperature effect on the SI values

4.4 Conclusions

In this study, an ECF bleaching WinGEMS simulation was linked to the Donnan Equilibrium model to simulate the addition of whitewater into the bleach section shower water. The recycling of white water into the bleach tower washer shower was achieved by stepwise reducing the freshwater addition in the bleach tower shower. The linked model helped to access the impact of whitewater recycling on the calcium ion distribution in the solution and on the fiber surface. The saturation index was calculated by importing the changes in Ca^{2+} ions which acted as an input to the Donnan equilibrium model.

The sensitivity analysis helped to understand the changes in the SI value with changes in the amount of freshwater replacement, the point of addition of white water i.e the pulp consistencies, the system pH, temperature, and the concentration of Ca^{2+} ions in the white water. The sensitivity analysis revealed that for all the parameters, the value of SI increases for both the calcium oxalate and the calcium carbonate scaling as the amount of white water addition in the

bleach section increases. The first instance of calcium oxalate scaling in the bleaching section was encountered for the D_1 stage at around 25.0% freshwater replacement with 200.0 ppm Ca^{2+} content in the white water for 5.0% pulp consistency. Calcium carbonate scaling was not predicted in the Ep and E_{OP} stages as these stages operate at alkaline pH values.

This analysis is done considering a particular ECF bleaching sequence modeled in WinGEMS software. Each stage of the bleaching sequence used to study the scale buildup has a purge stream that prevents the buildup of NPEs, Ca^{2+} in this study, in the system. To apply the system to another study, the bleaching sequence needs to be modified to account for the differences. Also in the Donna equilibrium model, the entire free calcium calculated is considered for scale modeling, however, some of the calcium present in the solution would be complexed to the organic material present in the effluent and would not contribute towards scaling. As a result the presence and nature of the organic matter in the effluent stream also need to be considered while modeling the scaling in the bleaching section.

Chapter 5. Techno-Economic Analysis of CO_2 Capture from Pulp and Paper Mill Lime Kiln

5.1 Introduction

Of all the greenhouse gases (GHGs), carbon dioxide (CO_2) is the primary GHG emitted through human activities. In the U.S., industrial processes accounted for 16.0% of the CO_2 emissions, and the pulp and paper industry accounted for 1.2% (30 MMT/y) of these industrial emissions in 2019 (EPA, 2020). The primary sources of CO_2 emissions in pulp and paper manufacturing are from the recovery boiler, bark boiler, and Lime Kiln (Onarheim et al., 2017b). The economic feasibility of CO_2 capture from the pulp and paper sector has not been studied extensively as the CO_2 emissions are primarily of biomass origin. Because all the existing regulations and policy instruments consider only fossil-fuel CO_2, there are limited incentives for CO_2 capture (Jönsson, Kjärstad and Odenberger, 2014). While the MonoethanolAmine (MEA) solvent-based absorption desorption process for CO_2 capture has been widely studied for oil, gas, iron and steel, cement, and chemicals production (Leeson et al., 2017), it is neither fully explored nor a mature technology for the pulp and paper industry. Also, there is a wide range of capture costs in the literature for this process (e.g., (Hektor and Berntsson, 2007), (Onarheim et al., 2017a), (Garðarsdóttir et al., 2018), (Nwaoha and Tontiwachwuthikul, 2019), (Yang, Meerman and Faaij, 2021)) making it difficult to assess its potential for the pulp and paper industry.

To the best of our knowledge, four studies provide estimates for CO_2 capture costs from pulp and paper industry emissions. Onarheim et al. (2017b) studied CO_2 capture and storage from various sources of a hypothetical Kraft pulp mill and a pulp and board mill. The capture process was MEA-based absorption desorption. The result showed that it is technically feasible to retrofit post-combustion CO_2 capture to an existing pulp mill or pulp and board mill. Another study

(Onarheim et al., 2017a) performed the techno-economic analysis of retrofitting post-combustion amine scrubbing to a pulp mill and an integrated pulp mill. The economic evaluations included estimating capital expences, total installed cost, total plant cost, and the discounted cash flow calculations. They utilized in-house cost databases of ÅF- consult Oy and Techincal Center of Finland (VTT) and quotes from vendors if required for the CO_2 capture plant. Also, a higher exponent value (0.7) for the "rule of six-tenths" was selected when estimating equipment costs. For 90% CO_2 capture from the Lime Kiln flue gas, the capture cost was calculated as $91 per tonne CO_2, which is the only cost estimate for CO_2 capture from pulp and paper mill Lime Kiln available in the literature. We will refer to this study (Onarheim et al., 2017a) as the reference study in this paper. Gardarsdottir et al. (2014) evaluated the technical performance of post-combustion CO_2 capture integrated with three different industries, including a kraft pulp mill recovery boiler. The study concludes that a pulp mill can become a negative net contributor to global CO_2 emissions. However, the study didn't provide any techno-economic evaluations for the CO_2 capture process.

Recently, Gardarsdottir et al. (2018) carried out an economic evaluation of 90% CO_2 capture from the recovery boiler flue gas. The study calculated the equipment costs using Aspen In-Plant Cost Estimator and assumed a generic cost level for all the sources. The estimated cost was $61.8 per tonne of CO_2. Nwaoha et al. (2019) also evaluated the cost of CO_2 capture from the recovery boiler flue gas. The paper considered two different solvents, MEA and 2-amino-2-methly-1-propanol and MEA blend, and three process configurations for each solvent. The equipment costs were calculated using reference guesstimate/ballpark estimates from the literature and scaling up to the equipment sizes suggested by the process simulation. The CO_2 capture costs varied from $129.0 to $147.2 per tonne of CO_2.

In this study, we perform a techno-economic analysis for CO_2 capture using the MEA-based absorption desorption process for pulp and paper mill Lime Kiln and compare the capture cost to the only available CO_2 capture cost estimate in literature (Onarheim *et al.*, 2017a). The CO_2 capture from the Lime Kiln section of a pulp and paper mill considers the system in addition to the existing pulp and paper mill. For the comparison, the same Lime Kiln flue gas specifications (Onarheim *et al.*, 2017b) are utilized in the analysis. Detailed process and techno-economical analysis for these two studies are provided in the report sponsored by the International Energy Agency Greenhouse gas R&D Programme (IEAGHG) and prepared by ÅF- consult Oy and Techincal Center of Finland (VTT) (IEAGHG, 2016). A variant of split-flow configuration was modeled using Aspen Rate-Based Distillation to reduce the reboiler heat duty. Further, the CO_2 capture plant is equipped with an amine reclaimer recovering the solvent lost to heat stable salts. Unlike the report, a conventional 30 Wt.% MEA CO_2 absorption desorption process is simulated in our study using Rate-Based Distillation in Aspen Plus to reduce convergence issues in Aspen Plus. The equipment costs are calculated using CAPCOST (Turton *et al.*, 2018). The present study applies, for the first time, the CAPCOST factor-based modular program for technoeconomic analysis of a solvent-based CO_2 capture process using MEA as the solvent for pulp and paper mill Lime Kiln. CAPCOST uses custom equations to perform the equipment cost calculations which provides transparency and editability while dealing with various equipment, different process configurations, and flowsheet optimization. Further, a sensitivity analysis was carried out to understand the impact on capture cost of varying flue gas CO_2 compositions and the changes in the MEA solvent, electricity, and steam costs.

5.2 Process simulation and economic analysis

5.2.1 Kraft pulp and paper mill

The Kraft pulping process is explained in detail in Chapter 2 with the help of Figure 2.1. The weak black liquor, after washing, is concentrated and burned in the recovery boiler for chemical and energy recovery. The recovery boiler smelt is dissolved in water to form green liquor and causticized with the reburned Lime (CaO) to form white liquor used in the cooking process, completing the cycle (Gary A.Smook, 2015). CO_2 emissions from the bark boiler and recovery boiler are considered biogenic as the CO_2 is released from burning wood derived fuels. In the Lime Kiln (Figure5.1), CO_2 is released during the calcination of Limestone (Onarheim *et al.*, 2017b).

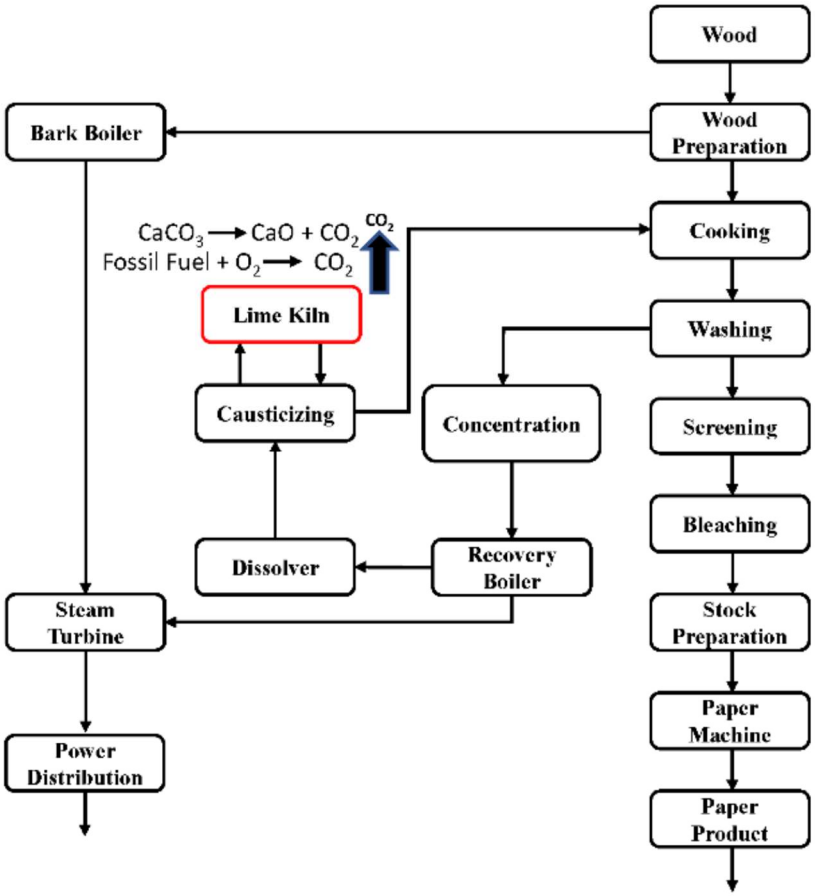

Figure 5.1 Overview of a Kraft pulp and paper mill

5.2.2 Aspen Plus simulation of the MEA-based absorption process for CO_2 capture from Lime Kiln

Aspen Plus simulation model was constructed utilizing the main design parameters listed in the reference study to simulate the CO_2 capture process from the same Lime Kiln flue gas. The economic analysis was carried out using the equations and data in CAPCOST. Table 5.1 summarizes the assumptions for calculating the capture costs and the utility and raw material costs used in the calculations. The MEA cost is taken from Kohl and Nielsen (1997) and inflated using the producer price index for the year 2016.

Table 5.1 Economic analysis assumptions, utility costs, and raw material prices

Parameter	Value	units
Operation hours	8400.0	Hours (h)
Plant operation	20.0	Years (m)
Interest rate	20.0	% (i)
Maintenance & repair costs	6.0	% of $C_{Capital}$
Insurance & taxes	2.0	% of $C_{Capital}$
Makeup-water	0.12	$/tonne
Operators	13.0	-
Supervisory level costs	18.0	% of C_{Labor}*
Start-up & MEA costs	10.0	% of $C_{Capital}$
General & Administrative costs	18.0 % C_{Labor} + 0.9 % $C_{Capital}$	
Plant overhead	70.8 % C_{Labor} + 3.6 % $C_{Capital}$	
Contingency	15.0	% C_{BM}**
Contractor Fee	3.0	% C_{BM}
Auxiliary facility cost	50.0	% C_{BM}
Steam (5 barg)	9.4	$/tonne
Cooling water	0.0157	$/tonne
Electricity	0.0674	$/kWh
Make-up MEA	2,100.0	$/tonne

* Labor cost
**Bare module costs

Figure 5.2 shows the Aspen Plus flowsheet developed for the solvent-based CO_2 capture process, excluding the CO_2 compression train (Figure 5.3) in the reference study. The absorption cycle is a temperature-dependent acid-base reaction where the flue gas CO_2 (weak acid) reacts with a solvent (a weak base) (1). The "CO2 loaded" solution (rich MEA) is stripped off of its CO_2 by reverse reaction (Eq. 10), regenerating the lean solvent and a gaseous CO_2 product (Bhown and Freeman, 2011). The absorption-desorption reactions for primary amines like MEA can be represented in Eq.10 (Kohl and Nielsen, 1997).

$$RNH_2 + CO_2 \leftrightarrow RNHCOO^- + H^+ \qquad (10)$$

The flue gas from the Lime Kiln stack is cooled and quenched in the direct contact cooler (DCC). The cooled flue-gas enters the absorber column from the bottom, and the lean MEA regenerated from the stripper column enters from the top. Solvent MEA, after absorbing CO_2 from the flue gas, is pumped and heated in a rich/lean heat exchanger with the stripper column bottoms (lean MEA) before being sent to the stripper column. The CO_2 and some water vapor are recovered as the top product of the stripper column, the CO2OUT stream in Figure 5.2. The lean MEA, recovered as the stripper bottoms, passes through the rich/lean heat exchanger and is mixed with makeup water and amine. The lean MEA is further cooled with cooling water before being sent back to the absorber. The flue gas specifications are given in Table 5.2. We used the specifications given in the reference study for comparison.

Table 5.2 Lime Kiln flue gas data

Parameter	Units	Value
Temperature	°C	250.0
Mass flow	MTPY	684 000.0
CO_2	mol %	20.4
N_2	mol %	47.4
O_2	mol %	1.2
H_2O	mol%	30.9
SO_x	ppm	50.0
NO_x	ppm	175.0
TRS	ppm	15.0
Particulates	ppm	30.0

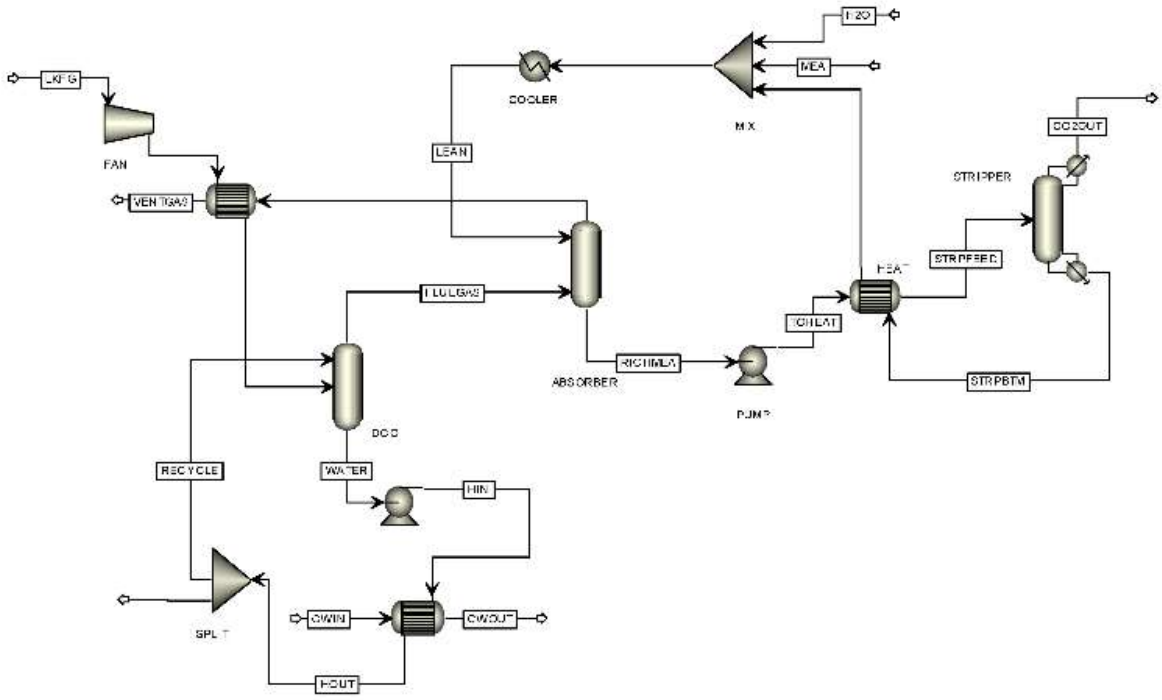

Figure 5.2 Aspen Plus model of CO_2 capture

Aspen Plus version, the property package, the model, and the built-in units used for the columns and other equipment are summarized in Table 5.3. The KEMEA package contains kinetics and rate constants, which allows modeling the MEA system more accurately with an electrolyte-NRTL model. RadFrac unit operation is used to model the absorber and stripper

columns. The absorber does not have a condenser or a reboiler. The stripper has a condenser at the top and a reboiler at the bottom. Both absorber and stripper columns employ the rate-based model. Pressure drops in the piping and equipment are neglected. The stripper column operates at 1.8 bar(a) to prevent potential solvent degradation due to high pressure and higher stripper bottom temperatures [113].

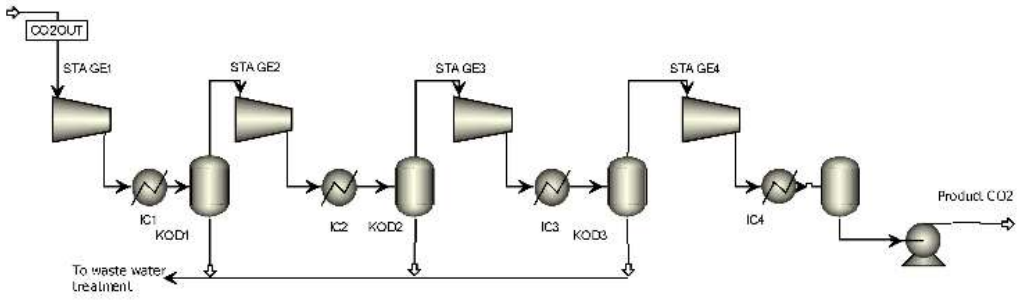

Figure 5.3 CO_2 compression train

To replicate the process conditions for the temperature and pressure from the reference work, a four-stage compressor train is used to compress the product CO_2 to 110.0 bar at 33.0°C. The Aspen Plus flowsheet for the compressor train is presented in Figure 5.3. The property packages and the unit operations used in Aspen Plus simulation are given in Table 5.3.

Table 5.3 Property package and the equipment model used

Parameter	Package/units
Aspen Plus	V10.0
Property Package	KEMEA (Kent-Eisenberg)
Absorber Column	RadFrac (Rate-based model)
Stripper Column	RadFrac (Rate-based model)
Lean/rich heat exchanger	HeatX
MEA cooler	HeatX
Compressor	Compr
Intercoolers	Heater

5.2.3 Economic analysis of the MEA-based absorption process

The CO_2 capture costs include capital and operating costs. CAPCOST is used to evaluate the capital costs for the columns (DCC, absorber, and stripper), heat exchangers (condenser, reboiler, rich/lean heat exchanger, intercoolers, and the solvent cooler), compressors/fan, and drivers for compressors and pumps. The costs are adjusted for inflation using the 2016 Chemical Engineering Plant Cost Index (CEPCI) value of 542.0 [114]. The total annualized cost (TAC) of the process, including the compression train, is shown in Eq. 11,

$$TAC\ \left(\frac{\$}{y}\right) = AF\ \times\ C_{Capital} + C_{Operating} \qquad (11)$$

where, $C_{Capital}$ and $C_{Operating}$ are capital and operating costs, and AF is the annualization factor.

The equipment installation costs for estimating the capital cost are calculated using the equipment bare module costs from CAPCOST. The absorber and stripper columns are modeled as packed columns. The column diameters are taken from the converged Aspen plus file and the packed height per stage (HETP) in meters is calculated using Eq. 12 [115]:

$$HETP\ = \frac{100}{a_p} + 0.1 \qquad (12)$$

where, a_p is the surface area per volume of the packing. The capital cost includes the bare module costs, contingency, contractor fee, plant start-up costs, and auxiliary facilities costs. The operating costs comprise the labor costs, the process utility, and the raw materials costs.

The annualization factor, AF, is calculated in Eq. 13,

$$AF = \frac{i(1+i)^m}{(1+i)^m - 1} \qquad (13)$$

where, i is the interest rate, and m is the plant operation year.

The total CO_2 capture cost is calculated by using Eq. 14:

$$CO_2\ capture\ costs\ \left(\frac{\$/yr}{t-CO_2/yr}\right) = \frac{TAC}{Captured\ CO_2} \quad (14)$$

The degradation of amine by the presence of SO_x in the flue gas is accounted for by considering MEA degradation losses due to SO_x in the economic evaluation. Separate treatment for the NO_x removal was not considered as NO_x present in the flue gas is regarded as inert. The amount of NO_2 is below the recommended limit, and a separate NO_2 removal setup is not required [116].

5.3 Overview of the reference study economic analysis

5.3.1 CO_2 capture setup of the reference study

A 30.0% MEA based CO_2 capture process was simulated in Aspen Plus using the Aspen Rate-Based Distillation model for processing the flue gas given in Table 5.2. A solvent split-flow configuration was used to reduce the stripper column reboiler duty. The overall CO_2 capture rate was set at 90.0%.

5.3.2 Economic analysis of the reference study

Economic analysis results were reported in terms of Earning Before Interest, Taxes, Depreciation, and Amortization (EBITDA). For the mill and the CO_2 capture plant, the cost calculations included the capital investments (CAPEX) and the operating costs (OPEX). Equipment costs were estimated using in-house cost databases of ÅF consult Oy and VTT, and quotes from vendors when necessary. When the capacity of the equipment was different from the quoted capacity, a scaling factor of 0.6 was applied to estimate the equipment cost using Eq. 15. In Eq. 15, the exponent n was assumed to be 0.7 for the CO_2 capture plant.

$$\frac{C}{C_0} = \left(\frac{S}{S_0}\right)^n \quad (15)$$

In Eq. 15, C is the scaled capital cost, C_0 is the actual purchased cost, S is the target capacity, and S_0 is the design capacity. IEAGHG economic assessment model developed in-house was applied to calculate the CO_2 avoided costs using a discounted cash flow (DCF) analysis. For CO_2 capture from the Lime Kiln section, the amount of CO_2 avoided is equal to the amount of CO_2 captured. Based on the DCF calculations, the cost of CO_2 capture from the Lime Kiln section was \$91.0 per tonne CO_2, which, at a CO_2 capture rate of 0.2 ton CO_2 per air dried tonne pulp (adt_{pulp}) produced translates to \$22.0 per adt_{pulp}. The cost estimates were developed in EUR (Quarter 2 of 2015). An exchange rate of 1.0 EUR = 1.1 USD was used for currency conversion.

5.4 Results and discussions

5.4.1 CO_2 capture costs evaluation and comparison with the reference study

The base case CO_2 capture cost for the process simulated using design and operation values from the reference study, the theoretical mill Lime Kiln, is given in Table 5.4. The costs are rounded off to the nearest 1000. For the operating capacity of the mill and the CO_2 capture rate of 23.3 t/h, the amount of CO_2 capture is 0.2 ton CO_2 per adt_{pulp}, translating the capture cost of \$76.0 per tonne CO_2 to \$18.0 per adt_{pulp}.

Table 5.4 Summary of CO_2 capture costs for the base case

Parameter	Value
Total capital cost [$]	19,606,000.0
Total annualized capital cost [$/y]	4,019,000.0
Total operating cost [$/y]	6,105,000.0
Total raw material cost [$/y]	461,000.0
Total utilities cost [$/y]	5,380,000.0
CO_2 capture [t/y]	196,000.0
CO_2 capture cost [$ per tonne CO_2]	76.0
CO_2 capture cost [$ per tonne pulp produced]	18.0

For the economic analysis of this study, the equipment costs given in Table 5.5 are calculated using the equations given in CAPCOST. These equations require the equipment sizes, which are directly obtained from the Aspen Plus simulation. Various factors contributing to the estimation of equipment grassroot costs (C_{GR}) are given in Figure 5.4. Figure 5.4 also includes the calculations for estimating the bare module cost (C_{BM}), which is defined as the direct and indirect expenses incurred for equipment purchase and installation. Adding contingency and contractor fees to C_{BM} gives the total module cost (C_{TM}). Finally, including the auxiliary facilities costs in the C_{TM} provides the C_{GR} for each piece of equipment.

Table 5.5 Equipment-wise breakdown of the capital costs

CO_2 capture plant section	Reference study ($ million)	This study ($ million)
Direct Contact Cooler	0.7	2.4
Amine absorber section	5.3	3.1
Amine circulation system	0.5	0.9
Stripper section	11.6	2.3
Compression & dehydration	1.4	7.1
Auxiliary facility costs	0.2	2.5
Start-up costs	3.8	1.3
CAPEX	23.5	19.6

The total capital cost is annualized for the plant operation time and includes the columns, exchangers, pumps, dehydration and compression, auxiliaries, and the start-up costs. The contributions of individual equipment to the total capital cost are shown in Table 5.5, which also lists the values from the reference study [116] for comparison.

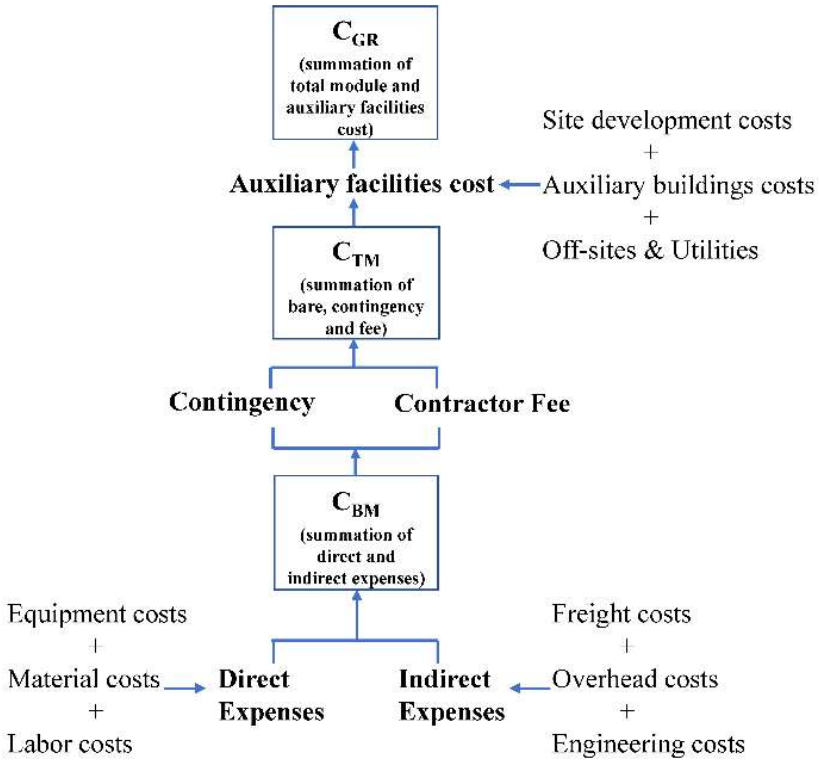

Figure 5.4 Factors considered in CAPCOST for estimating equipment costs

Table 5.5 reveals the differences in equipment costs. For the reference study, the total installed cost, including the project contingency, forms the total plant cost of the CO_2 capture plant. The total installation cost of the CO_2 capture plant includes the installation costs for each piece of equipment individually. The equipment costs for the reference study were adjusted using the 2015 CEPCI value, which is ca. 3.0% higher than the CEPCI value of 542.0 considered in this techno-economic analysis. The reference study separately calculated the costs incurred in Engineering, Procurement, and Construction (EPC) and construction for the entire CO_2 capture plant. Further, in the reference study, a project contingency of 10.0% was added to the total plant installation costs. The estimated value of total installation costs (TIC) with the required mill modification, and other CAPEX of spare parts, start-up costs, owner's cost interest, and working capital forms the total capital requirement (TCR). The CO_2 capture costs were estimated within a ± 50.0% accuracy,

assuming that the implementation of CO_2 capture technologies in the pulp and paper industry is not a mature technology. A 30.0% increase in the capital costs for the columns and the solvent circulation was applied to account for the solvent split-flow configuration in the reference study [117].

As the equipment costs calculated using CAPCOST rely on the sizes estimated by Aspen Plus, the contribution of equipment costs to capital costs for different sections are different from those reported in the reference study (Table 5.6). The EPC and constructions costs have been included in the factors considered while calculating the C_{GR}. On the contrary, in the reference study, the construction and the EPC costs have been calculated separately for the entire facility, and the total plant installation cost was the summation of the equipment, the construction, and the EPC costs. Further, the setup used for the CO_2 capture (a split-flow configuration) in the reference study [21] is different from that used in this study. A reclaimer for the degraded MEA is used in stripper column setup; however, a conventional absorption setup is used to simulate the process in this study. A disadvantage of the split flow configuration is the requirement of a higher solvent circulation flowrate to achieve a similar CO_2 recovery compared to the conventional configuration. Corrosion is another issue related to the use of split-flow configuration due to the higher percentage of the MEA components in the solvent. Also, the capital investment for the split flow configuration is higher due to the requirement of a larger absorber column, additional heat exchangers, pumps, and the associated pipings [116]. The cost of the amine absorber section in the reference study is around 70.0% higher than the costs of the absorber section in this study (Table 5.5).

The second term in Eq. 11 is the operating costs, including fixed and variable costs. These costs for the reference study and the present work are provided in Table 5.6. The total operating costs are similar (Table 5.6). However, unlike the reference study [77], we did not consider the

costs incurred for CO_2 transportation and storage in operating costs. The reference study [77] considered the fixed costs, variable costs, income from electricity sold to the grid, and the CO_2 storage and transportation costs for calculating operating costs. The fixed costs consisted of direct-indirect labor, insurance, local taxes, and maintenance. Chemical and utility costs, and waste processing and disposal charges were included in the variable costs. Also, for the base case and the case with Lime Kiln CO_2 capture in the reference study, the biomass feedstock costs are the same nullifying the impact of changes in the input biomass costs while calculating the Levelized cost of pulp.

Table 5.6 Operating cost details ($ million/y)

Operating costs	Subsection	Reference study ($ million/y)	This study ($ million/y)
Fixed costs	Operating labor Direct supervisory Plant overhead Insurances and taxes Maintenance	3.9	2.3
Variable costs	Utilities Chemicals	3.6	5.2

The breakdown of the capture costs for the reference study and this work is shown in Figure 5.5 in terms of million $/y. A cost difference is observed for the CAPEX and the fixed cost portion of the OPEX. The direct labor cost in the reference study is 1.3% lower than the direct labor cost used in this study. However, in the reference study, the indirect labor costs which include the costs of administration and the general overhead are 40.0% of the direct labor costs, and for this study, the contribution of the direct labor costs in the administration and the general overhead costs is at 18%. The higher percentage contribution of the labor costs leads to a higher contribution of the

indirect labor cost for the fixed costs in the reference study. For the reference study, the loss of electricity exported due to steam use from within the mill for the stripper column reboiler is considered a loss in revenue. The OPEX is similar for both studies; as a result, the difference in the capture costs is attributed to the difference in the total CAPEX, which is higher for the reference study [116].

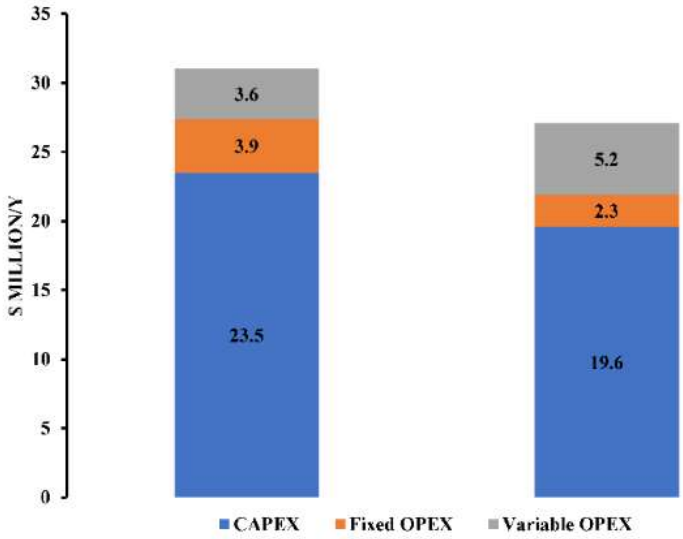

Figure 5.5 CAPEX and OPEX comparison

Table 5.7 provides the energy consumption of the main equipment of the present study. Stripper column reboiler steam alone contributes to around 52.0% and the electricity costs contribute to 23.0% of the total operating costs.

Table 5.7 Energy consumption of the main equipment

Equipment	Energy consumption
Stripper Reboiler	3.3 $\frac{GJ}{t-CO_2}$
Stage 1 compressor	629.0 kW
Stage 2 compressor	724.0 kW
Stage 3 compressor	479.0 kW
Stage 4 compressor	338.0 kW

The cost of the stripper section is higher for the reference study; however, the compressor costing is higher for the present study. The stripper section cost in the reference study includes the costs of the stripper column, water wash column, condenser and reflux drums, reboilers, and the associated pumps. The reference study did not include the cost breakdown for the individual equipment and the sizing for the condenser, the reboiler, and the reclaimer for the stripper section, making a one-to-one comparison impossible. Per CAPCOST estimates, the reboiler, condenser, and pump contribute more than 50.0% of the total stripper section costs. Table 5.8 summarizes the stripper section equipment and costs of the individual components for this study.

Table 5.8 Stripper section costing: CAPCOST

Stripper section	Costs ($ million)
Stripper column (including packings & internals)	1.1
Condenser	0.4
Reboiler & pump	0.8

When the stripper section costs are compared to the absorber section for the reference study, the stripper section cost is more than two times the cost of the absorber section. The absorber column has a larger diameter, 3.9 m, and is taller, 25.0 m, than the stripper column, which has a diameter of 2.9 m and a height of 20.0 m in the reference study [116]. Considering only the size difference of the absorber and the stripper columns, the pricing of the stripper column should be lower. Table 5.9 provides the equipment sizing for this study. Also, both absorber and stripper columns have the same packing material, Sulzer mellapack 250Y. However, the stripper column section has a condenser, a reboiler, and an MEA reclaimer, making the stripper column section as a whole expensive as compared to the absorber section.

Table 5.9 Specification for main equipment in this study

Equipment	Sizing
Direct contact cooler	Ø2.7 m × H10.1 m
Absorber	Ø3.9 m × H25.3 m
Stripper	Ø2.9 m × H19.8 m
Rich/lean heat exchanger	1621.0 m^2
Reboiler	700.0 m^2
Condenser	177.0 m^2
Solvent cooler	574.0 m^2

A significant difference is observed in the compressor and dehydration section cost between the reference study and the present work. A cost breakdown of the compressor and dehydration section was also not given in the reference study. A breakdown of the individual component costs in each section of the CO_2 capture plant and the equipment sizes would have enabled a more direct comparison.

The CO_2 capture process flow diagram can be divided into three main sections to compare the section-wise contribution to equipment costs. Table 5.10 lists the three main sections, the major equipment in each section, and the percentage section-wise cost distribution. Table 5.10 reveals that the major contributor to the reference study's capital costs is the CO_2 capture section, followed by the compressor and dehydration, and then the pretreatment sections. We guestimate that 1) the use of an MEA solvent split configuration for reducing reboiler heat duty, 2) the higher cost of the stripper column and its auxiliary units of the reboiler, condenser, and the MEA solvent reclaimer, and 3) the use of a higher exponent value for estimating equipment costs in (4) by the reference study led to a higher contribution of the CO_2 capture section. However, the capital cost estimated by CAPCOST suggests that the compressor unit is the major contributor to the total capital cost, followed by the CO_2 capture section and then the pretreatment. The pretreatment unit's contribution to the entire capital cost is the least for both approaches. If we did not assume n^{th} plant

for our economic analysis (similar to assuming a higher exponent in (6) for the equipment cost calculations) and include a 30.0% increment in the column costs, the CAPEX for this study would be comparable to the reference study. Considering a 30.0% increment in the column costs, the CAPEX difference between the reference and this economic analysis reduces from 16.6% to 11.2%.

Table 5.10 CO_2 capture process section-wise cost breakdown

Section	Major equipment	Reference study (%)	This study (%)
Pretreatment	Flue gas blower Vent gas heater Direct Contact Cooler (column & packing)	3.5	15.3
CO_2 capture	Pump & cooler Absorber section (column & packing) Amine circulation system (pumps & heat exchangers) Stripper section (column & packing) Condenser & reboiler	89.3	39.8
Compression& dehydration	Compressor package Heat exchangers Dehydration unit	7.2	44.9

5.4.2 Sensitivity of the capture cost for the base case of this study

The variable cost in OPEX includes the utilities, mostly steam and electricity, and chemicals, the makeup MEA. Steam is consumed in the stripper column reboiler, electricity for the compressor unit, and MEA solvent for CO_2 absorption. The capture cost sensitivity is evaluated with varying MEA solvent, electricity, and steam costs. Further, we analyzed the cost sensitivity to changes in flue gas inlet CO_2 mol%.

Figure 5.6 (blue) gives the CO_2 capture costs variation with changing flue gas CO_2 composition (mol%) from 18.0 mol% to 22.0 mol %. As the CO_2 mol% increases, an increase is observed in the equipment sizes; however, the capture costs decrease because of the relatively higher change in the amount of CO_2 captured. These observations align with previously reported conclusions [118].

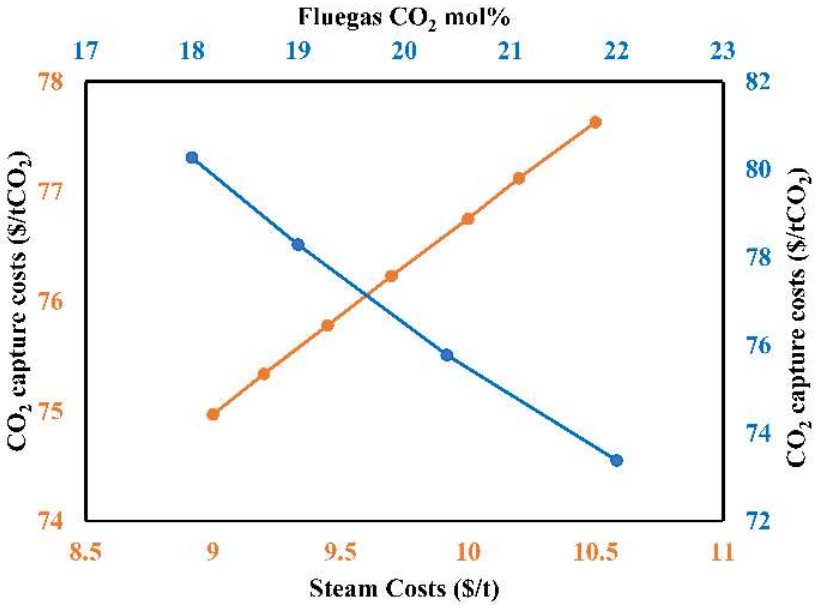

Figure 5.6 Capture cost sensitivity with the flue gas CO_2 mol% and steam costs

For this study, the medium pressure steam in the stripper column reboiler contributes to ca. 65.0% of the total utility costs and 22.5% of the total CO_2 capture costs. The sensitivity of the CO_2 capture costs to the steam cost changes, from \$9.0 to \$10.5 per tonne of medium pressure steam, is evaluated and shown in Figure 5.6 (orange). The steam cost changes significantly impact the OPEX due to its largest share in the utility costs. Hence, there is a linear correlation between the

capture cost and the steam cost. For an increase of $1.0 per tonne in steam costs, the CO_2 capture costs increase by 2.4% (Figure 5.6).

The MEA solvent makeup is needed due to the MEA losses from the absorber and the stripper columns and also to account for the MEA degradation due to the presence of SO_x in the flue gas. The MEA makeup and degradation losses account for 5.5% of the total CO_2 capture costs. The sensitivity of the CO_2 capture costs is evaluated for the MEA cost values of $1000.0 and $5000.0 per tonne of MEA in Figure 5.7 (blue). Almost a 5% increase is observed in the capture cost when the MEA prices increase from $1000.0 to $5000.0 per tonne.

Electricity is used in the compressor and dehydration section, contributing to almost 26.0% of the total utility costs. Electricity makes up 8.8% of the CO_2 capture costs. The capture cost as a function of the electricity price is illustrated in Figure 5.7 (orange). The literature study [77] also observed an increase in the capture costs with increasing electricity costs.

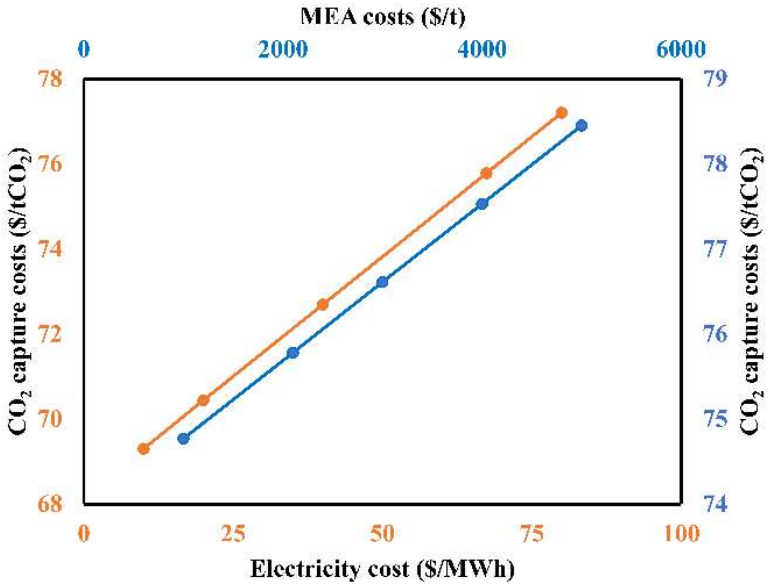

Figure 5.7 Capture costs sensitivity with the MEA and electricity costs

5.5 Conclusions and future directions

This techno-economic analysis evaluated the CO_2 capture costs from pulp and paper mill Lime Kiln and compared the costs to published capture cost data (in the reference study). The capital investment was estimated using CAPCOST in contrast to in-house tools and vendor quotes used in the reference study. A significant difference is observed in the capital cost between the reported value and this study. The difference in the overall capture cost is mainly attributed to the costing equations and the methodology used in evaluating the base equipment, EPC, construction, and fixed operating costs. The literature study estimated the costs considering a high degree of uncertainty due to the lower maturity of the MEA-based CO_2 capture process for use in the pulp and paper industry. In contrast, CAPCOST uses the sizing parameters estimated by the Aspen Plus simulation and calculates the equipment costs assuming n^{th} power law. Considering the decrease in the electricity sold to the grid, the reference study took steam integration into account, leading to a lower utility cost than observed in this study. However, OPEX for both approaches was found to be similar to each other.

We conducted a sensitivity analysis on the capture cost by varying the inlet flue gas composition (CO_2 mol%), and steam, electricity, and MEA prices. The results revealed that the capture costs vary from \$70.0 to \$82.0 per tonne of CO_2 captured. Our study provides a basis for cost calculations, with details on TEA, and helps for future process simulation and optimization studies. The use of CAPCOST modular program provides transparency to replicate cost calculations and utilize this approach to evaluate the CO_2 capture costs in the pulp and paper industry.

Future work will focus on processing flue gas data from two different Lime Kiln sections, a real integrated paper mill, and a liner board mill, analyzing the capture costs for different input

conditions and production rates. Optimization of the CO_2 capture process considering the equipment sizing and the operating conditions as decision variables for capture cost minimization will be performed. Further, steam integration from within the mill will be explored to reduce the total capture costs, and in-mill application of captured CO_2 with an existing federal tax credit for carbon capture and sequestration (Section 45Q - Internal revenue code) will be studied. We also plan to analyze the cost sensitivity with the economic parameters.

Chapter 6. Carbon dioxide capture from the Kraft mill Lime Kiln: process and techno-economic analysis

6.1 Introduction

In Chapter 5 we performed the techno-economic analysis on theoretical mill data and compared the capture costs to the only Lime Kiln CO_2 capture cost data available in the literature. In this Chapter, we applied the approach used in Chapter 5 and examined the techno-economic analysis and process flowsheet optimization of capturing CO_2 from the Lime Kiln flue gas using actual mill data from two different mills. To achieve this, we couple a process simulator, ASPEN Plus, with a derivative-free optimization (DFO) solver, which identifies the optimum process design and operating conditions that minimize the CO_2 capture cost.

Apart from emitting CO_2 in the production process, the pulp and paper mills, depending on the type of the mill, also utilize CO_2 as a raw material for bioproducts. Scattered studies on the applications of CO_2 in pulp and paper mills have been reported in the literature. Kuparinen et al. [75] have given the possible application of CO_2 in the pulp and paper mill, stating that the application of CO_2 depends on the mill-specific details, chosen practices, and the type of woody raw material. Also, CO_2 has been used for multiple processes, including neutral papermaking, near-neutral bleaching, brown stock washing, and effluent treatment [119–122]. As a result, the pulp and paper mills could be a site for negative CO_2 emissions by utilizing the captured CO_2 [75]. Most strikingly, section 45Q of the Internal Revenue Code (IRC) intends on incentivizing the investment in carbon capture and sequestration and doesn't distinguish between biogenic and non-biogenic sources of CO_2 [123]. Under this section, the pulp and paper mills utilizing CO_2 could be eligible for the section 45Q utilization tax credits.

Additionally, we analyze possible steam integration from within the mill to further reduce the CO_2 capture costs. A sensitivity analysis is done to examine the changes in the CO_2 capture costs with changing flue gas conditions and the utility costs.

Kraft pulping, Aspen plus modeling of the MEA solvent-based process with the optimization framework, and the economic analysis are introduced in the next section. The results and discussion section analyzes the DFO parametric study, the impact of steam integration on the cost analysis, the in-mill CO_2 application, and sensitivity analysis. Finally, the last section states the conclusions and prospects of this study.

6.2 Process simulation and optimization framework

6.2.1 Kraft pulp and paper mill

The Kraft pulping process along with the sources of CO_2 is explained in detail in Chapter 2 with the help of Figure 2.1.

In this study, the Lime Kiln is selected as a case for CO_2 capture, while CO_2 emitted from the Lime Kiln is still primarily of biomass origin, the Lime Kiln is the only source of fossil fuel-based CO_2 and has the highest concentration of CO_2 in the flue gases [124]. Also, it is shown earlier that the CO_2 capture costs decrease as the CO_2 concentration increases [125,126].

6.2.2 ASPEN Plus process simulation

Two southern United States softwood-based kraft pulp mills provided the Lime Kiln flue gas process conditions and composition (Table 6.1). The absorption cycle is a temperature-dependent acid-base reaction wherein the flue gas CO_2 (weak acid) reacts with a solvent (a weak base). After reacting with CO_2, the "CO_2 loaded" solution (rich MEA) is regenerated to reverse the reaction,

thus liberating gaseous CO_2 [127]. The absorption-desorption reactions for primary amines like MEA can be represented as [128]:

$$RNH_2 + CO_2 \leftrightarrow RNHCOO^- + H^+ \quad (16)$$

The ASPEN Plus configuration for solvent-based CO_2 capture is shown in Figure 6.1. The Lime Kiln flue gas is cooled and quenched in a direct contact cooler (DCC). The cooled flue gas enters the absorber column from the bottom, and the lean MEA, solvent regenerated from the stripper column, enters the absorber from the top. Solvent MEA, absorbing CO_2 from the flue gas, is pumped and heated in a rich/lean heat exchanger with the stripper column bottoms (lean MEA) before sending it to the stripper column. The rich MEA solution is stripped of its CO_2 in the stripper column. The CO_2 and some water vapor are recovered as the top product from the stripper column CO2OUT stream. A four-stage compressor train is used to compress the product CO_2 to 110 bar at 33°C. The lean MEA from the stripper's bottom passes through the rich/lean heat exchanger and is mixed with make-up water and make-up amine. This mixed lean MEA is further cooled at an exchanger with cooling water and is sent back to the absorber.

Table 6.1 Lime Kiln fluegas data

		Mill A	**Mill B**
Parameter	Units	Value	Value
Stack Flow Rate	m^3/h	137209.0	127562.0
Temperature	°C	113.0	75.0
Water	mol %	33.9	36.5
CO_2	mol %	20.0	16.7
O_2	mol %	4.6	7.1
N_2	mol %	41.4	39.6

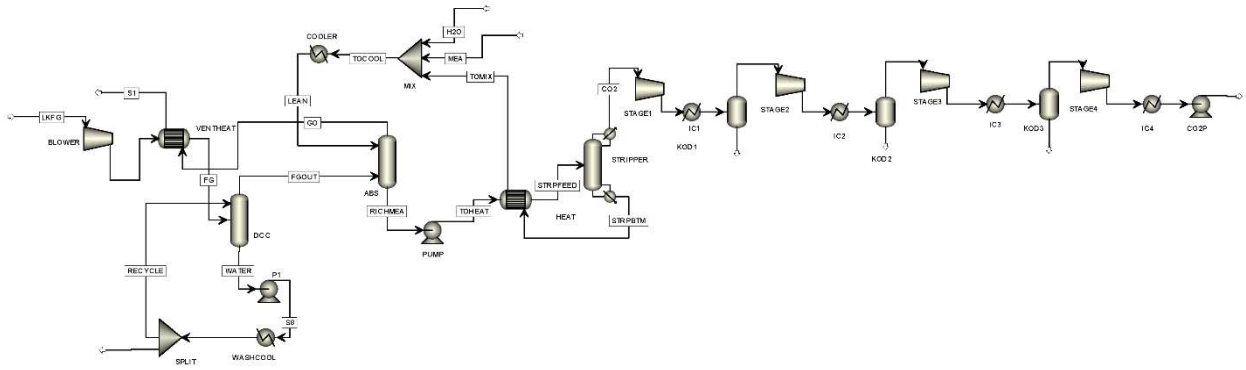

Figure 6.1 ASPEN Plus flowsheet of CO_2 capture

CO_2 absorption-desorption is simulated in Aspen Plus V10.0. KEMEA (Kent-Eisenberg) data package is used to model the thermodynamic and transport properties. The package contains kinetics and rate constants, which allows modeling the MEA system more accurately with an electrolyte-NRTL model using RadFrac distillation. RadFrac unit operation is used to model the absorber and stripper columns. The absorber is a simple RadFrac column without a condenser and a reboiler. The stripper has a condenser at the top and a reboiler at the bottom. Both absorber and stripper columns are modeled using the Rate-based model. Pressure drop in the piping and each piece of equipment is neglected. The stripper column operates at 1.9 bar pressure to prevent potential solvent degradation due to high pressure and higher stripper bottom temperatures [113]. COMPR block is used in Aspen plus to simulate the CO_2 compressors.

6.2.3 Optimization environment

Derivative-free optimization (DFO) is a framework to solve optimization problems that do not require an explicit mathematical expression of the problem or its derivatives. Instead, this framework utilizes the objective function values for sets of decision variables with an algorithmic specific search strategy to gradually improve the best set of decision variables. The procedure for a DFO framework can be found in Figure 6.2. In a DFO framework, the objective function is

treated as a black-box model, which is able to provide the objective function value of the optimization problem when given a set of decision variables. The framework begins by providing the black-box model a set, or sets, of decision variables to obtain the objective function value(s). The set of decision variables and the objection function pair is then passed back to the DFO algorithm, where a new set of decision variables is determined and evaluated. This process is repeated until a termination criterion is met. There are a different number of termination criteria; however, one of the most commonly used is the maximum number of black-box evaluations [129]. The objective function, a multivariant optimization problem, to be minimized within the DFO framework, is the CO_2 capture cost given by equation 4. Eight degrees of freedom that act as a decision variable for the DFO tool have been identified for optimization: 1) DCC stages, 2) flue gas temperature, 3) absorber stages, 4) stripper stages, 5) MEA solvent lean loading, 6) MEA solvent wt.%, 7) stripper inlet temperature, and 8) amount of CO_2 captured. The absorber and the stripper stages were treated as integer values, while the remaining process parameters were continuous. A Python script was used to link the ASPEN Plus simulator and the derivative-free optimization solver. The solver used is glcSolve from the TOMLAB optimization suite [130], with a termination criterion of 2,000 black-box evaluations. At the framework's termination, the absorber stages, stripper stages, the MEA solvent lean loading, MEA solvent wt.%, stripper inlet temperature, and the amount of CO_2 captured are determined for the minimum CO_2 capture costs value.

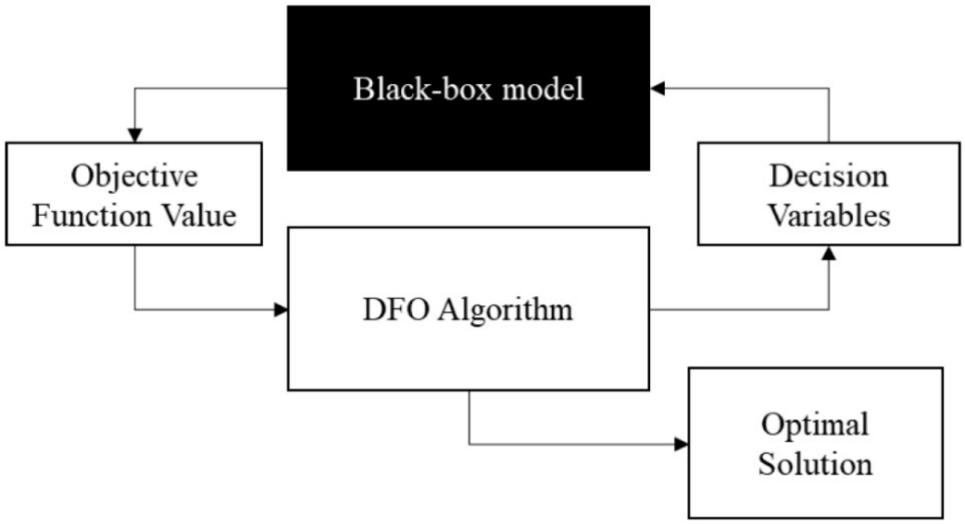

Figure 6.2 The derivative-free optimization framework

6.2.4 Economic analysis

The CO_2 capture costs include fixed capital costs and operating costs. Equations and data from the module factor-based software CAPCOST are used to evaluate the fixed capital costs for the columns (DCC, absorber and stripper), heat exchangers (condenser, reboiler, rich/lean heat exchanger, and the solvent cooler), and the pump [114]. The cost data is adjusted for inflation using the Chemical engineering plant cost index value, CEPCI, 596.2 [131]. The total annualized cost for the system is calculated using the following formula,

$$TAC\left(\frac{\$}{y}\right) = AF \times C_{Capital} + C_{Operating} \tag{17}$$

The Annualization factor, A.F., was calculated as follows,

$$AF = \frac{i(1+i)^n}{(1+i)^n - 1} \tag{18}$$

Where i is the interest rate, and n is the plant operation year.

The total CO_2 capture cost used for flowsheet optimization is calculated as

$$CO_2\ capture\ costs\ \left(\frac{\$}{t-CO_2}\right) = \frac{TAC}{Captured\ CO_2} \quad (19)$$

Where, $C_{operating}$ and $C_{Capital}$ are operating costs and capital costs, respectively.

The overall assumptions used for the calculation of capture costs are:

- A Grassroots facility with 8,400 hours of operation per year is considered.
- Twenty years (n) of plant operation and a 20.0% interest rate (i) are considered with no salvage value.
- Maintenance and repair costs are at 6.0% of the fixed capital investment.
- Operating supplies are at 0.9% of the fixed capital cost investment.
- Insurance and taxes are taken at 2.0% of the fixed capital investments.
- Thirteen operators are required as operating labor with an annual salary of $ 66,910.0 was determined using the method defined in Turton et al. [114].
- Direct supervisory and clerical level costs are taken at 18.0% of the labor costs.
- Laboratory charges are taken at 15.0% of the labor costs.
- Plant overhead cost is a summation of 70.8% of the labor costs and 3.6% of the fixed capital cost investment.
- General and Administrative expense cost is a summation of 17.7% of the labor costs and 0.9% of the fixed capital costs.
- Startup and MEA costs are taken at 10.0% of fixed capital investment.
- Make-up water costs are $0.2/1,000 kg, and the make-up MEA costs are taken from [128] and inflated as per CEPCI value.
- The steam (5 barg) costs, process cooling water, and electricity are $9.4/1,000 kg, $15.7/1,000 $m^{3,}$ and $0.0674/kWh, respectively [114].

The absorption setup's equipment costs primarily include the costs of the absorber column, the stripper column, and the exchanger costs. The absorber and stripper columns are packed bed columns with the packed height per stage (HETP) calculated using Eq. 20 [115]:

$$HETP\ (m) = \frac{100}{a_p} + 0.1 \tag{20}$$

Where a_p is the surface area per volume of the packing.

6.3 Results and discussions

6.3.1 Derivative-Free Optimization (DFO) parametric study

The optimal process configuration by the DFO solver and some critical process parameters are shown in Table 6.2 below. The equipment costs are shadowed by the total operating costs, which include the reboiler steam, cooling water, electricity, and make-up chemicals. Steam contributes to almost 53.0% of the total operating costs for both mills. The impact of steam consumption on the total capture costs was compared with literature data [125,132] and made up the most significant portion of the operating costs.

Table 6.2 Optimal process configuration for the MEA-based CO_2 capture system

Variable	**Mill A** Value	**Mill B**
Captured CO_2 (%)	94.8	94.4
Absorber stages	10	12
Stripper stages	7	7
Solvent lean loading	0.281	0.275
MEA solvent concentration (wt. %)	45.0	45.0
MEA solvent flow rate $\left(\frac{\boldsymbol{m^3}}{\boldsymbol{t-CO_2}}\right)$	21.6	20.2
Stripper inlet temperature (°C)	98.7	99.4
Reboiler heat duty $\left(\frac{\boldsymbol{GJ}}{\boldsymbol{t-CO_2}}\right)$	3.9	3.8

Table 6.3 summarizes the equipment costs for the optimized flowsheet. The costs are rounded off to the nearest 1000. The difference in the costing of the absorber columns is due to the higher number of absorber stages for the Mill B data. However, the Mill A absorber column has a slightly larger diameter than the Mill B absorber column as the Mill A solvent circulation rate is almost 1.3 times higher than that of Mill B. Furthermore, a higher capital cost for the Mill A stripper column is attributed to the fact that the amount of CO_2 stripped in the Mill A stripper column is almost 1.2 times higher than Mill B. This higher amount of CO_2 stripping and the higher solvent regeneration leads to a stripper column with a larger diameter and thus a higher cost for the Mill A stripper column. Also, the higher MEA circulation rate for Mill A leads to a higher exchanger cross-sectional area increasing the equipment capital costs for Mill A.

Table 6.3 Optimized flowsheet equipment costs and specification

	Mill A		Mill B	
	Costs (US $)	Specification	Costs (US $)	Specification
Absorber	2316000.0	Ø4.9 m × H12.2 m	2456000.0	Ø4.7 m × H13.2 m
Stripper	844000.0	Ø3.6 m × H6.1 m	655000.0	Ø3.2 m × H5.5 m
Rich/lean heat exchanger	1135000.0	1554.0 m^2	1016000.0	1414.0 m^2
Reboiler	1172000.0	1204.0 m^2	1065000.0	1049.0 m^2
Condenser	1386000.0	743.0 m^2	1160000.0	617.0 m^2
Solvent cooler	753000.0	1082.0 m^2	682000.0	986.0 m^2

Table 6.4 provides the results of cost evaluation for the optimized process flowsheet for both the mills. The total annualized costs and the operating costs are higher for Mill A as compared to Mill B. Although, for the optimized flowsheet, the percentage of CO_2 capture from both the mill data is similar, the flue gas for Mill A has a higher CO_2 mol% entering the capture system. The higher CO_2 concentration in the flue gas leads to a higher amount of CO_2 captured for Mill A. This higher amount of CO_2 captured in the case of Mill A leads to overall lower CO_2 capture costs for Mill A.

Table 6.4 CO_2 capture costs

Parameter	**Mill A** Value	**Mill B** Value
Total capital cost [$]	23,270,000.0	21,658,000.0
Total annualized capital cost [$/y]	20,097,000.0	18,179,000.0
Total operating cost [$/y]	9,977,000.0	8,605,000.0
Total utilities cost [$/y]	8,254,000.0	6,942,000.0
CO_2 capture [t/y]	309,000.0	260,736.0
CO_2 capture cost [$ per t-CO_2]	64.9	69.7

Few studies have worked towards the CO_2 capture from the Lime Kiln section of the pulp and paper industry. Onarheim et al. [21] studied CO_2 capture from pulp and paper mill Lime Kiln section and for 90% CO_2 capture from the Lime Kiln flue gas, the capture cost was calculated at $91 per tonne CO_2. Detailed comparative cost analysis between the study and the method used in this work is previously done [88].

Further, accounting for the 45Q tax credit, a $50.0 per tonne CO_2 reduction in cost is incorporated in each cost estimate operation W.J. Sagues et al. [84] estimated Lime Kiln CO_2 capture costs to be in the range of $2.1 per tonne CO_2 to $5.0 per tonne CO_2. The Levelized capital and operating expenses for CO_2 capture were estimated using chemical process models and were assessed using AspenTech process simulation software.

The following sub-sections discuss how the total capture costs, i.e., the cost minimization function, vary with changing decision variables' values. DFO solver determines the minimum value of CO_2 capture costs by changing the decision variables. For a particular decision variable, the CO_2 capture costs vary depending on the other seven decision variables' levels, which leads to

multiple values of CO_2 capture costs being evaluated at a particular level of a single decision variable. The y-axis of the figures' trends in the following sub-sections, 6.3.1.1 to 6.3.1.8, represents CO_2 capture costs in $ per tonne of CO_2. The x-axis corresponds to the numerical values of decision variables. Each dot in figures 6.3 to 6.11 represents individual runs of the model with other varied decision variables. The plot in orange is for Mill A and in blue is for Mill B.

6.3.1.1 Effect of absorber stages

Figure 6.3 shows capture cost variation by changing the number of absorber stages. The absorber column is the equipment that facilitates the absorption reaction between the solvent and CO_2. The absorber column would be treating an enormous amount of flue gas flow rate in the CO_2 capture system [113], making the absorber column a critical piece of equipment contributing to capital costs. The absorber column's height was varied by changing the number of stages in the column; as the absorber stages increase, the capital costs increase. The minimum value of the capture cost is at 10 and 12 stages for Mill A and Mill B respectively. There is a decrease in the absorber capital costs by almost 77.0% as the stages decrease from 39 to 10 for both the mill data. The DFO algorithm changes other decision variables' values for a particular absorber stage, leading to different capture costs values at a specific absorber stage. The absorber column's lowest capital cost is at ten stages; however, the values of other decision variables result in process configuration with higher overall capture costs for those stages as seen from the higher capture cost values for stages 10 to 23.

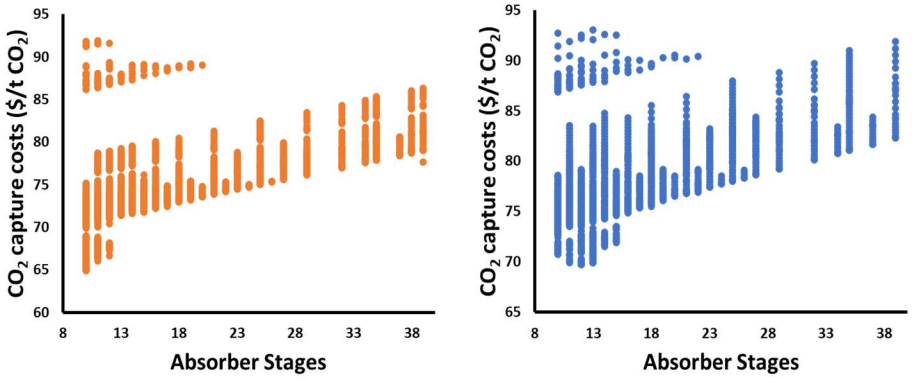

Figure 6.3 Impact of absorber stages on capture costs

6.3.1.2 Effect of stripper stages

The impact of the stripper stages on the capture costs is shown in Figure 6.4. The lowest value of the capture cost is at the stripper stage 7 for both the mill data. The stripper stages above 8 are not explored by the algorithm because of the stripper column flooding, causing a convergence problem.

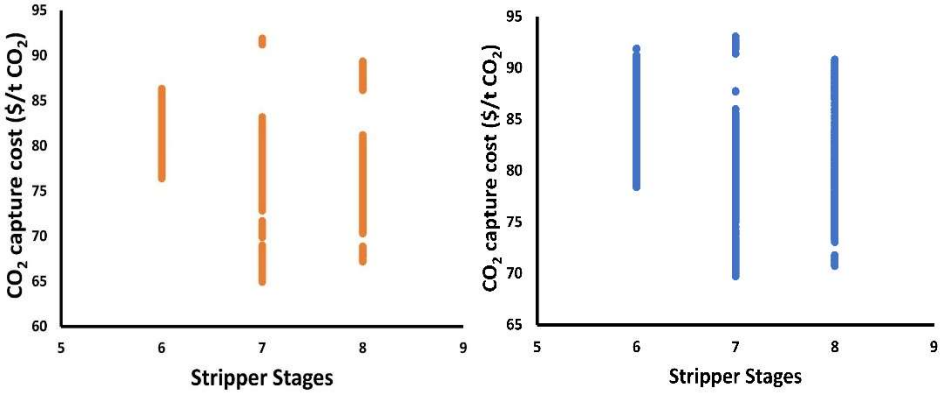

Figure 6.4 Impact of stripper stages on capture costs

6.3.1.3 Effect of stripper inlet temperature

Figure 6.5 shows the variation of the capture costs with varying stripper inlet temperature. The capture cost decreases slightly as the stripper inlet temperature increases from 91.0°C to 100.0°C, with the lowest capture costs at 98.7°C for Mill A and 99.4°C for Mill B. As the stripper inlet temperature increases, the fraction of reboiler heat required to increase feed temperature to the stripper bottom temperature decreases. A slight increase in capture costs above 98.7°C for Mill A is mainly due to the process configurations leading to higher overall capture costs.

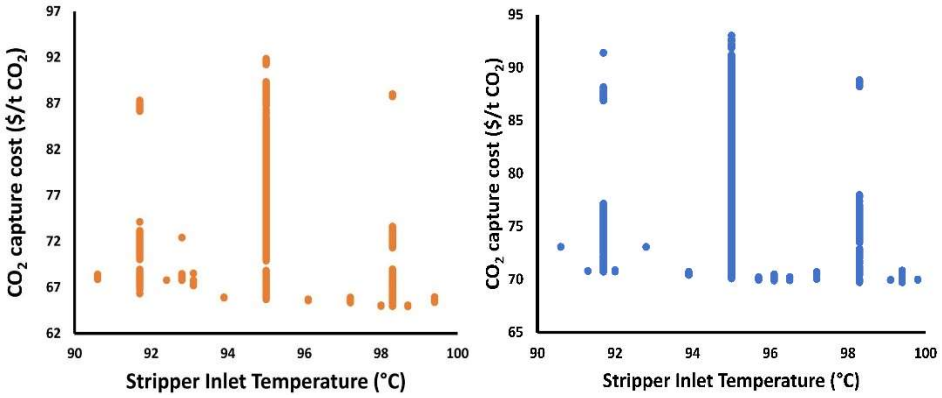

Figure 6.5 Impact of stripper inlet temperature on capture costs

6.3.1.4 Effect of the solvent lean loading

Figure 6.6 gives the variation of capture costs with solvent lean loading. The lowest capture cost was at a solvent lean loading of 0.281 for Mill A and 0.275 for Mill B respectively. Lower the value of solvent loading, lower the solvent circulation rate required to capture the desired CO_2 from flue gas. Also, at a lower value of lean loading, the solvent has more MEA, boosting the absorption rate. However, a large amount of heat duty required for solvent regeneration tends to overshadow the accelerated absorption at a lower value of lean loading. The reboiler duty decreases by almost 36% as the MEA solvent lean loading increases from 0.17 to 0.281 for Mill

A and Mill B reboiler heat duty decreases by almost 38% as the solvent lean loading increases from 0.17 to 0.275. The higher solvent regeneration duty at lower values of solvent lean loading increases the overall capture costs as steam is the major contributor to the total utility costs.

Moreover, the higher solvent lean loading value is also associated with reduced CO_2 absorption rates, increasing the solvent circulation rate and the equipment costs. The reboiler heat duty changes and the associated steam costs with lean loading are also recorded by [133–135]. The DFO solver did not explore the territory between 0.17 and 0.225 for both the mill data due to possibly higher capture costs.

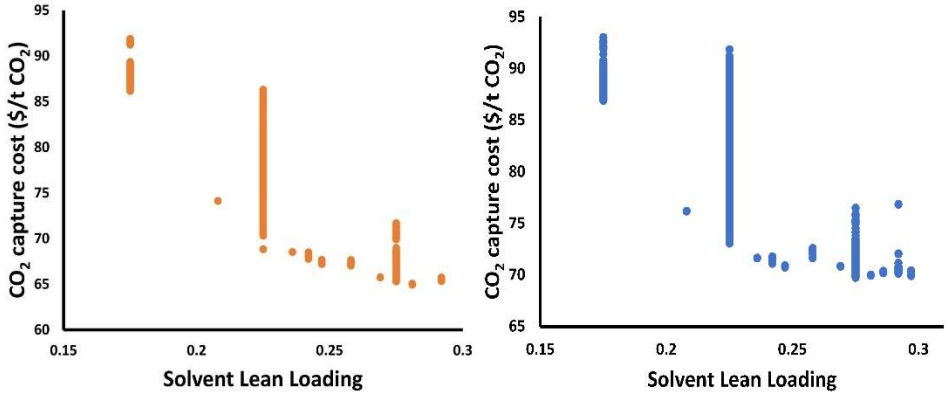

Figure 6.6 Impact of solvent lean loading on capture costs

6.3.1.5 Effect of Monoethanolamine weight percentage

Figure 6.7 shows the capture costs variation, varying the MEA solvent concentration. The lowest capture cost was at a solvent concentration of 45.0 wt.%. The change in solvent concentration affects the reboiler heat duty in two ways 1) as the solvent concentration increases, the amount of water evaporated in the stripper column decreases, 2) an increase in the solvent concentration also leads to a lower solvent circulation rate and a lower sensible heat requirement in the reboiler. An increase in the solvent concentration from 25.0 to 45.0 Wt. % leads to a rise in the MEA flow rate

by almost 64.0% for Mill A and 53.0% for Mill B respectively. This decrease in the solvent flow rate leads to a reduction in the reboiler energy consumption. A decrease in the solvent flow rate and the regeneration duty with increasing solvent concentration was also reported [136]. The MEA concentration change also impacts the capital cost leading to a cost reduction in the rich/lean heat exchanger's by almost 8 times for Mill A and almost 5 times for Mill B respectively as the MEA concentration increases from 25.0% to 45.0 Wt.%. The higher MEA concentration at a constant lean loading value leads to a decrease in the reboiler temperature due to the higher partial pressure of CO_2. A decrease in the reboiler temperature outweighs concentration effects, reducing thermal degradation in the system [137]. The reduction in thermal degradation could reduce corrosion as the MEA degradation products have shown to increase the corrosion rates [128], [138]. Further, with higher MEA concentration, corrosion inhibitors are required. The MEA concentrations above 45.0 Wt.% lead to a process configuration with a rise in the fixed operating costs and consecutively higher overall capture costs.

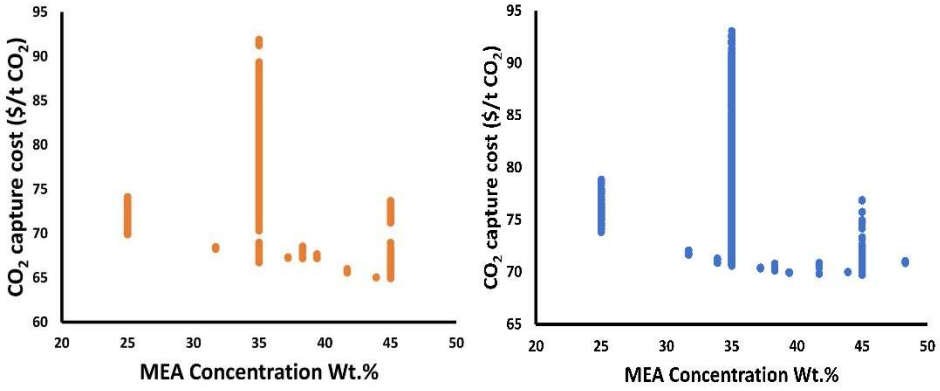

Figure 6.7 Impact of solvent concentration (wt. %) on capture costs

6.3.1.6 Effect of the amount of CO_2 capture

Figure 6.8 gives the variation of capture costs with the amount of CO_2 captured. The total costs of CO_2 capture decrease slightly with an increasing amount of CO_2 captured. The minimum capture cost was seen at 94.8% of CO_2 capture for Mill A and 94.4% of CO_2 capture for Mill B. The capture costs tend to flatten at higher amounts of CO_2 capture.

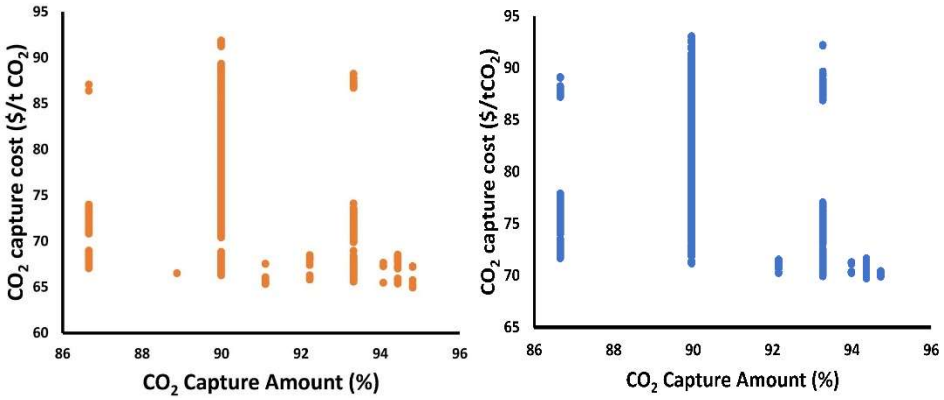

Figure 6.8 Impact of the amount of CO_2 capture (%) on capture costs

6.3.1.7 Effect of DCC stages on capture costs

Figure 6.9 gives the variation of capture costs with the direct contact cooler stages. The reduction in capital costs is seen with the reduction in the number of DCC stages for both the mill data.

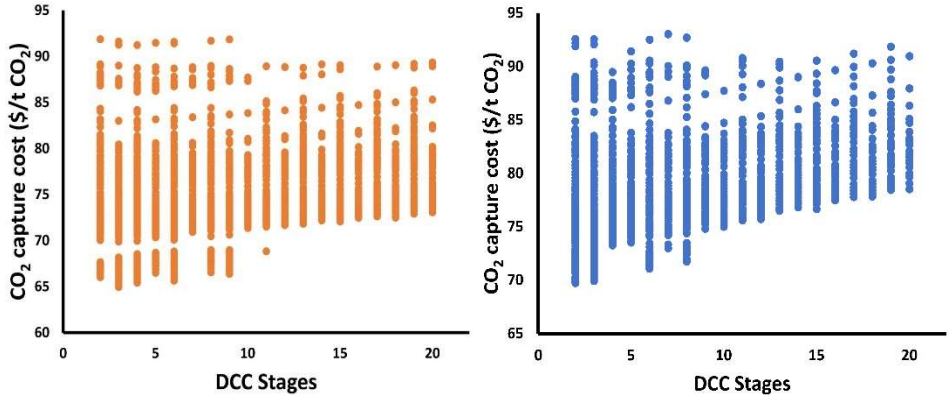

Figure 6.9 Impact of the DCC stages on capture costs

6.3.1.8 Effect of flue-gas temperature on capture costs

Figure 6.10 gives the variation of capture costs with the flue-gas temperature entering the absorber column. The CO_2 absorption in MEA solvent is favored at lower temperatures and higher temperatures in the absorber column also lead to higher solvent losses from the absorber column. As a result, the capture costs are lower at the lower values of the flue gas.

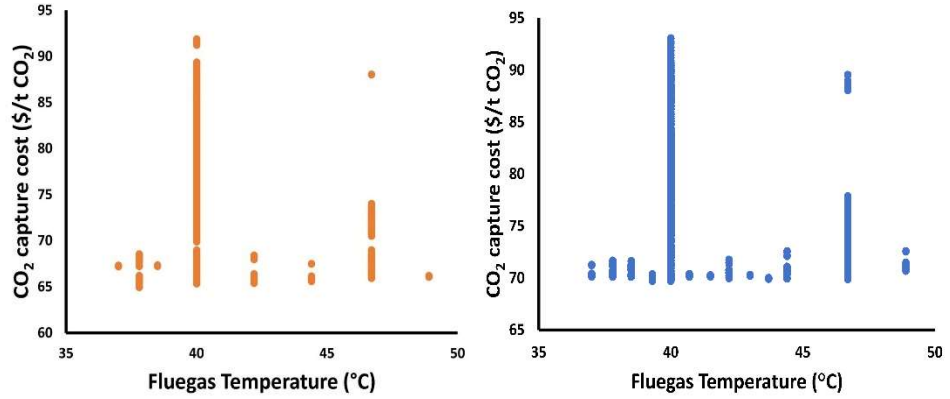

Figure 6.10 Impact of flue-gas temperature on capture costs

6.3.2 Integration of the CO_2 capture system within a pulp and paper mill

The possibility of using extracted steam from the pulp and paper mill in the CO_2 capture system and the in-mill CO_2 application is studied. Section 6.3.2.1 discusses the use of extracted steam from the mill's steam island system into the stripper column reboiler, and section 6.3.2.2 discusses the in-mill application of captured CO_2 with an existing federal tax credit for carbon capture and sequestration (Section 45Q - Internal revenue code).

6.3.2.1 Economic impact of the steam integration on the CO_2 capture costs

A typical steam turbine island system for an integrated pulp and paper mill is shown in Figure 6.11 [21]. Steam generated from the bark boiler combined with the steam generated from the recovery boiler is expanded in a steam turbine. The steam turbine plant comprises an extraction-condensing turbine and a power generator. High Pressure (H.P) steam from the bark and recovery boiler at 505.0°C and 103.0 bar (a) is expanded across an extraction-condensing set of turbines to generate power using a set of generators. In the first stage extracted steam at 30.0 bar is used for soot blowing in the recovery boiler, whereas the 13.0 bar and 4.0 bar extracted steam is used in the process at various points of application. The first three-stages comprise a high-pressure turbine section, and the last two constitute the low-pressure turbine section. The steam extracted from the steam turbine island is used at various locations within the mill. The process condensate generated is mixed with the turbine condensate and sent to the boiler feed water (BFW) tank [21].

COMPR block is used in ASPEN Plus to simulate the steam turbine. The values of isentropic efficiencies, the extracted steam pressure levels, and the amount of steam extracted from the turbine are taken from [21,116,139].

The MEA-based CO_2 capture process is costly because of the high-energy requirements [140], and the most significant impact comes from the steam demand in the stripper column of the CO_2 capture plant. The possibility of steam integration from within the mill is explored. In this study, the extracted steam at 4.2 bar is investigated as a possible source for the stripper reboiler steam. In Figure 6.12, the dashed red line gives a possible steam extraction point from the steam island towards the stripper column reboiler.

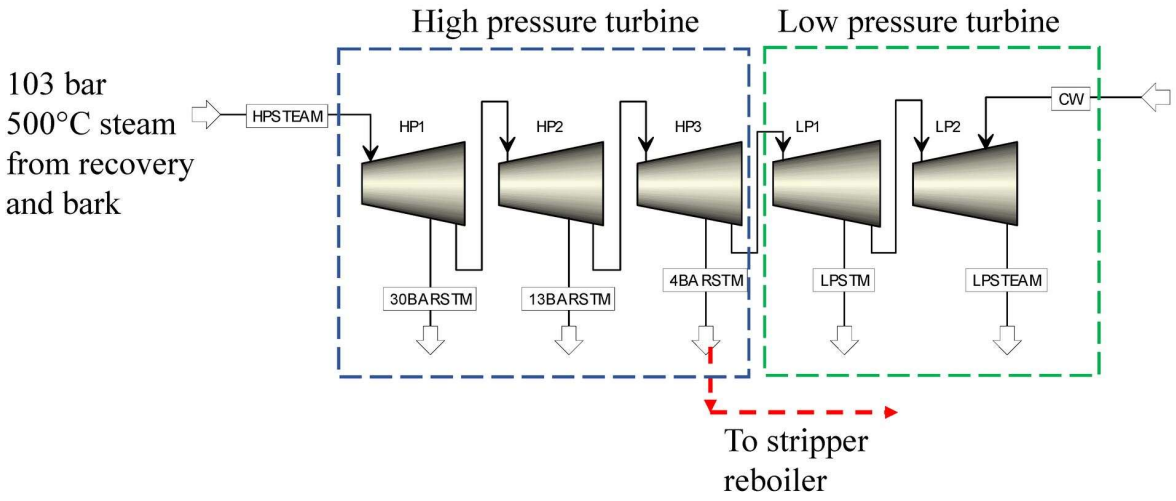

Figure 6.11 Steam extraction point for the capture process

Steam integration would reduce the capture costs by 27.0% for Mill A and around 25.0% for Mill B, with a net reduction of 6.6 MWh of electricity export to the grid for Mill A and 5.4 MWh for Mill B respectively. For Mill A, a decline in the electricity export to the grid results in a \$12.0 per tonne CO_2 cost penalty. However, the cost savings of \$17.7 per tonne of CO_2 from the use of extracted steam in the stripper reboiler overshadows the cost penalty and for Mill B, a reduction in the electricity export to the grid results in an \$11.5 per tonne CO_2 cost penalty. However, the cost savings of \$17.1 per tonne of CO_2 overshadows the electricity lost penalty. The cost savings are similar for both the mill data. For Mill A, the amount of reboiler steam required

for solvent regeneration is 1.2 times higher than that for Mill B. At the same time, the amount of CO_2 captured for Mill A is 1.2 times higher reducing the electricity loss costs and balancing out the costs for reboiler steam. A decrease in CO_2 capture costs using extracted steam in the stripper reboiler was also reported [141]. Table 6.5 gives the details on the steam turbine section and steam savings in the stripper column reboiler for both the mills.

Table 6.5 Impact of CO_2 capture on the steam and electricity balances

		Mill A without CO_2 capture	Mill A with CO_2 capture	Mill B without CO_2 capture	Mill B with CO_2 capture
Steam Production (t/h)		1163.0	1163.0	1177.0	1177.0
Steam extracted for process applications (t/h)	30 bar Extracted steam	31.4	31.4	31.8	31.8
	13 bar extracted steam	249.7	249.7	252.7	252.7
	4.2 bar extracted steam	529.9	598.8	536.4	548.9
Steam extracted for CO_2 capture (t/h)	4.2 bar	-	68.6	-	56.3
Electricity generated (MWh)	High-pressure section	172.9	172.9	175.1	175.1
	Low-pressure section	33.4	26.8	32.9	28.5
Electricity demand in the mill (MWh)		119.8	119.8	125.3	125.3
Electricity exported to the grid (MWh)		79.8	73.2	83.5	78.2

6.3.2.2 In-mill CO_2 utilization

Potential lies for the pulp and paper mills in improving the cash flow through in-mill CO_2 utilization. The eligibility of an entity depends if the CO_2 is captured and permanently isolated or displaced from the atmosphere [84]. Considering 2026 as the year for calculating the capture cost with $50 per tonne of CO_2 captured as the 45Q sequestration tax credit levels off in 2026. The capture costs for both the mills are calculated and seven potential applications of in-mill CO_2 are discussed.

Tall oil manufacture

The tall oil soap rises as a top layer when the black liquor is concentrated and allowed to settle. The top layer is skimmed off and maybe subsequently acidified to convert the tall oil soaps to crude tall oil, i.e., free fatty and resin acids, which are used to make coatings, sizing paper, paints varnishes, etc. Generally, sulfuric acid is used for acidulation purposes [142]. However, CO_2 being a weak acid can partly replace the sulphuric acid used for acidulation [75].

Lignin separation

Lignin is separated from the black liquor, as it often is a bottleneck for increasing the pulp production in mills. Biofuels can be produced from the separated lignin, producing an additional product that can replace the oil that can be transported and sold for additional revenue [75,143]. Part of the mineral acid used in the acid treatment can be replaced by CO_2.

Precipitated calcium carbonate

PCC is used as a filler in the paper machine section as it has a high scattering coefficient that helps in increasing the opacity of the paper produced [144]. PCC is manufactured by bubbling the CO_2 through calcium hydroxide solution.

Brown stock washing (BSW)

Lower washing losses are achieved in the BSW section of the pulp and paper mill by reducing the pH by CO_2 addition. The pH is lowered in one or more washing stages, attaining an improved washing-out of the pulp from substances contribution to COD [145].

pH control for stock preparation and Near-Neutral Bleaching

CO_2 treatment of the alkaline pulp before processing in the paper machine assembly for improving the drainage of the pulp in the wet end section of the paper machine [146]. Reduction in the bleaching costs by maximizing chlorine dioxide bleaching efficiency can be achieved by carrying out the final chlorine dioxide brightening at a near-neutral condition using CO_2 for pH control [120].

Effluent treatment

Replacement of the mineral acids in the acidulation stage by use of CO_2 in the effluent treatment by carbonating the process of water treatment to maintain the pH at neutral [122].

The applications of CO_2 in the mill would displace the CO_2 from the environment and also make the mill self-sufficient concerning in-mill CO_2 requirements. The existing federal tax credit for carbon capture and sequestration would help in improving the process economics making the system attractive for investments and incorporating carbon capture techniques in the pulp and paper mills. Considering the steam integration and the federal tax credit, the CO_2 capture costs for Mill A come at -$2.5 per tonne CO_2 captured and Mill B at $2.6 per tonne CO_2 captured. The negative value of CO_2 capture costs implies that the tax credit for Mill A acts as a source of income. A negative CO_2 capture cost value for CO_2 capture from the pulp and paper mill Lime Kiln was also reported by [84].

6.3.3 Sensitivity analysis

The sensitivity analysis is done to understand: 1) the impact of flue gas CO_2 concentration on capture costs, 2) how the flue gas flow rate affects the CO_2 capture costs and 3) the impact of the utility costs on the CO_2 capture costs. The base case, an optimized flow sheet, was used to perform the sensitivity analysis.

Figure 6.12 gives the variation of CO_2 capture costs with changing flue gas CO_2 concentration (mol%). The flue gas CO_2 concentration was varied from 5.0 mol % to 25.0 mol % to gauge the impact of CO_2 concentration change on the total capture costs. Initially, for lower flue-gas CO_2 concentrations, there is a sharp decline in capture costs as the concentration increases. The capture costs decrease by almost 31.0% as the CO_2 mol % increase from 5.0 to 10.0%. However, a moderate decline in capture costs is observed at higher flue-gas CO_2 concentrations. The capture costs decrease by almost 7.0% as the CO_2 mol % increase from 20.0 to 25.0%. As the CO_2 mol % increases, an increase is seen in the equipment sizes; however, the capture costs decrease because of the relatively higher change in the amount of CO_2 captured. A reduction in the capture costs with increasing flue-gas CO_2 concentration was reported in literature data [118,125,126].

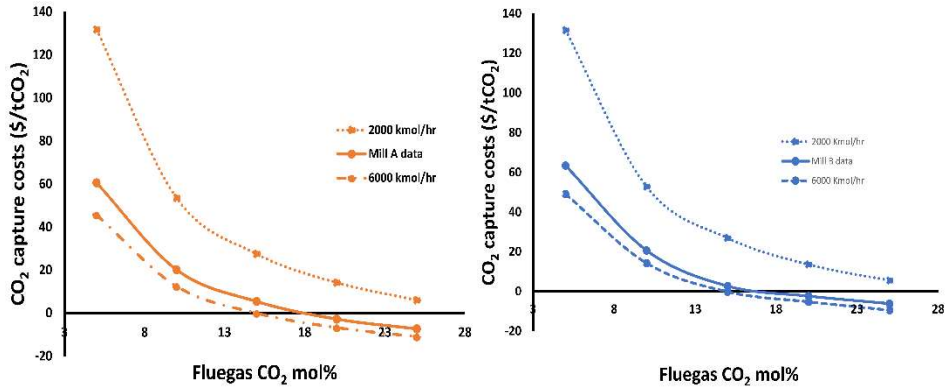

Figure 6.12 Capture costs as a function of flue gas flowrate and flue gas CO_2 concentrations

Figure 6.12 also gives the variation of CO_2 capture costs with changing flue gas flowrate. The flue gas flow rate was changed from 2000.0 kmol/hr to 6000.0 kmol/hr, and the capture costs were calculated. The flow rate was varied so that the actual flow rate is around the midpoint of the lower and upper values of the flue gas flowrate. For the same CO_2 concentration at different flue gas flow rates, the difference in capture costs was higher at the lower flue gas flow rate values. As the flue gas flow rate increased, the difference in the capture costs was reduced. The decreased difference can be explained as the flue gas flow rate increases and the CO_2 captured increases at the same flue gas composition. For both mills, the flue gas CO_2 concentration of >15.0 mol% and a flue gas flowrate of 6000.0 kmol/hr leads to a negative value of CO_2 capture costs, indicating a net earning for the mill.

The CO_2 capture cost sensitivity is evaluated by the MEA solvent and electricity costs. To evaluate the CO_2 capture costs sensitivity to the utilities, the utility costs are varied in the range of ±50.0% of the base utility costs.

MEA solvent losses take place from the absorber and the stripper column top and also MEA degradation losses are accounted for in the calculation of the operating costs. The MEA makeup and degradation losses account for around 5.0% of the total CO_2 capture costs for Mill A

and almost 4.5 % for Mill B. The sensitivity of the CO_2 capture costs to changing MEA costs is illustrated in Figure 6.13.

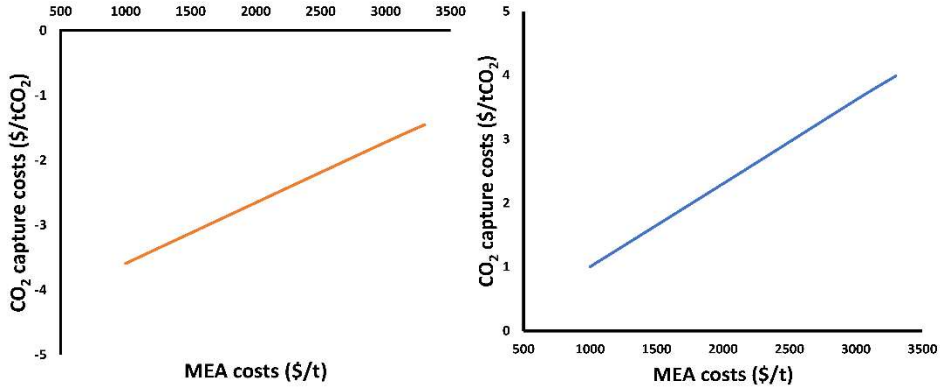

Figure 6.13 Capture costs as a function of MEA costs

Electricity costs account for 21.0% of the total operating costs making up to 10.0% of the total CO_2 capture costs for both the mill data. The CO_2 capture costs increase as the electricity costs increase (Figure 6.14). Electricity is majorly utilized by the liquid CO_2 pump and compressors in the compression and dehydration section and the inlet flue gas blower.

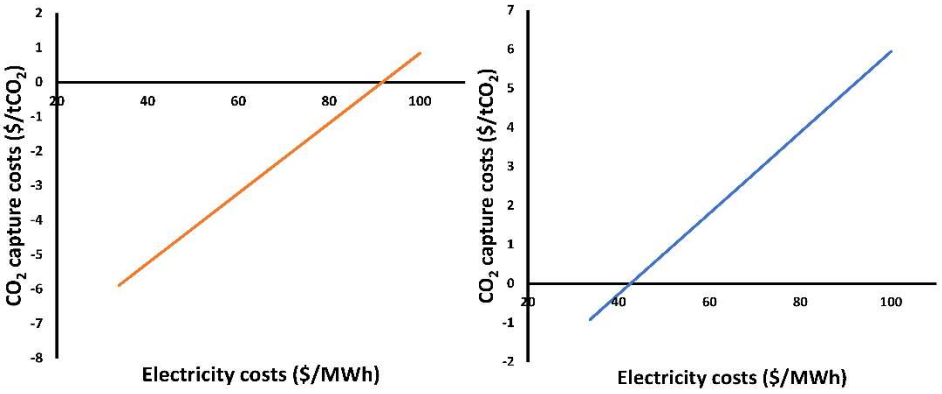

Figure 6.14 Capture costs as a function of electricity costs

6.4 Conclusion and prospects

In this study, we did a techno-economic analysis and process flowsheet optimization of the CO_2 capture from a pulp and paper and a linerboard mill using an MEA absorption process. The approach utilized preparing an MEA-based CO_2 absorption simulation in Aspen plus and linking the prepared simulation to a DFO tool using python script. We employed the CAPCOST modular program for doing the CO_2 capture costs calculations. The results showed that for the optimized flowsheet, total annualized costs and utility costs were higher for Mill A. However, a higher CO_2 capture from Mill A results in an overall lower capture costs for Mill A compared to Mill B.

Further, steam integration from within the mill to reduce the total capture costs, and in-mill application of captured CO_2 with an existing federal tax credit for carbon capture and sequestration (Section 45Q - Internal revenue code) are studied. A reduction in the electricity export from the mill is observed when the mill steam is used for the stripper column reboiler. However, the costs due to steam savings mask the loss of revenue from the reduced electricity exports. After taking into account the steam savings and CO_2 utilization, the total capture costs for Mill A were -$2.5 per tonne of CO_2 and $2.6 per tonne of CO_2 for Mill B. The capture costs sensitivity was performed by varying the inlet flue gas flowrate, flue gas CO_2 mol%, and the electricity and MEA prices. The results revealed that the capture costs vary from -$5.9 to $5.9 per tonne of CO_2 captured.

The steam integration and the CO_2 utilization potential depend on the type of the mill, location, and the industrial ecology of the pulp and paper industry. Before realizing the true benefits of integrating the pulp and paper mill with the CO_2 absorption system, a thorough evaluation of the entire framework needs to be done.

6.5. Acknowledgment

The authors acknowledge our industrial partners, a linerboard and a pulp and paper mill in the USA, for providing their Lime Kiln flue gas data for this study.

Chapter 7. Conclusions and future work

This work is aimed at reducing the freshwater from the ECF bleaching section and capturing CO_2 from the Lime Kiln section of a pulp and paper mill. A simulation-based approach was developed to study the bleaching section and perform a techno-economic analysis of CO_2 capture. An integrated softwood mill is selected for study on the bleaching section. First, a 5-stage Elemental Free Chlorine bleaching section was simulated using Windows General Energy and Material Balance Systems (WinGEMS) to develop a process of an integrated softwood line of a Kraft pulp mill. Three levels of research work are considered which include unit operations, a combination of unit operations, and a combination of various processes. Data for building the simulation was taken from a softwood mill which provided the materials flow, the bleach tower freshwater flows, and important pulp properties. Steady-state equations for the ECF bleaching sequence $D_0E_{OP}D_1E_PD_2$ are included in the simulation. The simulation model captures the effects of carry-over from brown stock washers (BSW) and extraction stage washers on the pulp brightness. Also, the prepared simulation model can predict changes in the kappa number, brightness, and COD values with changes in the operating parameters. Industry data were used to verify the model outputs and the percent difference between industry operation date and simulation results in terms of key pulp properties such as pulp brightness and pulp kappa number was in the range of 0.2 to 5.5%, respectively.

A high degree of interaction between various processes leads to a built-up of NPEs in the system. To tackle the problem of the NPEs build-up, for the first time, the 5-stage bleaching model was used to simulate the replacement of freshwater in the bleach tower washers with the paper machine section white water. The simulation was used to track the NPEs and the water flows in

the bleaching section. To study the partition of the Ca^{2+} ions on the fiber surface and the surrounding solution, the Donnan equilibrium model was linked with the 5-stage bleaching model using the dynamic data exchange (DDE) feature in WinGMES. After simulating white water addition, the free Ca^{2+} ions are calculated using the value of partition coefficient 'λ', and taking the inputs of the metal ion concentration from the ECF bleaching section of the WinGEMS model. The amount of free Ca^{2+} ions in the solution was used to calculate the scaling tendency in the bleaching section. Usually, the calcium oxalate scaling is formed in the extraction section and the calcium oxalate scaling is formed in the acidic chlorine dioxide stages. The sensitivity analysis helped to understand the changes in the SI value with changes in the amount of freshwater replacement. Different parameters were considered while calculating the value of SI like the point of addition of white water, the pulp consistencies, the system pH, temperature, and the concentration of Ca^{2+} ions in the white water. The SI value sensitivity analysis revealed that for all the parameters, the value of SI increases for both the calcium oxalate and the calcium carbonate scaling as the amount of white water addition in the bleach section increases. For the calcium oxalate scale in the bleaching section, the first instance of scaling was encountered for the D_1 stage at around 25% freshwater replacement with 200 ppm Ca^{2+} content in the white water for 5% pulp consistency. However, the calcium carbonate scaling was not predicted in the Ep and E_{OP} stages as these stages operate at alkaline pH values and the value of the solubility product, and therefore the scaling also depends on the amount of CO_2 dissolved in water.

This study explored the application of the bleaching section simulation for predicting the amount of effluent reduction due to white water recycling in the bleaching section. However, the WinGEMS simulation for sequence $D_0E_{OP}D_1E_PD_2$ of softwood line can be used to optimize the parameters of the bleaching section. It is very well established that chlorine dioxide usage in the

bleaching section can be optimized by varying the temperature and dosages of oxygen and peroxide in the E_{OP} stage. The simulation can be used to optimize the usage of chlorine dioxide and also further improve the effluent quality. The simulation can also be extended to optimize the steam consumption in the bleach section. Integrating the simulation with the rest of the mill simulation would also help in understanding and giving insights into the process from wood chips to the paper machine section. In the pulp and paper mill, the simulation can also help the plant personnel as a prediction tool for determining the chemical dosages, the utility consumption, and the effluent quality in the bleaching section for a specific target of the pulp brightness and the kappa number.

The second part of the research focused on the CO_2 capture from the Lime Kiln section of the pulp and paper industry. The simulation approach included the preparation of a Monoethanol amine solvent-based CO_2 capture flowsheet in Aspen plus. First, a techno-economic analysis was performed by processing a published theoretical Lime Kiln flue gas data into the absorption setup. CAPCOST modular program was linked to the Aspen plus file using a python script and the equipment costs were calculated. The total capture costs, the equipment costs, the utility costs, and the economic evaluation methodology in the published literature were compared. A significant difference is observed in the capital costs of this study and the published report. The costing equations, the methodology for calculating the base equipment costs, EPC, construction, and fixed operating costs were the main factors leading to a difference in the total capture costs for both the studies. Analyzing the cost breakdown, the highest difference in the capital costs was observed in the stripper section and the compressor and dehydration sections. However, the operating costs for both studies were similar. The sensitivity analysis provided a range of the CO_2 capture costs by varying the flue gas CO_2 composition and the utility costs.

The approach used to do the CO_2 capture techno-economic analysis was extended to calculate CO_2 capture costs by processing two real mill Lime Kiln data. In this work, a techno-economic assessment of carbon dioxide capture from Lime Kiln flue gas of a pulp and paper mill (Mill A) and a linerboard mill (Mill B), using a Monoethanolamine (MEA) absorption desorption process, was carried out. We coupled the ASPEN Plus simulator with a derivative-free optimization (DFO) tool to identify the overall optimal configuration for minimizing the total capture cost. The capture costs were calculated using CAPCOST. Eight degrees of freedom, the direct contact cooler stages, the absorber stages, the stripper stages, solvent lean loading, solvent weight concentration, stripper inlet temperature, the flue gas inlet temperature, and the amount of CO_2 captured were selected for process and flowsheet optimization. Additionally, we evaluate the effect of steam integration, and Section 45Q of the existing federal tax credit for carbon capture and sequestration on the CO_2 capture costs. Considering the steam integration and Section 45Q, the total capture costs for were -$2.5 per tonne of CO_2 for Mill A and $2.6 per tonne of CO_2 for Mill B. Further, the CO_2 capture costs sensitivity was performed by varying the inlet flue gas flowrate, flue gas CO_2 mol%, and the electricity and MEA prices. The sensitivity analysis results showed that the capture costs vary from -$5.9 to $5.9 per tonne of CO_2 captured.

Historically the pulp and paper industry is looked at as a sector emitting bio-based CO_2 and hence not heeded upon as a potential source of carbon capture. However, recent alarming trends of CO_2 emissions and the associated temperature rise have focused the attention of researchers on the topic of bio-based CO_2 capture. Ways to implement the carbon capture include giving tax Incentives which ensures that the manufacturing sector pays necessary attention to the major source of CO_2. Studies, though theoretical, have brought into play the techniques used for capturing carbon dioxide from various other sectors like the power plant, cement industries, etc.,

and applying those techniques to the pulp and paper industry. Identification of carbon-emitting clusters and considering a combined carbon capture scenario would further strengthen the cause of carbon dioxide capture and utilization.

Overall, this research using the simulation approach enabled to have an understanding of the softwood line 5-stage ECF bleaching section, the scaling tendency, the white water recycling capacity using WinGEMS simulation, and the donna equilibrium theory. Also, the simulation approach was utilized to study the techno-economic analysis of CO_2 capture from the pulp and paper mill Lime Kiln section. The research done would provide a platform for further research on the topic of effluent reduction and CO_2 capture from the pulp and paper industry. This in turn would help to reduce the environmental footprint of the sector.

Every industrial sector has its intricacies and nuances. Simulation and modeling earlier have and in the future would help to bridge the gaps between various methods and schemes used for emissions and waste reduction from different sectors including the pulp and paper industry. Direct retrofitting a particular technology from one sector to another might not be completely feasible however, accessing the necessary degrees of freedom and the process parameters can be done using the available technological tools.

References

[1] Journal of Pollution Effects & Control. Longdom Publ SL n.d. https://www.longdom.org/scholarly/industrial-pollution-journals-articles-ppts-list-2683.html.

[2] Broniewicz E. ENVIRONMENTAL MANAGEMENT IN PRACTICE. 2011.

[3] EPA. Production-Related Waste Managed by Industry , 2019 Total Disposal or Other Releases by Industry. 2019.

[4] Dieter, C.A., Maupin, M.A., Caldwell, R.R., Harris, M.A., Ivahnenko, T.I., Lovelace, J.K., Barber, N.L., and Linsey KS. Estimated use of water in the United States in 2015: U.S. Geological Survey Circular 1441. 2018. https://doi.org/10.3133/cir1441.

[5] Industry P. Conservation of Water in the Pulp and Paper Industry through Recycle, Re-use, and Reclamation. Ind Eng Chem 1956;48:2151–5. https://doi.org/10.1021/ie50564a031.

[6] Sappi. Water Use and Treatment in the Pulp and Paper Industry. EQ Insights 2012;5:1–7.

[7] Lovelady EM, El-Halwagi M, Krishnagopalan GA. An integrated approach to the optimisation of water usage and discharge in pulp and paper plants. Int J Environ Pollut 2007;29:274.

[8] Jacob J, Kaipe H, Couderc, F. et al. Water network analysis in pulp and paper processes by pinch and linear programming techniques. Chem Eng Commun 2002;189:184–206. https://doi.org/10.1080/00986440211836.

[9] Chew IML, Tan R, Ng, Denny Kok Sum et al. Synthesis of direct and indirect interplant water network. Ind Eng Chem Res 2008;47:9485–96. https://doi.org/10.1021/ie800072r.

[10] Manan ZA, Yin LT, Foo, Dominic Chwan Yee et al. Application of the water cascade

analysis technique for water minimisation in a paper mill plant. Int J Environ Pollut 2007;29:90–103. https://doi.org/10.1504/ijep.2007.012798.

[11] Shafiei S, Domenech S, Koteles R et al. System closure in an integrated newsprint mill, practical application of the genetic algorithm 2004;105:146–9. https://doi.org/10.1016/S0959-6526(02)00188-9.

[12] Koppol APR, Bagajewicz MJ, Dericks BJ et al. On zero water discharge solutions in the process industry. Adv Environ Res 2004;8:151–71. https://doi.org/10.1016/S1093-0191(02)00130-2.

[13] Nguyen KL, Hoadley A. Design and management of water circuits of a closed integrated unbleached kraft pulp mill. Appita J 2004;57:395–8.

[14] Shukla SK, Kumar V, Chakradhar B et al. Designing plant scale process integration for water management in an Indian paper mill. J Environ Manage 2013;128:602–14. https://doi.org/10.1016/j.jenvman.2013.06.012.

[15] de Oliveira KD, Cardoso M, Nicolato R. Process simulation for water consumption minimization in pulp mill. Lat Am Appl Res 2011;40:81–90.

[16] Mei I, Chew L, Chwan, Dominic et al. A model-based approach for simultaneous water and energy reduction in a pulp and paper mill. Appl Therm Eng 2013;51:393–400. https://doi.org/10.1016/j.applthermaleng.2012.08.070.

[17] Parthasarathy G, Krishnagopalan G. Systematic reallocation of aqueous resources using mass integration in a typical pulp mill. Adv Environ Res 2001;5:61–79. https://doi.org/10.1016/S1093-0191(00)00043-5.

[18] Agency USEP. Economic Impact Analysis Final Revisions to the National Emission Standards for Hazardous Air Pollutants Subpart S (MACT I and MACT III) 2012.

[19] U.S. Energy Information Administration - EIA - Independent Statistics and Analysis n.d. https://www.eia.gov/energyexplained/use-of-energy/industry.php.

[20] Klaas Jan Kramer, Eric Masanet and EW. Energy efficiency opportunities in the U.S. pulp and apper industry. n.d.

[21] Onarheim K, Santos S, Kangas, Petteri et al. Performance and costs of CCS in the pulp and paper industry part 1: Performance of amine-based post-combustion CO2 capture. Int J Greenh Gas Control 2017;59:58–73. https://doi.org/10.1016/j.ijggc.2017.02.008.

[22] US EPA. GHGRP Reported Data 2020. https://www.epa.gov/ghgreporting/ghgrp-reported-data.

[23] Arasto A. CCS and Pulp and Paper Industry 2015.

[24] Rao AB, Rubin ES. A technical, economic, and environmental assessment of amine-based CO_2 capture technology for power plant greenhouse gas control. Environ Sci Technol 2002;36:4467–75. https://doi.org/10.1021/es0158861.

[25] Feron PHM, Hendriks CA. CO_2 capture process principles and costs. Oil Gas Sci Technol 2005;60:451–9. https://doi.org/10.2516/ogst:2005027.

[26] Figueroa JD, Fout T, Plasynski S, McIlvried H, Srivastava RD. Advances in CO2 capture technology-The U.S. Department of Energy's Carbon Sequestration Program. Int J Greenh Gas Control 2008;2:9–20. https://doi.org/10.1016/S1750-5836(07)00094-1.

[27] Rubin ES. IPCC special report on Carbon dioxide capture and storage structure of the intergovernmental panel on climate change (IPCC) 2006:1–443.

[28] Gibbins J, Chalmers H. Carbon capture and storage. Energy Policy 2008;36:4317–22. https://doi.org/10.1016/j.enpol.2008.09.058.

[29] Hetland J, Anantharaman R. Carbon capture and storage (CCS) options for co-production

of electricity and synthetic fuels from indigenous coal in an Indian context. Energy Sustain Dev 2009;13:56–63. https://doi.org/10.1016/j.esd.2009.02.001.

[30] Authors CL, Abanades JC, Authors L, Feron P, Rubin E, Wilkinson M, et al. Capture of CO_2 n.d.

[31] Berntsson T, Axegård P, Backlund B et al. Swedish pulp mill bio refineries- A vision of future possibilities. Goteborg: 2008.

[32] Leeson D, Mac Dowell N, Shah N, Petit C, Fennell PS. A Techno-economic analysis and systematic review of carbon capture and storage (CCS) applied to the iron and steel, cement, oil refining and pulp and paper industries, as well as other high purity sources. Int J Greenh Gas Control 2017;61:71–84. https://doi.org/10.1016/j.ijggc.2017.03.020.

[33] Hektor E, Berntsson T. Reduction of greenhouse gases in integrated pulp and paper mills: Possibilities for CO_2 capture and storage. Clean Technol Environ Policy 2009;11:59–65. https://doi.org/10.1007/s10098-008-0166-3.

[34] Möllersten K, Gao L, Yan J et al. Efficient energy systems with CO2 capture and storage from renewable biomass in pulp and paper mills. Renew Energy 2004;29:1583–98. https://doi.org/10.1016/j.renene.2004.01.003.

[35] Garðarsdóttir SÓ, Normann F, Skagestad R et al. Investment costs and CO2 reduction potential of carbon capture from industrial plants – A Swedish case study. Int J Greenh Gas Control 2018;76:111–24. https://doi.org/10.1016/j.ijggc.2018.06.022.

[36] Darmawan A, Hardi F, Yoshikawa K, Aziz M, Tokimatsu K. Enhanced process integration of black liquor evaporation, gasification, and combined cycle. Appl Energy 2017;204:1035–42. https://doi.org/10.1016/j.apenergy.2017.05.058.

[37] Darmawan A, Ajiwibowo MW, Yoshikawa K, Aziz M, Tokimatsu K. Energy-efficient

recovery of black liquor through gasification and syngas chemical looping. Appl Energy 2018;219:290–8. https://doi.org/10.1016/j.apenergy.2018.03.033.

[38] EPA. EPA's treatment of biogenic carbon dioxide (CO2) emissions from stationary sources that use forest biomass for energy production. US Environ Prot Agency Off Atmos Programs Clim Chang Div 2018:6.

[39] Jönsson J, Kjärstad J, Odenberger M. Perspectives on the potential for CCS in the European pulp and paper industry. Syst Perspect Biorefineries 2014:81–91.

[40] Gary A.Smook. Handbook for pulp and paper technologists- Chapter 10 Chemical Recovery. 3rd ed. TAPPI Press; 2015.

[41] EPA. Available and emerging technologies for reducing Greenhouse gas emissions from the pulp and paper manufacturing industry. Improv Energy Effic Greenh Gas Reduct Pulp Pap Ind 2011:1–55.

[42] PCA. How Containerboard Is Made 2021. https://www.packagingcorp.com/how-containerboard-is-made (accessed July 29, 2020).

[43] AF&PA. Containerboard 2019. https://www.afandpa.org/our-products/paper-based-packaging/containerboard (accessed March 10, 2021).

[44] Valmet. Water handling 2019. https://www.valmet.com/pulp/wood-handling/water-handling/.

[45] Orville D. Mussey. Water Requirements of Pulp and paper industry. US Gov Print Off 1955. https://doi.org/10.3133/wsp1330A.

[46] Ravnjak D, Ilić G, Može A. Designing water reuse in a paper mill by means of computer modelling. Chem Biochem Eng Q 2004;18:13–9.

[47] Carlton W. Dence and Douglas W. Reeve, editor. Pulp Bleaching: Principles and Practice.

1st ed., TAPPI Press; 1996.

[48] Timaty AT, Sikdar SK. Security of Industrial Water Supply and Management. NATO Sci Peace Secur Ser C Environ Secur 2011:131–9. https://doi.org/10.1007/978-94-007-1805-0.

[49] Eric Kilby AC. Pulp and Paper Industry-Definitions and concepts. Routledge Handb Environ Displac Migr 2014:323–8. https://doi.org/10.4324/9781315638843-25.

[50] Bryant PS, Woitkovich CP, Malcolm EW. Pulp and paper mill water use in North America. Int Environ Conf 1996;2:451–60.

[51] Martinez J, Picon M. Retrofit Approach for the Reduction of Water and Energy Consumption in Pulp and Paper Production Processes. Environ Manag Pract 2011. https://doi.org/10.5772/20882.

[52] Cardoso M, de Oliveira KD, Costa GAA, Passos ML. Chemical process simulation for minimizing energy consumption in pulp mills. Appl Energy 2009;86:45–51. https://doi.org/10.1016/j.apenergy.2008.03.021.

[53] Dahlquist E. Process simulation for pulp and paper industries: Current practice and future trend. Chem Prod Process Model 2008;3. https://doi.org/10.2202/1934-2659.1087.

[54] Jour P, Lindgren K, Gutke K et al. Decreased water usage in a softwood ECF bleaching sequence - Full mill simulations. PEERS Conf 2017 Maximizing Success Through Innov 2017;2017-Novem:755–62.

[55] Maryna Mansfield and Volkmar Böhmer. The use of computer simulation to find effluent treatment and recirculation soutions for SAPPI pulp and paper mills. TAPPSA J 17-20 n.d.

[56] Savulescu L, Poulin B, Hammache A et al. Water and energy savings at a kraft paperboard

mill using process integration. Pulp Pap Canada 2005;106:29–31.

[57] Liang J, He Y, Zhao X et al. Pinch technology reduces wastewater at a paper mill. 2nd Int Conf Bioinforma Biomed Eng ICBBE 2008 2008:2753–6. https://doi.org/10.1109/ICBBE.2008.1020.

[58] Towers M. Energy reduction at a kraft mill: Examining the effects of process integration, benchmarking, and water reduction. Tappi J 2005;4:15–21.

[59] Keshtkar M, Ammara R, Perrier M et al. Thermal Energy Efficiency Analysis and Enhancement of Three Canadian Kraft Mills. J-for-Journal Sci Technol For Prod Process 2015;5:24–60.

[60] Mateos-Espejel E, Marinova M, Bararpour S et al. Energy implications of water reduction strategies in kraft process. Part II: Results. Pulp Pap Canada 2010;111:34–7.

[61] Kermani M, Périn-Levasseur Z, Benali M et al. A novel MILP approach for simultaneous optimization of water and energy: Application to a Canadian softwood Kraft pulping mill. Comput Chem Eng 2017;102:238–57. https://doi.org/10.1016/j.compchemeng.2016.11.043.

[62] Dogan I, Guniz A. Waste minimization in a bleach plant. Adv Environ Res 2004;8:359–69.

[63] V.P. Singh, Vivek Kumar DK. Mathematical model for waste minimization of a bleach plant in paper industry. Proc Appl Math Mech 2007;7:2150045–6. https://doi.org/10.1002/pamm.200701110.

[64] Chew, Irene Mei Leng, Foo D.C.Y., Lam H.L. et al. Simultaneous water and energy optimization for a pulp and paper mill. Chem Eng Trans 2011;25:441–6. https://doi.org/10.3303/CET1125074.

[65] Ibrić N, Ahmetović E et al. Simultaneous synthesis of non-isothermal water networks integrated with process streams. Energy 2017;141:2587–612. https://doi.org/10.1016/j.energy.2017.07.018.

[66] Huber P, Burnet A, Petit-Conil M. Scale deposits in kraft pulp bleach plants with reduced water consumption: A review. J Environ Manage 2014;141:36–50. https://doi.org/10.1016/j.jenvman.2014.01.053.

[67] Shukla SK, Kumar D, Kumar V et al. Process Integration in the Bleaching Section of a Paper Mill for Minimization of Fresh Water Consumption and Wastewater Generation. Environ Eng Manag J 2013;12:2435–42. https://doi.org/10.30638/eemj.2013.295.

[68] Atkins M, Walmsley M, Morrison A, Neale J. Process integration in pulp and paper mills for energy and water reduction - A review. Appita J 2012;65:170–7.

[69] Mateos-Espejel E, Savulescu L, Paris J. Base case process development for energy efficiency improvement, application to a Kraft pulping mill. Part I: Definition and characterization. Chem Eng Res Des 2011;89:742–52. https://doi.org/10.1016/j.cherd.2010.09.012.

[70] A. Blanco, E. Dahlquist, J. Kappen, J. Manninen, C. Negro RR. Use of modelling and simulation in the pulp and paper industry, Mathematical and Computer Modelling of Dynamical Systems: Methods, Tools and Applications in Engineering and Related Sciences 2009;15:5:409–23. https://doi.org/http://dx.doi.org/10.1080/13873950903375387.

[71] Vakkilainen EK. Kraft recovery boilers - Principles and practice. 2005.

[72] Adams TN. Lime kiln principles and operations. TAPPI Kraft Recover Course 2007 2007;1:83–113.

[73] EuLA. Kiln Types – EuLA: European Lime Association. n.d.

[74] Tran H. Lime kiln chemistry and effects on kiln operations. TAPPI Kraft Recover Course 2007 2007;1:114–50.

[75] Kuparinen K, Vakkilainen E, Tynjälä T. Biomass-based carbon capture and utilization in kraft pulp mills. Mitig Adapt Strateg Glob Chang 2019;24:1213–30. https://doi.org/10.1007/s11027-018-9833-9.

[76] Mathieu P. The IPCC special report on carbon dioxide capture and storage. 2006.

[77] Onarheim K, Santos S, Kangas P et al. Performance and cost of CCS in the pulp and paper industry part 2: Economic feasibility of amine-based post-combustion CO2 capture. Int J Greenh Gas Control 2017;66:60–75. https://doi.org/10.1016/j.ijggc.2017.09.010.

[78] Dutcher B, Fan M, Russell AG. Amine-based CO2 capture technology development from the beginning of 2013-A review. ACS Appl Mater Interfaces 2015;7:2137–48. https://doi.org/10.1021/am507465f.

[79] Möllersten K, Yan J, Moreira JR. Potential market niches for biomass energy with CO_2 capture and storage - Opportunities for energy supply with negative CO_2 emissions. Biomass and Bioenergy 2003;25:273–85. https://doi.org/10.1016/S0961-9534(03)00013-8.

[80] Möllersten K, Yan J, Westermark M. Potential and cost-effectiveness of CO_2 reductions through energy measures in Swedish pulp and paper mills. Energy 2003;28:691–710. https://doi.org/10.1016/S0360-5442(03)00002-1.

[81] Hektor E, Berntsson T. Future CO_2 removal from pulp mills - Process integration consequences. Energy Convers Manag 2007;48:3025–33. https://doi.org/10.1016/j.enconman.2007.06.043.

[82] Nwaoha C, Tontiwachwuthikul P. Carbon dioxide capture from pulp mill using 2-amino-2-methyl-1-propanol and monoethanolamine blend: Techno-economic assessment of advanced process configuration. Appl Energy 2019;250:1202–16. https://doi.org/10.1016/j.apenergy.2019.05.097.

[83] McGrail BP, Freeman CJ, Brown CF et al. Overcoming business model uncertainty in a carbon dioxide capture and sequestration project: Case study at the Boise White Paper Mill. Int J Greenh Gas Control 2012;9:91–102. https://doi.org/10.1016/j.ijggc.2012.03.009.

[84] Sagues WJ, Jameel H, Sanchez, D. L. et al. Prospects for bioenergy with carbon capture & storage (BECCS) in the United States pulp and paper industry. Energy Environ Sci 2020;13:2243–61. https://doi.org/10.1039/d0ee01107j.

[85] Luis P. Use of monoethanolamine (MEA) for CO_2 capture in a global scenario: Consequences and alternatives. Desalination 2016;380:93–9. https://doi.org/10.1016/j.desal.2015.08.004.

[86] Feron PHM, Cousins A, Jiang K, Zhai R, Garcia M. An update of the benchmark post-combustion CO_2-capture technology. Fuel 2020;273:117776. https://doi.org/10.1016/j.fuel.2020.117776.

[87] Möllersten K, Yan J, Moreira JR. Potential market niches for biomass energy with CO2 capture and storage - Opportunities for energy supply with negative CO2 emissions. Biomass and Bioenergy 2003;25:273–85. https://doi.org/10.1016/S0961-9534(03)00013-8.

[88] Parkhi A, Cremaschi S, Jiang Z. Techno-Economic Analysis of CO2 Capture from Pulp and Paper Mill Limekiln. IFAC-PapersOnLine 2022;In-Press.

[89] Mourtzis D, Doukas M, Bernidaki D. Simulation in manufacturing: Review and challenges. Procedia CIRP 2014;25:213–29. https://doi.org/10.1016/j.procir.2014.10.032.

[90] Atkins M, Morrison A, Walmsley M, Riley J. WinGEMS modelling and pinch analysis of a paper machine for utility reduction. Appita J 2010;63:281–7.

[91] Li J, Zhang Y, Liu H. Simulation of multiple effect evaporators for energy-saving studies in a chemical pulp mill. Proc World Congr Intell Control Autom 2015;2015-March:2791–7. https://doi.org/10.1109/WCICA.2014.7053169.

[92] Litvay C, Rudie A, Hart P. Use of excel ion exchange equilibrium solver with WinGEMS to model and predict NPE distribution in the MeadWestvaco Evandale, TX hardwood bleach plant. TAPPI Fall Tech Conf 2003:393–408.

[93] Brooks TR, Edwards LL, Nepote JC, Caldwell MR. Bleach plant close-up and conversion to TCF: a case study using mill data and computer simulation. Proc 1994 Int Pulp Bleach Conf 1994:13–20.

[94] Technology GI of. An Assessment of the Potential for Water Reuse in the Pulp na Paper Industry. Off Water Res Technol United States Dep Inter Under Res Grant 1981.

[95] Ulrich, D.A. and Kambhiranond, R. GEMS energy balances for a kraft pulpmill complex. Proceedings,"TAPPI Eng Conf 1988:259–63.

[96] Andersson P. A dynamic Na/S balance of a kraft pulp mill 2014:54.

[97] Jain S, Mortha G, Calais C. Kinetic models for all chlorine dioxide and extraction stages in full ECF bleaching sequences of softwoods and hardwoods. Tappi J 2009;8:12–21.

[98] Brogdon BN. Improved steady-state models for chlorine dioxide delignification sequences that includes washer carryover effects. PEERS Conf 2014 2014;14:7–20.

[99] Brogdon BN. Stoichimetric model of chlorine dioxide delignification of hardwood kraft

pulp with oxidant-reinforced extraction effects 2013;12:17–26.

[100] Brogdon BN. Revised steady-state model for chlorine dioxide brightening that considers extraction washer carryover effects. Tappi J 2016;15:178–85.

[101] Brogdon BN, Lucia LA. Using multistage models to evaluate how pulp washing after the first extraction stage impacts elemental chlorine-free bleach demand. Pulping Eng Environ Recycl Sustain Conf PEERS 2018 Tech Solut Today Beyond 2018:35–46. https://doi.org/10.32964/TJ17.11.621.

[102] Hart PW, Rudie AW. Mineral scale management, Part I. Case studies. Tappi J 2006;5:22–7.

[103] Rudie A, Hart P. Mineral scale management. Part II, Fundamental chemistry. TAPPI J 2006;5:17–23.

[104] Rudie A, Hart P. Mineral scale management Part III, Nonprocess elements in the paper industry. TAPPI J 2006;5:3–10.

[105] P. Huber, S. Nivelon, P. Ottenio MS and AB. Prediction of mineral deposits in kraft pulp bleaching lines through chemical process simulation. Adv Pulp Pap Res 2018;35:451–85. https://doi.org/10.15376/frc.2017.1.451.

[106] Hart PW, Santos RB. Kraft ECF pulp bleaching: A review of the development and use of techno-economic models to optimize cost, performance, and justify capital expenditures. Tappi J 2013;12:19–29. https://doi.org/10.32964/tj12.10.19.

[107] Towers M, Scallan AM. Predicting the ion-Exchange of Kraft Pulps Using Donnan Theory. J Pulp Pap Sci 1996;22:332–7.

[108] Rudie A, Hart P. Managing calcium oxalate scale in the bleach plant. Solutions 2005;88:45–6.

[109] Ferguson RJ. Predicting calcium oxalate scale. NACE - Int Corros Conf Ser 2002;2002-April:1–9.

[110] Rudie AW, Service UF. Fundamental Chemistry of Precipitation and Mineral Scale Formation Alan W. Rudie, USDA Forest Service, Forest Products Laboratory, Madison, WI Peter W. Hart, MeadWestvaco Corporation, Corporate Research Center, Chillicothe, OH 1980;i.

[111] Stefánsson A, Bénézeth P, Schott J. Carbonic acid ionization and the stability of sodium bicarbonate and carbonate ion pairs to 200°C - A potentiometric and spectrophotometric study. Geochim Cosmochim Acta 2013;120:600–11. https://doi.org/10.1016/j.gca.2013.04.023.

[112] Rudie A. Calcium in pulping and bleaching. TAPPI J 2000;83:36–7.

[113] Abu-Zahra MRM, Schneiders LHJ, Niederer JPM, Feron PHM, Versteeg GF. CO_2 capture from power plants. Part I. A parametric study of the technical performance based on monoethanolamine. Int J Greenh Gas Control 2007;1:37–46. https://doi.org/10.1016/S1750-5836(06)00007-7.

[114] Turton R, Joseph A. Shaeiwitz, Debangsu Bhattacharyya, Wallace B. Whiting. Analysis, Synthesis, and Design of Chemical Processes. 5 edition. Pearson; (June 22, 2018); 2018.

[115] Wankat PC. Separation Process Engineering. vol. 49. 2004.

[116] IEAGHG. Techno-Economic Evaluation of Retrofitting CCS in a Market Pulp Mill and an Integrated Pulp and Board Mill 2016.

[117] Lars Erik Ø. Removal of CO 2 from exhaust gas 2012:165.

[118] Nuchitprasittichai A, Cremaschi S. Optimization of CO_2 capture process with aqueous amines using response surface methodology. Comput Chem Eng 2011;35:1521–31.

https://doi.org/10.1016/j.compchemeng.2011.03.016.

[119] Hua, X., Owston, T. and Dorris G. “Carbon Dioxide for pH Control in Neutral Papermaking” Wet End and Water Systems Management For Papermakers. Pira Conf 2006.

[120] Zhi-hua Jiang; Berry Richard. Near-Neutral final chlorine dioxide brightening: Theory and Practice 2011:14–20.

[121] Luthe, C., Berry, R., Nadeau L. How does carbon dioxide improve brownstock washing? Tappi J 2003.

[122] Linde North America. When Being Green Matters - CO_2 pH control. 2015.

[123] Internal Revenue Service (IRS), Treasury Department. Final Rule on Section 45Q Credit Regulations 2021;1:1–187.

[124] Kristin O, Santos S, Hankalin V, Kangas P, Tsupari E, Karki J, et al. Retrofitting CO_2 capture to an integrated pulp and paper mill. Nord Pulp Pap Res J 2014;29:620–34. https://doi.org/10.3183/npprj-2014-29-04-p620-634.

[125] Husebye J, Brunsvold AL, Roussanaly S, Zhang X. Techno economic evaluation of amine based CO_2 capture: Impact of CO_2 concentration and steam supply. Energy Procedia 2012;23:381–90. https://doi.org/10.1016/j.egypro.2012.06.053.

[126] David J, Herzog H. The Cost of Carbon Capture. Massachusetts Inst Technol 2000.

[127] Bhown AS, Freeman BC. Analysis and status of post-combustion carbon dioxide capture technologies. Environ Sci Technol 2011;45:8624–32. https://doi.org/10.1021/es104291d.

[128] Kohl AL, Nielsen R. Gas Purification. 5 edition. Gulf Professional Publishing; 1997.

[129] Boukouvala F, Misener R, Floudas CA. Global optimization advances in Mixed-Integer Nonlinear Programming, MINLP, and Constrained Derivative-Free Optimization, CDFO.

Eur J Oper Res 2016;252:701–27. https://doi.org/10.1016/j.ejor.2015.12.018.

[130] Holmstr K, Anders OG, Edvall MM. USER ' S GUIDE FOR TOMLAB / CPLEX v12 . 1 2009:1–106.

[131] Maxwell C. Cost Indices. Towering Ski 2020. https://www.toweringskills.com/financial-analysis/cost-indices/ (accessed February 22, 2022).

[132] Zhang X, Song Z, Gani R, Zhou T. Comparative Economic Analysis of Physical, Chemical, and Hybrid Absorption Processes for Carbon Capture. Ind Eng Chem Res 2020;59:2005–12. https://doi.org/10.1021/acs.iecr.9b05510.

[133] Oh SY, Binns M, Cho H, Kim JK. Energy minimization of MEA-based CO_2 capture process. Appl Energy 2016;169:353–62. https://doi.org/10.1016/j.apenergy.2016.02.046.

[134] Duan L, Zhao M, Yang Y. Integration and optimization study on the coal-fired power plant with CO_2 capture using MEA. Energy 2012;45:107–16. https://doi.org/10.1016/j.energy.2011.12.014.

[135] Hassan SMN, Douglas P, Croiset E. Techno-economic study of CO_2 capture from an existing cement plant using MEA scrubbing. Int J Green Energy 2007;4:197–220. https://doi.org/10.1080/01971520600873418.

[136] Li K, Leigh W, Feron P, Yu H, Tade M. Systematic study of aqueous monoethanolamine (MEA)-based CO_2 capture process: Techno-economic assessment of the MEA process and its improvements. Appl Energy 2016;165:648–59. https://doi.org/10.1016/j.apenergy.2015.12.109.

[137] Davis JD. Thermal Degradation of Aqueous Amines Used for Carbon Dioxide Capture. PhD Thesis. Univ Texas Austin 2009;2:S165–70.

[138] Fytianos G, Ucar S, Grimstvedt A, Hyldbakk A, Svendsen HF, Knuutila HK. Corrosion

and degradation in MEA based post-combustion CO2 capture. Int J Greenh Gas Control 2016;46:48–56. https://doi.org/10.1016/j.ijggc.2015.12.028.

[139] Kangas P, Kaijaluoto S, Maattanen M. Evaluation of future pulp mill concepts - Reference model of a modern Nordic kraft pulp mill. Nord Pulp Pap Res J 2014;29:620–34.

[140] Zhang W, Liu H, Sun Y, Cakstins J, Sun C, Snape CE. Parametric study on the regeneration heat requirement of an amine-based solid adsorbent process for post-combustion carbon capture. Appl Energy 2016;168:394–405. https://doi.org/10.1016/j.apenergy.2016.01.049.

[141] Roussanaly S, Fu C, Voldsund M, Anantharaman R, Spinelli M, Romano M. Techno-economic Analysis of MEA CO_2 Capture from a Cement Kiln - Impact of Steam Supply Scenario. Energy Procedia 2017;114:6229–39. https://doi.org/10.1016/j.egypro.2017.03.1761.

[142] Nelson E. Lawson and Gamal. Amer. Acidulation and recovery of crude tall oil from tall oil soaps. United States Pat No 4,495,095 1985:2–5.

[143] Kouisni L, Holt-Hindle P, Maki K, Paleologou M. The LignoForce System™: A new process for the production of high-quality lignin from black liquor. Pulp Pap Canada 2014;115:18–22.

[144] Christopher J. Biermann. Handbook of pulping and papermaking-Chapter 8. Second. Academic Press; 1996.

[145] Monica Bokstrom, Raimo Rasimus. Method of washing of alkaline pulp by adding carbon dioxide to the pulp. 5,429,717, 1995.

[146] Hollerbach, George H., Jr.; Kleinberg W. Cellulosic pulp. EP88301311A, 1988.